

Design and Evaluation of Fluidized Bed Heat Recovery for Diesel Engine System

J.R. Hamm, R.A. Newby, E.J. Vidt, and T.E. Lippert
Westinghouse Electric Corporation

July 1985

Prepared for
National Aeronautics and Space Administration
Lewis Research Center
Cleveland, Ohio 44135
Under Contract DEN 3-345

for
U.S. DEPARTMENT OF ENERGY
Conservation and Renewable Energy
Office of Vehicle and Engine R&D
Washington, D.C. 20585
Under Interagency Agreement DE-AI01-80CS50194

DESIGN AND EVALUATION OF FLUIDIZED BED HEAT RECOVERY
FOR DIESEL ENGINE SYSTEMS

Prepared By

Westinghouse Electric Corporation
Research and Development Center
1310 Beulah Road, Pittsburgh, PA 15235

Principal Investigators
J. R. Hamm, R. A. Newby, E. J. Vidt and T. E. Lippert

Prepared For

National Aeronautics and Space Administration
Lewis Research Center
Under Contract DEN 3-345

ACKNOWLEDGEMENTS

This work was conducted for NASA under the technical direction of Mr. Murray Bailey whose many suggestions and contributions are recognized.

CONTENTS

	<u>Page</u>
ACKNOWLEDGEMENTS.....	i
1. SUMMARY AND CONCLUSIONS.....	1-1
2. INTRODUCTION.....	2-1
3. BACKGROUND.....	3-1
3.1 Diesel Engine Application With Heat Recovery.....	3-1
3.2 Fluidized Bed Characteristics in Heat Recovery Applications.....	3-2
4. COMPOUND ENGINE CONFIGURATION SCREENING.....	4-1
4.1 Organic Rankine Cycle.....	4-1
4.1.1 FLUORINAL-85 (F-85) Working Fluid.....	4-1
4.1.2 RC-1 - Working Fluid.....	4-5
4.2 Steam Rankine Cycle.....	4-9
4.3 Turbocompound Engine With Steam Injection.....	4-9
4.4 Open Brayton Cycle.....	4-16
4.5 Closed Brayton Cycle.....	4-23
4.6 Stirling Engine.....	4-34
4.7 Analysis of Screening Evaluations.....	4-42
5. EVALUATION OF SELECTED SYSTEMS.....	5-1
5.1 Organic Rankine Cycle.....	5-1
5.1.1 Truck Applications.....	5-1
5.1.2 Locomotive Application.....	5-4
5.1.3 Marine Application.....	5-4
5.2 Steam Injection Cycle.....	5-4
5.2.1 Truck Application.....	5-13
5.2.2 Locomotive and Marine Applications.....	5-13

5.3	Stirling Engine.....	5-13
5.3.1	Truck Application.....	5-22
5.3.2	Locomotive and Marine Applications.....	5-24
5.4	Performance of Selected Systems.....	5-24
6.	PRELIMINARY DESIGN AND COSTS OF FLUIDIZED BED HEAT EXCHANGERS FOR SELECTED SYSTEMS.....	6-1
6.1	Conceptual Description of the Heat Recovery Unit.....	6-1
6.2	Design Procedure.....	6-3
6.4	Organic Rankine Cycle.....	6-7
6.5	Steam Injection Cycle.....	6-7
6.6	Stirling Engine Cycle.....	6-11
6.7	Fluid Bed Heat Exchanger Cost Estimate.....	6-16
7.	SYSTEM DESCRIPTION AND ARRANGEMENT.....	7-1
7.1	Truck Application.....	7-1
7.1.1	Organic Rankine Cycle.....	7-1
7.1.2	Steam Injection Cycle.....	7-4
7.1.3	Stirling Engine.....	7-4
7.2	Locomotive Application.....	7-7
7.2.1	Organic Rankine Cycle.....	7-7
7.2.2	Steam Injection Cycle.....	7-11
7.2.3	Stirling Engine.....	7-11
7.3	Marine Application.....	7-15
7.3.1	Organic Rankine Cycle.....	7-15
7.3.2	Steam Injection Cycle.....	7-15
7.3.3	Stirling Engine System.....	7-18
8.	SYSTEM COSTS AND ECONOMIC ASSESSMENT.....	8-1
8.1	System Component Weights and Costs.....	8-1
8.1.1	Rankine Cycle System*.....	8-1
8.1.2	Steam Injection Cycle System.....	8-1
8.1.3	Stirling Engine System.....	8-11
8.2	Comparison of System Weights.....	8-11
8.2.1	Truck Application.....	8-11
8.2.2	Locomotive Applications.....	8-11

8.2.3 Marine Application.....	8-12
8.3 Economic Assessment of Turbocompound Diesel Engine Systems.....	8-12
9. REFERENCES.....	9-1
APPENDIX A.....	A-1
APPENDIX B.....	B-1
APPENDIX C.....	C-1
APPENDIX D.....	D-1
APPENDIX E.....	E-1
APPENDIX F.....	F-1
APPENDIX G.....	G-1

LIST OF FIGURES

<u>Figure</u>		<u>Page</u>
4.1	Turbocharged diesel with subposed organic Rankine cycle	4-2
4.2	Turbocompound diesel with subposed organic Rankine cyle	4-3
4.3	Fluidized Bed Heat Exchanger Temperature Profile, organic Rankine cycle with regenerative feed heating	4-6
4.4	Fluidized Bed Heat Exchanger Temperature Profile, organic Rankine cycle with regenerative feed heating	4-7
4.5	Fluidized Bed Heat Exchanger Temperature Profile, organic Rankine cycle	4-8
4.6	Turbocharged diesel with subposed steam Rankine cycle	4-10
4.7	Turbocompound diesel with subposed steam Rankine cycle	4-11
4.8	Fluidized Bed Heat Exchanger Temperature Profile, steam Rankine cycle	4-13
4.9	Turbocompound diesel with steam injection between compressor drive expander and power expander	4-14
4.10	Fluidized Bed Heat Exchanger Temperature Profile. Turbocompound engine with steam injection between compressor drive and power expanders	4-17
4.11	Turbocompound diesel with steam injection ahead of compressor drive expander	4-18
4.12	ATCPD/A Model for Steam Injection System	4-19
4.13	Turbocharged diesel with subposed open Brayton cycle	4-21
4.14	Turbocharged diesel with subposed intercooled open Brayton cycle	4-24
4.15	Turbocharged diesel with subposed recuperated open Brayton cycle	4-25
4.16	Fluidized Bed Heat Exchanger Temperature Profile intercooled open Brayton cycle	4-26
4.17	Turbocharged diesel with subposed closed Brayton cycle	4-28

4.18	Fluidized Bed Heat Exchanger Temperature Profiles for closed Brayton cycle	4-29
4.19	Adiabatic diesel engine with subposed closed Brayton cycle	4-30
4.20	Adiabatic diesel engine with subposed closed Brayton bottoming cycle	4-31
4.21	Adiabatic diesel engine with subposed closed Brayton bottoming cycle	4-32
4.22	Adiabatic diesel engine with subposed Stirling cycle	4-35
4.23	Temperature profile of fluidized bed heat exchanger for Stirling engine subsystem with intermediate heat transfer loop	4-36
4.24	Single stage FBHX heater integrated with Stirling engine	4-39
4.25	Adiabatic diesel engine with subposed Stirling engine using heat pipes	4-40
5.1	Turbocharged diesel with subposed organic Rankine cycle	5-2
5.2	Turbocompound diesel with steam injection ahead of compressor drive expander	5-11
5.3	Fluidized bed heat exchanger temperature profile. Turbocompound engine with steam injection ahead of compressor drive expander	5-12
5.4	Adiabatic diesel with suposed Stirling engines using heat pipes	5-20
5.5	Fluidized bed heat exchanger temperature profile, Stirling engine	5-21
5.6	Basic Mod-I Stirling engine	5-23
6.1	Fluid bed heat recovery unit schematic	6-2
6.2	Fluid bed heat exchanger for organic Rankine bottoming cycle	6-8
6.3	Fluid bed heat exchanger for steam injection	6-12
6.4	Fluid bed heat exchanger for Stirling injection	6-15

7.1	Heavy duty long haul truck tractor	7-2
7.2	Typical truck installation of organic Rankine cycle system	7-3
7.3	Typical truck installation of steam injection cycle	7-5
7.4	Water tank for steam injection cycle on truck	7-6
7.5	Heat pipe system for supposed Stirling engine	7-8
7.6	Typical truck installation of Stirling engine units	7-9
7.7	General Electric 3600 hp C36-7 Diesel-Electric Locomotive	7-10
7.8	Arrangement for organic Rankine cycle system in locomotive	7-12
7.9	Arrangement for steam injection system in locomotive	7-13
7.10	Arrangement of Stirling engine system in locomotive	7-14
7.11	RBC/Vessel Installation	7-16
7.12	Installation of RC-1 organic Rankine cycle system on deck of push-pull boat for inland river service	7-17
7.13	Installation of steam injection cycle system on deck of push-pull boat for inland river service	7-19
7.14	Stirling engine system arrangement for marine application	7-20
B1	Compressor drive expander dimensions for steam injection cycle	B-2
B2	Power expander and gearbox dimensions for steam injection cycle	B-3
C1	Beal number as a function of heater temperature (after Walter, 1979)	C-2
C2	Conventional V-belt accessory drive	C-3
C3	Beal number as a function of heater temperature showing Stirling engine design parameters	C-2
D1	TECCO reference system power conversion unit (PCU)	D-2

LIST OF TABLES

<u>Table</u>		<u>Page</u>
2.1	Adiabatic Diesel Engine Design Point Data	2-2
2.2	Exhaust Pressure Corrections for Engine Performance	2-2
2.3	Candidate Bottoming Cycles Evaluated in Task 1 Screening	2-3
4.1	Performance Summary of Adiabatic Diesel Engine with Organic Rankine Bottoming Cycle	4-4
4.2	Performance Summary of Adiabatic Diesel Engine with Steam Rankine Bottoming Cycle	4-12
4.3	Performance Summary of Adiabatic Turbocompound Diesel Engine with Steam Injection Between Compressor Drive and Power Expanders	4-15
4.4	Performance Summary of Adiabatic Turbocompound Diesel Engine with Steam Injection Ahead of the Power Expander	4-20
4.5	Performance Summary of Adiabatic Diesel Engine with Subposed Open Brayton Cycle	4-22
4.6	Performance Summary of Adiabatic Diesel Engine with Subposed Open Brayton Cycle	4-27
4.7	Conditions for Maximum Performance of Closed Brayton Bottoming Cycle for Adiabatic Diesel Engine	4-33
4.8	Performance Summary of Adiabatic Diesel Engine with Subposed Stirling Cycle	4-37
4.9	Performance Summary of Adiabatic Diesel Engine with Subposed Stirling Cycle	4-38
4.10	Performance Summary of Adiabatic Diesel Engine with Subposed Stirling Cycle	4-41
4.11	Evaluation of Candidate Bottoming Cycles	4-42
5.1	ATCD with Organic Rankine Cycle Using RC-1 (Reference Conditions Truck Application)	5-3

5.2	ATCD with Organic Rankine Cycle Using RC-1 (High Temperature Conditions-Truck Application)	5-5
5.3	ATCD with Organic Rankine Cycle Using RC-1 (Low Temperature Conditions - Truck Application)	5-6
5.4	Adiabatic Diesel Exhaust Gas Temperature Sensitivity Analysis for the Turbocharged Engine with Organic Rankine Bottoming Cycle	5-7
5.5	ATCD with Organic Rankine Cycle Using RC-1 (Reference Conditions-Locomotive Application)	5-8
5.6	ATCD with Organic Rankine Cycle Using RC-1 (Reference Conditions-Marine Application)	5-9
5.7	Performance of RC-1 Organic Rankine Cycle in Marine Application	5-10
5.8	ATCPD/A with Steam Injection (Reference Case) for Truck Application	5-14
5.9	ATCPD/A with Steam Injection (High Temperature Case) for Truck Application	5-15
5.10	ATCPD/A with Steam Injection (Low Temperature Case) for Truck Application	5-16
5.11	Adiabatic Diesel Exhaust Gas Temperature Sensitivity Analysis for the Turbocompound Engine with Steam Injection Ahead of Compressor-Drive Expander	5-17
5.12	ATCPD/A with Steam Injection (Reference Case) for Marine Application	5-18
5.13	ATCPD/A with Steam Injection ((Reference Case) for Marine Application	5-19
5.14	Mass and Energy Balance for ATCD with Dual Stirling Engines Using Heat Pipes (Reference Case for Truck Application)	5-26
5.15	Mass and Energy Balance for ATCD with Dual Stirling Engines Using Heat Pipes (High Temperature Case for Truck Application)	5-27
5.16	Mass and Energy Balance for ATCD with Dual Stirling Engines Using Heat Pipes (Low Temperature Case for Truck Application)	5-28

5.17	Stirling Engine Performance Summary for Truck Application	5-29
5.18	Performance of System with Subposed Stirling Engines for Truck Application	5-30
5.19	Mass and Energy Balance for ATCD with Stirling Engines Using Heat Pipes (Reference Case for Locomotive Application)	5-31
5.20	Mass and Energy Balance for ATCD with Dual Stirling Engines Using Heat Pipes (Reference Case for Marine Application)	5-32
5.21	Performance of System with Subposed Stirling Engines for Marine Application	5-33
5.22	Performance of Selected Systems for Three Applications	5-34
6.1	Summary Table Diesel Heat Recovery Unit Characteristics	6-6
6.2	Common Organic Rankine Cycle Heat Recovery Unit Overall Characteristics	6-9
6.3	Common Organic Rankine Cycle Heat Recovery Unit Stage Characteristics	6-10
6.4	Common Steam Injection Cycle Heat Recovery Unit Overall Characteristics	6-13
6.5	Common Steam Injection Cycle Heat Recovery Unit Stage Characteristics	6-14
6.6	Common Stirling Cycle Heat Recovery Unit Recovery Unit Overall Characteristics	6-17
6.7	Common Stirling Cycle Heat Recovery Unit Stage Characteristics	6-18
6.8	Estimated Price for Heat Recovery Fluid Bed Organic Rankine	6-19
6.9	Estimated Price for Heat Recovery Fluid Bed Steam Injection	6-20
6.10	Estimated Price for Heat Recovery Fluid Bed Stirling Engine	6-21

8.1	Summary of Rankine Bottoming Cycle Component Costs for Adiabatic Diesel-Heavy Duty Truck Application	8-2
8.2	Summary of Rankine Bottoming Cycle Component Costs for Adiabatic Diesel - Locomotive Application	8-3
8.3	Summary of Rankine Bottoming Cycle Component Costs for Adiabatic Diesel - Marine Application	8-4
8.4	Summary of Steam Injection Cycle Component Costs for Adiabatic Diesel - Heavy Duty Truck Application	8-5
8.5	Summary of Steam Injection Cycle Component Costs for Adiabatic Diesel - Locomotive Application	8-6
8.6	Summary of Steam Injection Cycle Component Costs for Adiabatic Diesel - Marine Application	8-7
8.7	Summary of Stirling Engine Cycle Component Costs for Adiabatic Diesel - Heavy Duty Truck Application	8-8
8.8	Summary of Stirling Engine Cycle Component Costs for Adiabatic Diesel - Locomotive Application	8-9
8.9	Summary of Stirling Engine Cycle Component Costs for Adiabatic Diesel - Marine Application	8-10
8.10	NASA Reference Economic/Operational Data Diesel Engines	8-13
8.11	NASA Reference Simple Payback Period Turbocharged + RC-1 Bottoming vs Turbocompound-Aftercooled Truck Application	8-14
8.12	NASA Reference Simple Payback Period Turbocharged + Steam Injection vs Turbocompound-Aftercooled Truck Application	8-15
8.13	NASA Reference Simple Payback Period Turbocharged + Stirling Engine vs Turbocompound-Aftercooled Truck Application	8-16
8.14	NASA Reference Simple Payback Period Turbocharged + RC-1 Bottoming vs Turbocompound-Aftercooled Locomotive Application	8-17
8.15	NASA Reference Simple Payback Period Turbocharged + Steam Injection vs Turbocompound-Aftercooled Locomotive Application	8-18

8.16	NASA Reference Simple Payback Period Turbocharged + Stirling vs Turbocompound-Aftercooled Locomotive Application	8-19
8.17	NASA Reference Simple Payback Period Turbocharged + RC-1 Bottoming vs Turbocompound-Aftercooled Marine Application	8-20
8.18	NASA Reference Simple Payback Period Turbocharged + Steam Injection vs Turbocompound-Aftercooled Marine Application	8-21
8.19	NASA Reference Simple Payback Period Turbocharged + Stirling Engine vs Turbocompound-Aftercooled Marine Application	8-22
8.20	Summary of Simple Payback Period (Yrs)	8-23
B1	Turboexpander Data for Steam Injection Cycle	B-4
B2	Planetary Gearboxes for Steam Injection System	B-5
F1	Turbine Data for Organic Rankine Cycle with RC-1	F2
F2	Planetary Gearbox Data for Organic Rankine Cycle with RC-1	F3
G1	Scaling of Stirling Engines	G2
G2	Planetary Gearboxes for Stirling Engines	G3

1. SUMMARY AND CONCLUSIONS

A preliminary conceptual design study was conducted to evaluate the potential of utilizing fluidized bed heat exchangers in place of conventional counter-flow heat exchangers for heat recovery from adiabatic diesel engine exhaust gas streams.

The advantages of utilizing fluidized bed heat exchangers for exhaust gas heat recovery are increased heat transfer coefficients and the potential to operate reliably with highly depositing exhaust gases. In contrast with the counterflow heat exchanger, however, the fluidized bed is a uniform temperature device. This has implications on the practical limits of heat recovery achieved vs. the desired power cycle operating temperature; and typically requires a multi-stage approach for the fluidized bed system design.

Fluidized bed heat recovery systems were evaluated in three different heavy duty transport applications: heavy duty diesel truck, diesel locomotive, and diesel marine pushboat. The three applications are characterized by differences in overall power output and related annual utilization as follows:

<u>Application</u>	<u>Horsepower</u>	<u>Utilization (hphr/rated x 8760)</u>
Truck	373 hp	* 12%
Locomotive	3600 hp	63%
Pushboat	5600 hp	71%

$$* \text{ Truck hphr} = \frac{\text{annual gallons} \times \text{fuel density}}{\text{specific fuel consumption}}$$

For each application, the exhaust gas source is a turbocharged-adiabatic diesel core. Representative subposed exhaust gas heat utilization power cycles were selected for conceptual design efforts including design layouts and performance estimates for the fluidized bed heat recovery heat exchangers. The selected power cycles were: Organic Rankine with RC-1 working fluid, Turbocompound Power Turbine with Steam Injection, and Stirling Engine.

In general, the heat recovery heat exchanger designs consist of two stages of fluidized beds with in-bed and above-bed tubes, followed by a final convective heat exchanger stage. The diesel exhaust gases enter the first fluid bed stage such that a mode of turbulent fluidization is maintained and at a temperature sufficiently high to minimize sticky soot particle deposits. The second stage fluid bed operates at lower gas temperature and removal of deposits formed on the heat exchanger tubes and bed particles is promoted by the churning and circulating motion of the bed particles. For the maximum heat recovery desired in power cycle applications, a finned-tube convective section is needed above the low temperature fluid bed and serves as the final heat recovery stage.

The subposed Rankine power cycle consisted of a closed loop system with the RC-1 working fluid vaporized in the heat recovery heat exchanger and expanded through an auxiliary turbine unit that is geared to the diesel output shaft. The expanded vapor is condensed in a heat rejection heat exchanger (condenser).

The Turbocompound Power Turbine with Steam Injection power cycle was an open cycle system with steam generated in the heat recovery heat exchanger and then injected (mixed) into the exhaust gas stream for expansion through both the turbocharger turbine and the downstream turbocompound power turbine. The power turbine is geared to the diesel output shaft. The power output of both turbines is increased due to the increased mass flow rate.

The Stirling Engine power cycle is unique in that the heat recovery heat exchanger does not include any convective section. Heat is recovered in a series of two fluidized bed stages; each stage being coupled to its own dedicated Stirling engine via a heat pipe. The operating temperature of the two Stirling engines differs according to the series arrangement of the fluid beds.

For the truck and locomotive applications, the heat rejection required for the Rankine and Stirling systems is accomplished via air cooled heat exchangers (radiators). The considerable amount of water required for the Turbocompound Power Turbine with Steam Injection cycle is carried in an onboard tank. In the marine pushboat application, river water is utilized to meet cycle cooling requirements as well as the water supply needs of the steam injection cycle.

The study results indicate that use of an exhaust gas heat recovery power cycle produces a 5 to 11 percent improvement in specific fuel consumption over that of a reference turbocompound/aftercooled engine system. The magnitude of the improvement depends on the particular power cycle configuration.

The fuel economy results were used in conjunction with capital cost estimates and fuel price data to determine payback times for the various cases. These were based on simple payback assumptions without considerations of maintenance burdens or the cost of money. The results show a wide range of payback times (1.2 to 15.4 years) depending on the power cycle and application. For all power cycles, payback was faster in the marine and locomotive applications than in the truck application.

For the truck application, a specific comparison was made of the multi-stage fluidized bed heat recovery system including final convective stage vs. a conventional counterflow heat exchanger. For equal heat transfer duty, the fluidized bed system was approximately one-third larger, heavier, and more costly. A review of the cost estimates indicated that approximately two-thirds of the overall cost in the fluidized bed approach is associated with the final convective stage.

A number of conclusions may be drawn from the results of the study:

1. The fluidized bed approach to diesel exhaust gas heat recovery is feasible for a range of heavy duty transport applications.

2. The multi-stage approach, including a final convective heat exchanger stage, impacts the size, weight, and cost of the overall heat recovery system.

3. The size and weight implications of the fluidized bed systems make them relatively more attractive for the larger locomotive or marine applications with greater annual utilization.

4. Future studies should include system performance and cost tradeoffs that would eliminate the use of a final convective heat exchanger stage in series with the fluidized beds.

5. Future payback calculations should include maintenance burdens and cost of money considerations.

6. The particulate removal characteristics projected for the fluidized bed systems make them relatively more attractive for use in large systems utilizing heavy fuels.

7. Experimental programs are needed to definitize the diesel particulate removal characteristics of the fluidized bed systems by agglomeration and/or by in-bed catalytic combustion.

2. INTRODUCTION

Over the past decade, spurred by significantly increased fuel costs, the Department of Energy has supported technology efforts for development of efficient engine systems for heavy duty transport. The adiabatic diesel engine concept offers substantial improvements in engine efficiency through reduced heat loss. Characteristic of the adiabatic diesel is an increased exhaust gas temperature that also affords the opportunity for engine turbocharging and turbocompounding coupled with exhaust gas heat recovery to further improve fuel economy. Cost effective systems for heat recovery are required however to realize any commercial benefits of the compound engine systems.

The purpose of this study is to evaluate the application of a fluid bed heat exchanger for heat recovery from adiabatic diesel engines. Various thermodynamic cycles for convecting heat recovered to work are explored and defined for three specific diesel engine applications; heavy duty truck, railroad locomotive and marine vessel. For each application three different compound engine configurations are defined that include the primary adiabatic diesel coupled with a selected subposed cycle that utilizes a fluid bed heat exchanger system. The design and operating parameters of the primary diesel engines (heavy duty truck) were provided by NASA Lewis, Table 2.1. NASA also provided the basis for correcting the diesel engine performance for changes in exhaust pressure associated with the application of the subposed cycle, Table 2.2.

Preliminary thermodynamic screening evaluations were conducted to define attractive candidate subposed cycle configurations, Table 2.3. From these studies and in consultation with cognizant NASA technical personnel, three specific heat recovery systems (Organic Rankine, Steam Injection and Stirling Engine) were selected for conceptual design and

economic evaluation for each of the three identified applications (truck, locomotive and marine). The scope of this effort has included detailed thermodynamic definition, the conceptual design of the fluid bed heat exchanger including weight and costs and the identification of subsystem components and estimation of their size, weight and cost. Also, for each application and subposed cycle, a conceptual arrangement drawing is provided to show overall physical size and identify possible equipment packaging within defined constraints. A preliminary economic assessment is made based on simple payback period assuming fuel costs, engine duty and annual production requirements.

Table 2.1
ADIABATIC DIESEL ENGINE DESIGN POINT DATA

Code	ATCD/A	ATCD	ATCPD/A	ATCPD
N - rpm	1900	1900	1900	1900
Gas Flow Rate - lb/min	47.6	48.1	48.2	47.9
Turbine Inlet Temp. - °F	1290	1440	1380	1575
Turbine Outlet Temp. - °F	1120	1240	1055	1140
Power - hp	320	318.5	340	335
SFC - lb/hphr	0.310	0.315	0.293	0.297
Air/Fuel Ratio	27.8	28.9	29.0	28.9

where ATCD/A: Adiabatic Turbocharged Diesel/Aftercooled
 ATCD: Adiabatic Turbocharged Diesel
 ATCPD/A: Adiabatic Turbocompound Diesel/Aftercooled
 ATCPD: Adiabatic Turbocompound Diesel

Table 2.2
EXHAUST PRESSURE CORRECTIONS FOR ENGINE PERFORMANCE

$$\text{Corrected SFC} = \text{SFC} + 0.04 * (P/P)_{\text{exh}}$$

$$\text{Corrected POWER} = \text{POWER} / (1 + 0.129 * (P/P)_{\text{exh}})$$

$$\text{Corrected Temp.} = \text{Temp.} + T$$

$$T = 1018.9 * (1 - 1 / (1 + 0.129 * (P/P)_{\text{exh}}))$$

Table 2.3
CANDIDATE BOTTOMING CYCLES EVALUATED IN TASK 1 SCREENING

<u>Bottoming Cycle</u>	<u>Engine Type</u>			
	ATCD/A	ATCD	ATCPD/A	ATCPD
Organic				
Rankine	X	-	X	-
Water				
Rankine	X	-	X	-
Steam Injection	X	X	NA	NA
Air				
Open Brayton				
Simple	X	X	-	-
Recuperated	X	-	-	-
Intercooled	X	-	-	-
Helium				
Closed Brayton	X	X	-	-
Stirling	X	X	-	-

3. BACKGROUND

3.1 Diesel Engine Application With Heat Recovery

The application of engine compounding with the adiabatic truck diesel has been studied for some limited subposed cycles. The Thermo Electron Corporation(1) has evaluated the organic Rankine cycle using an RC-1 (60 mole percent pentafluorobenzene and 40 mole percent hexafluorobenzene) working fluid. Their work has included stability studies of the RC-1 fluid at cycle conditions and system design and economic analysis premised on a 300 horsepower reference diesel engine. The heat recovery unit consisted of a separate vapor generator and condenser-regenerator modules. Subsystem components including the feed pump, turbine expander, filters, boost pump and gearbox were identified, sized and costed. This study has served as a primary reference and comparison where the vapor generator is replaced with the fluid bed heat exchanger unit. Reference 2 summarizes the economic findings from current program studies that featured subposing Rankine and Brayton cycles with the reference truck diesel engine but using other than fluid bed heat exchanger systems. These screening studies indicate that improved fuel economy can be realized but that these power cycles may not be competitive on an economic payback basis.

Most of the railroad locomotives used in the United States today are powered by turbocharged Diesel engines. Reference 3 is a study evaluating alternative fuels and engines for railroad locomotives. As part of this study, two diesel base engines of 3000 hp are evaluated for costs and fuel economy. These reference engines are compared with other diesel alternatives including two adiabatic engine cases with turbocompounding that used either the Stirling or Rankine subposed cycle heat recovery. It is concluded that if the adiabatic diesel engine can

be adapted to locomotive service, the fuel savings will be impressive (26%) and that the addition of the bottoming cycle further enhances fuel economy. Annualized life cycle cost comparisons were made but involved alternative fuels that did not permit a direct comparison with the standard locomotive diesel engine.

A third study (Reference 4) used as a primary reference in the current work describes the application of a Rankine bottoming cycle to a 5600 hp marine diesel engine. The study includes a preliminary design of the bottoming cycle, performance projections, diesel engine interface and power coupling options, component and system costs, preliminary economics and market assessment and a demonstration program plan. This study projects significant economic and fuel saving benefits utilizing the Rankine Bottoming Cycle (RBC) in marine push-tow boat industry. It was identified that the only major obstacles to RBC implementation on some ships are its large weight and space requirements.

3.2 Fluidized Bed Characteristics in Heat Recovery Applications

Fluidized beds display several characteristics making them uniquely suitable for dirty, corrosive, high-temperature, fouling gas heat recovery applications:

(1) fluidized beds promote very high heat transfer coefficients to heat transfer surfaces immersed in them

(2) their high rates of thermal mixing protect tube materials from excessively high metal temperatures experienced at the hot end of many high-temperature heat recovery applications

(3) proper selection of particle characteristics and operating conditions can result in a self-cleaning behavior for tube deposits

(4) some depositing gases, diesel exhausts being prime examples, will form flaky deposits on bed particles and tubes that drop off, retaining a relatively large, agglomerated form suitable for efficient downstream collection

(5) gas cleaning functions can be integrated into the fluid bed heat recovery by the addition of appropriate sorbents, getters and catalyst particles or other reactants to the bed

(6) their high rates of thermal mixing means that in some applications where the working fluid temperature approaches the hot gas temperature either staging of the fluid bed or the use of a convective heat recovery section is required

(7) fluid beds can be arranged in a variety of staged configurations yielding efficient heat recovery.

The physics of fluidization has been a topic of great academic and industrial activity over the past 50 years and much fundamental and practical information is now available. The nature of fluidized beds has been closely related to the behavior of gas voids passing through the bed and the motion that these voids impart to the particles in the bed. The high rates of particle mixing, the high rates of heat transfer to objects immersed in a fluid bed, the nature of gas and particle contacting, particle elutriation, particle attrition, and many other features of fluidized beds have been correlated to the bubbling nature of the bed. In turn, the bubbling nature relates directly to the properties of the particles and the gas, and, to a smaller extent, to the vessel and its internals design. Nonetheless, the design of industrial fluidized beds, a technology widespread in the process industries, is still largely empirical and is hindered by a variety of uncertainties. The greatest uncertainties relate to the scaleup of fluid bed processes from laboratory scale equipment to commercial scale equipment. In the diesel heat recovery application under consideration in this program the scaling factor for the available design basis is quite small and scaleup is not a major problem.

In the specific area of heat recovery, fluidized beds have been under consideration for many applications, and some commercial fluid bed heat recovery systems are being marketed. Applications for stationary waste heat recovery, waste heat disposal, thermal energy storage, and

solids heating or cooling have been proposed or are under development. For example, highly fouling liquid fluidized bed heat exchangers have been successfully applied and look promising for many difficult applications.⁽⁵⁾

High-temperature, stationary fluid bed heat recovery development has been proceeding under DOE support of both the Thermal Electron Corporation and Aerojet Liquid Rocket Company. The Thermal Electron Corporation fluid bed concept uses two very shallow fluid bed stages, one to remove high-temperature heat from the waste stream and the other to preheat combustion air.⁽⁶⁾ The fluid bed particles are mechanically circulated between the two beds and no internal heat transfer surfaces are placed in the beds. The Aerojet fluid bed heat recovery system uses a relatively deep bed containing a row of horizontal finned tubes.^(6,7) A brush system is used to clean the underside of the distributor plate of deposits, as in the commercial Stone-Platt technology. The largest technical hurdle for both of these high-temperature applications seems to be the fabrication of an economical distributor plate for the high-temperature environment.

A two-stage, shallow fluid bed heat recovery unit (a Stone-Platt unit) was evaluated for use with diesel engine exhaust gases by the United Technologies Research Center under DOE sponsorship.^(8,9) No testing was performed under actual diesel exhaust conditions. Commercially, the Stone-Platt Fluidfire Company (UK) appears to be the world leader in fluid bed heat recovery.^(10,11) Two U.S. companies, Granco Equipment Company, Grand Rapids, Michigan and Fennell Corporation, Harvey, Illinois are licensees for the technology. The Fluidfire units are stationary units of multiple shallow bed design with internal heat transfer surface. The Econo-Therm Corporation also markets a fluid bed heat recovery unit based on raining fluid bed technology, requiring no heat transfer surface, but requiring continuous circulation of solids between two vessels.⁽¹²⁾ Related technology development in fluidized bed combustion and other fluidized bed heat transfer applications have

provided some valuable input for stationary heat recovery system development.

Some applications of fluidized bed combustion to transportation uses (marine) have been under development by the Japanese⁽¹³⁾ where effects of ship motion on the fluidization has been evaluated. Again, Stone-Platt seems to be a leader in the marine application of fluidized bed diesel engine heat recovery, having built a fully operational unit for Shell International Marine Ltd.⁽¹⁴⁾ The 2000 kW unit consists of three independent beds using mechanical cleaning of the distributor plate. Stone-Platt have identified design solutions for the impact of ship roll and pitch on the fluidization performance. Marine applications are also under study by various U.S. agencies.

Applications of fluidized bed to small diesel engine heat recovery has been under study by an Italian university team for Fiat.^(15,16) A conventional 60 kW diesel test engine has been operated with a fluid bed heat recovery unit, and it was observed that a specially designed diesel exhaust gas distributor functioned well in its hot condition with limited deposits. It was also determined that diesel exhaust deposits would not form on a surface with a temperature greater than about 900 °F. Significant deposits did form on heat transfer surfaces in the bed during operation which led to only a limited reduction in heat recovery effectiveness. These deposits could be easily removed by periodic thermal cycling of the tubes.

4. COMPOUND ENGINE CONFIGURATION SCREENING

Cycle screening evaluations were carried out on the following adiabatic diesel compound engine configurations

- o Organic Rankine cycle
- o Steam Rankine cycle
- o Turbocompound with steam injection
- o Open Brayton cycle
- o Closed Brayton cycle
- o Stirling engine

The results of these screening tests are presented in the following text.

4.1 Organic Rankine Cycle

4.1.1 FLUORINAL-85 (F-85) Working Fluid

A series of preliminary performance calculations were made for organic Rankine bottoming cycles to determine the effect of throttle conditions, regenerative feedheating, and adiabatic engine configuration with FLUORINAL-85 (F-85) as the working fluid. Figures 4.1 and 4.2 show cycle schematics. The results of these calculations are summarized by the first four cases given in Table 4.1. These results indicate that the ATCPD/A engine configuration (Case 4) with throttle conditions corresponding to the maximum recommended working temperature of F-85, i.e. 600°F, and regenerative feedheating would give the best system performance.

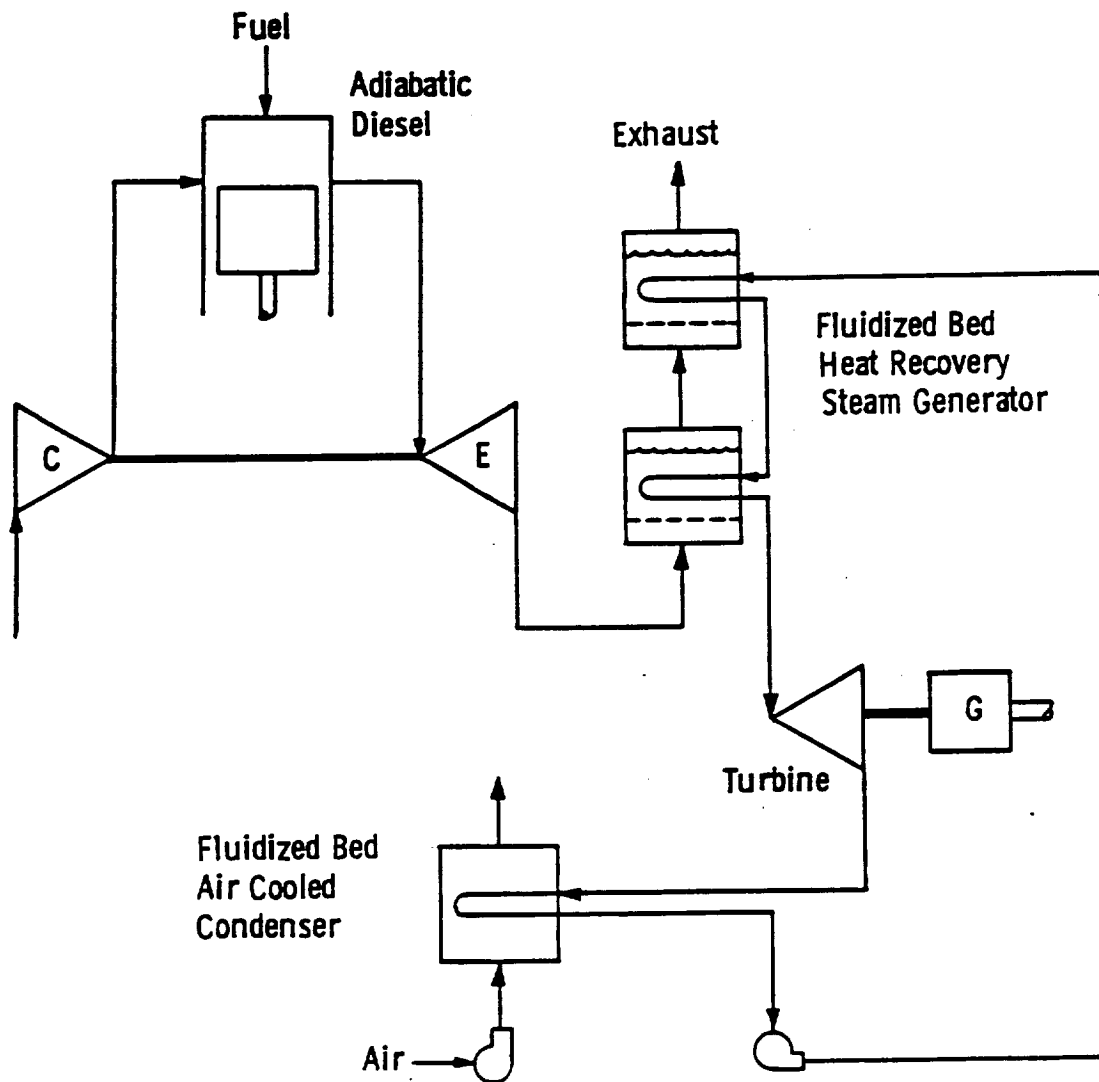


Fig. 4. 1-Turbocharged diesel with subposed organic Rankine cycle.

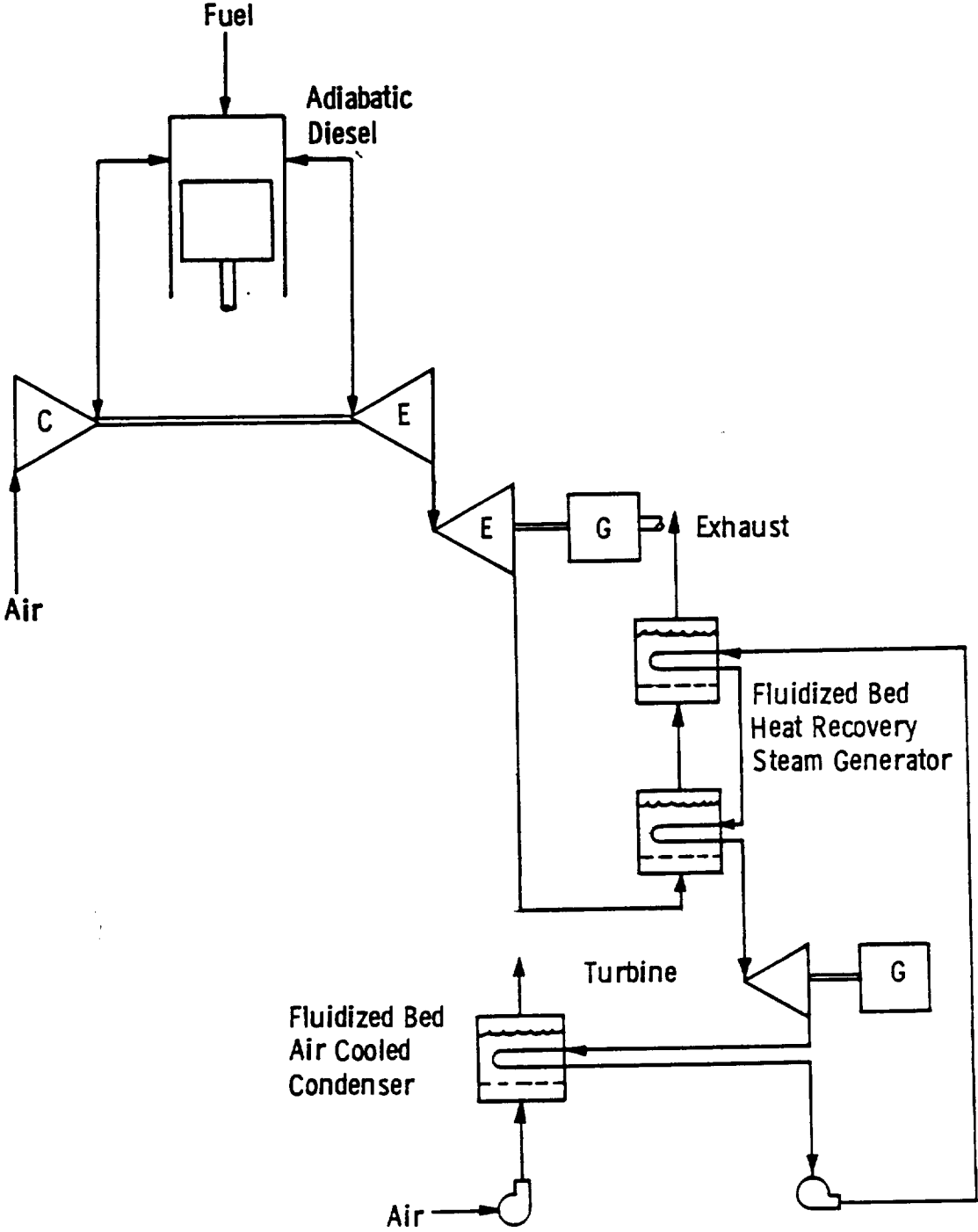


Fig. 4-2—Turbocompound diesel with subposed organic Rankine cycle.

Table 4.1
 PERFORMANCE SUMMARY OF ADIABATIC DIESEL ENGINE WITH
 ORGANIC RANKINE BOTTOMING CYCLE

Case	1	2	3	4	5
	ATCD/A			ATCPD/A	ATCD
Engine Configuration	<— Turbocharged —>			Turbocompound	
Working Fluid	F-85 —————>			RC-1	
$(\Delta P/P)_{hx}$	0.05 —————>			0.03	
Corr. $(T_{exh})_{ad}$ - °F	1126.5 —————>			1061.5	1245
Corr. Eng. Power - hp	318 —————>			338	317.1
Corr. Eng. SFC - lb/hphr	0.312 —————>			0.295	0.316
P_{throt} - psia	300	700	—————>	—————>	800
T_{throt} - °F	550	600	—————>	—————>	750
T_{cond} - °F	160	—————>	—————>	—————>	135
$(\Delta T_{pinch})_{hx}$ - °F	75	—————>	—————>	—————>	30
$(\Delta T_{approach})_{hx}$ - °F	75	75	75	75	150
Regenerative Heater	No	No	Yes	No	Yes
T_{stack} - °F	410	420	480	430	347
Working Fluid Flow Rate - lb/s	0.513	0.500	0.598	0.450	
Gross Pwr - hp	29.7	34.0	40.7	30.8	62.4
Pump Pwr - hp	0.7	1.5	1.8	1.3	6.2
Net Pwr - hp	29.00	32.5	38.9	29.3	56.2
System Performance					
Power	346.6	350.5	356.9	367.3	373.3
SFC - lb/hp hr	0.286	0.283	0.278	0.271	0.269
PIF Note 1	1.0194	1.0309	1.0497	1.0803	1.098

(1) Relative to ATCPD/A Engine Configuration, PIF is Performance Improvement Factor

In all of these four cases, two stages of fluidized bed were used. As indicated in Section 3, deposition problems in the distributor plate of the second bed are expected to be minimized if the temperature of the first bed is maintained equal to or greater than 900°F. The temperature profile for the Case 3 cycle conditions with a first stage bed temperature of 900°F ($\Delta T_{\text{approach}} = 300^\circ\text{F}$) and a $\Delta T_{\text{pinch}} = 75$ is shown in Figure 4.3. This gives a stack temperature of 530°F. The actual Case 3 temperature profile is shown in Figure 4.4 where no constraint is placed on the first bed temperature and the ΔT_{pinch} and $\Delta T_{\text{approach}}$ are both 75°F. The resultant stack gas temperature is 480°F. This shows that the organic Rankine subposed cycle system performance is significantly affected by the $\geq 900^\circ\text{F}$ constraint on the first bed temperature.

4.1.2 RC-1 - Working Fluid

Performance calculations were also made for a subposed organic Rankine cycle using RC-1 (60 mole percent pentafluorobenzene and 40 mole percent hexafluorobenzene) as the working fluid. RC-1, which has a maximum recommended working temperature of 750°F, was used by the Thermo Electron Corporation in Reference 1. In addition it was determined that the use of a convective third stage in the heat exchanger would eliminate the performance penalty imposed by the $\geq 900^\circ\text{F}$ constraint on the temperature of the first bed in the two stage design.

The design conditions and the performance of the RC-1 cycle with two fluidized bed stages and a convective third stage are shown in Case 5 of Table 4.1. The profile of the heat exchanger is shown in Figure 4.5. The ATCD engine configuration was used to match the conditions used by TECO in Reference 1. The performance which results is only slightly better than Case 4 with engine configuration ATCPD/A and no regenerative feedheater. This indicates that the performance with F-85 working fluid, engine configuration ATCPD/A, a regenerative feedheater, and a two-stage fluidized bed heat exchanger with the first stage bed temperature equal to 900°F might be competitive with RC-1 working fluid,

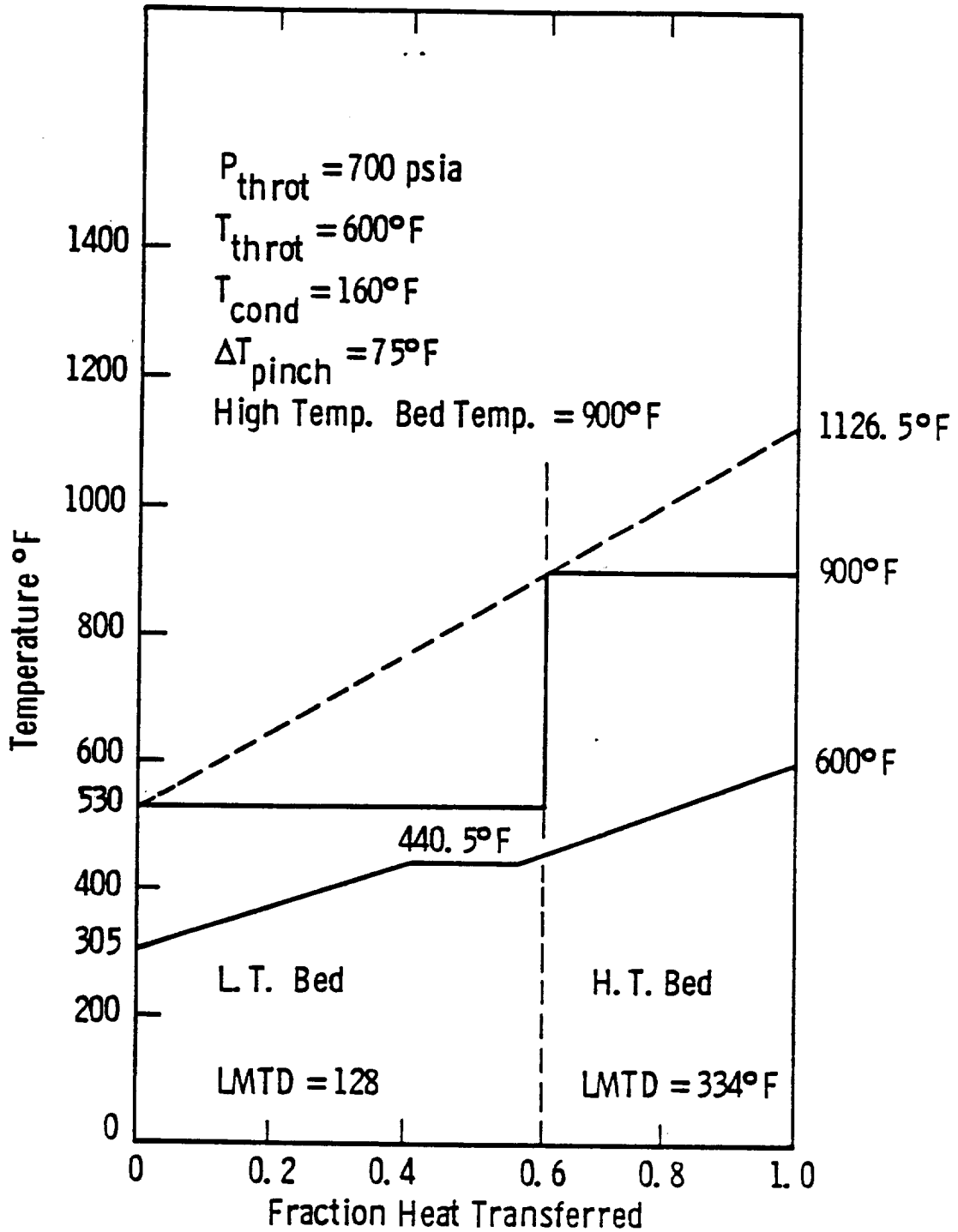


Fig. 4. 3—Fluidized bed heat exchanger temperature profile, organic Rankine cycle with regenerative feed heating

Curve 749101-A

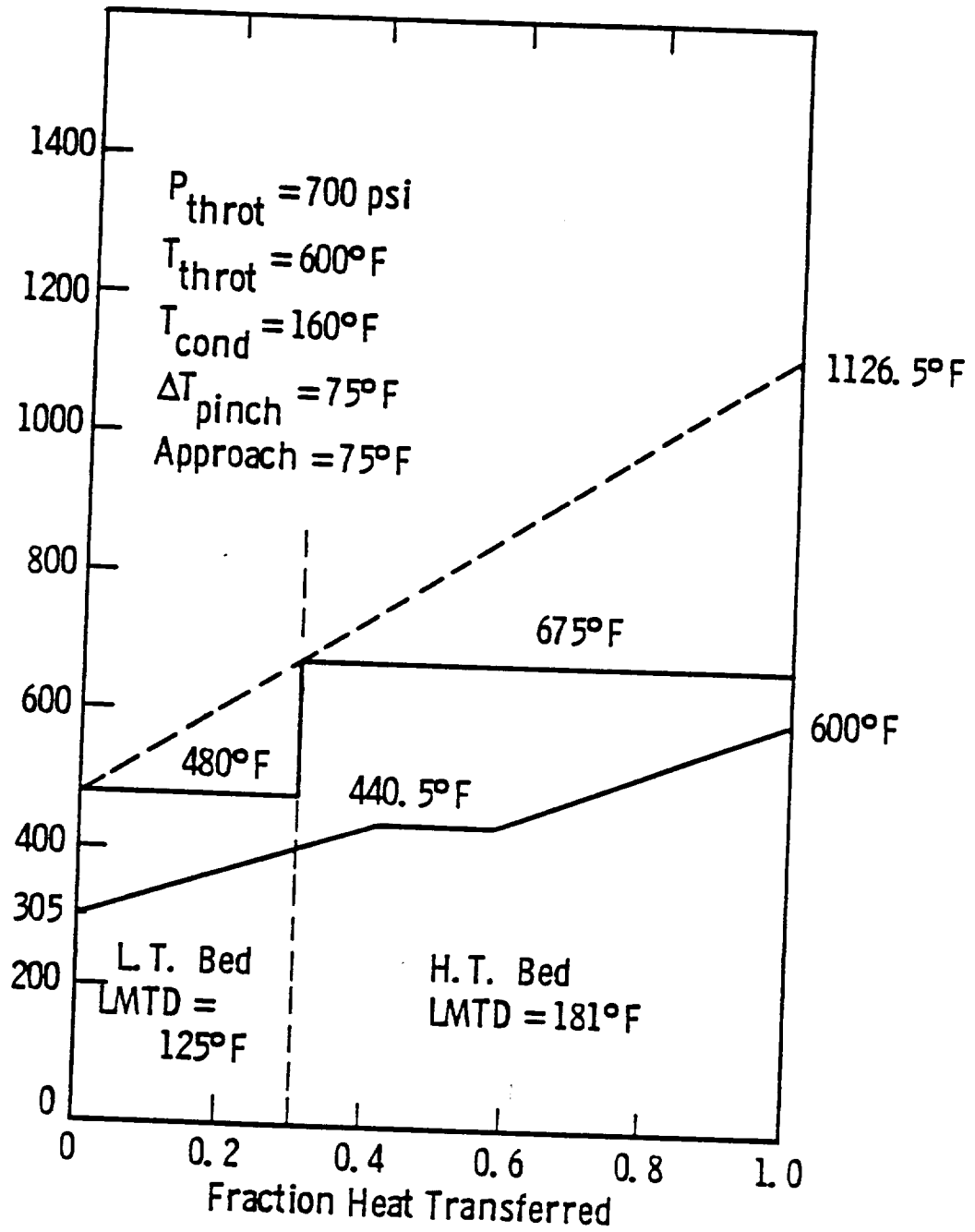


Fig. 4.4—Fluidized bed heat exchanger temperature profile, organic Rankine cycle with regenerative feed heating

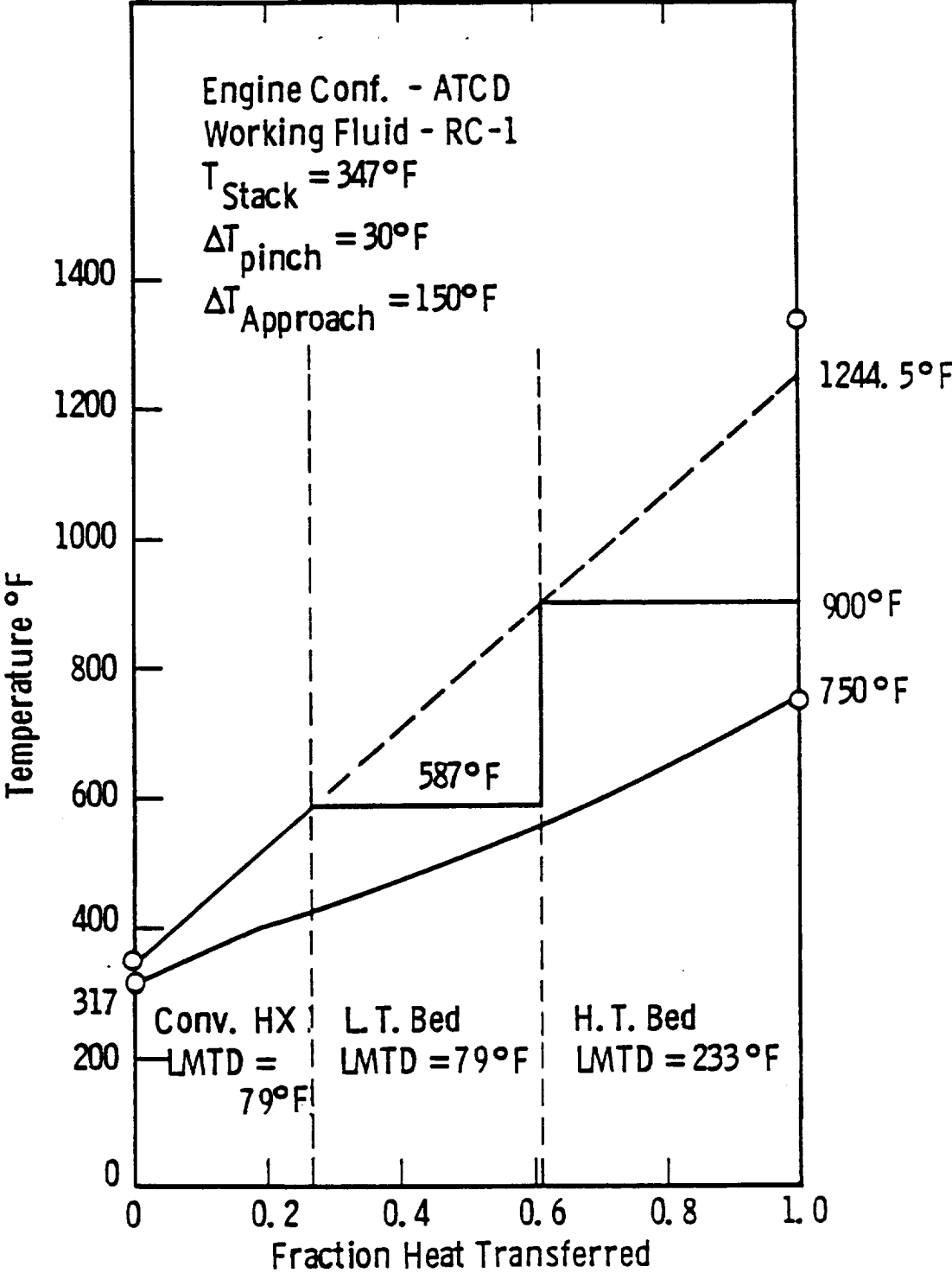


Fig. 4.5—Fluidized bed heat exchanger temperature profile, organic Rankine cycle

engine configuration ATCD, a regenerative feedheater, and the three stage heat exchanger.

4.2 Steam Rankine Cycle

A series of preliminary performance calculations were made for steam Rankine bottoming cycles to determine the effect of throttle conditions, heat exchanger temperature differences, and adiabatic engine configuration. Figures 4.6, and 4.7 show cycle schematics. A two-stage fluidized bed heat exchanger was assumed for all cases. The results of these calculations are summarized in Table 4.2. These results show that system performance is a weak function of throttle conditions and heat exchanger pinch temperature difference. The adiabatic engine configuration is, however, shown to have a significant effect on the performance of the steam Rankine bottoming cycle.

Examination of Figure 4.8 shows that increasing the first stage fluidized bed temperature to 900°F while keeping the pinch temperature difference constant would have no effect on the system performance. It would, however, have a significant effect on the log mean temperature differences (LMTD) of the two beds. For the high temperature bed, the LMTD would increase and that for the low temperature bed would increase so that the changes in bed surface area would tend to balance.

4.3 Turbocompound Engine With Steam Injection

A series of preliminary performance calculations were made for the system shown in Figure 4.9 where the steam is injected between the compressor drive expander and the power expander of a turbocompound engine and the fluidized bed heat exchanger has two stages. The results of these calculations are summarized in Table 4.3. Turbocharged engine performance corrected for back pressure was used to simulate the turbocompound engine. Cases 1 through 3 show that the performance of the system with an after cooler improves significantly with increasing injection pressure. Comparing Cases 1 and 4 shows that the use of an

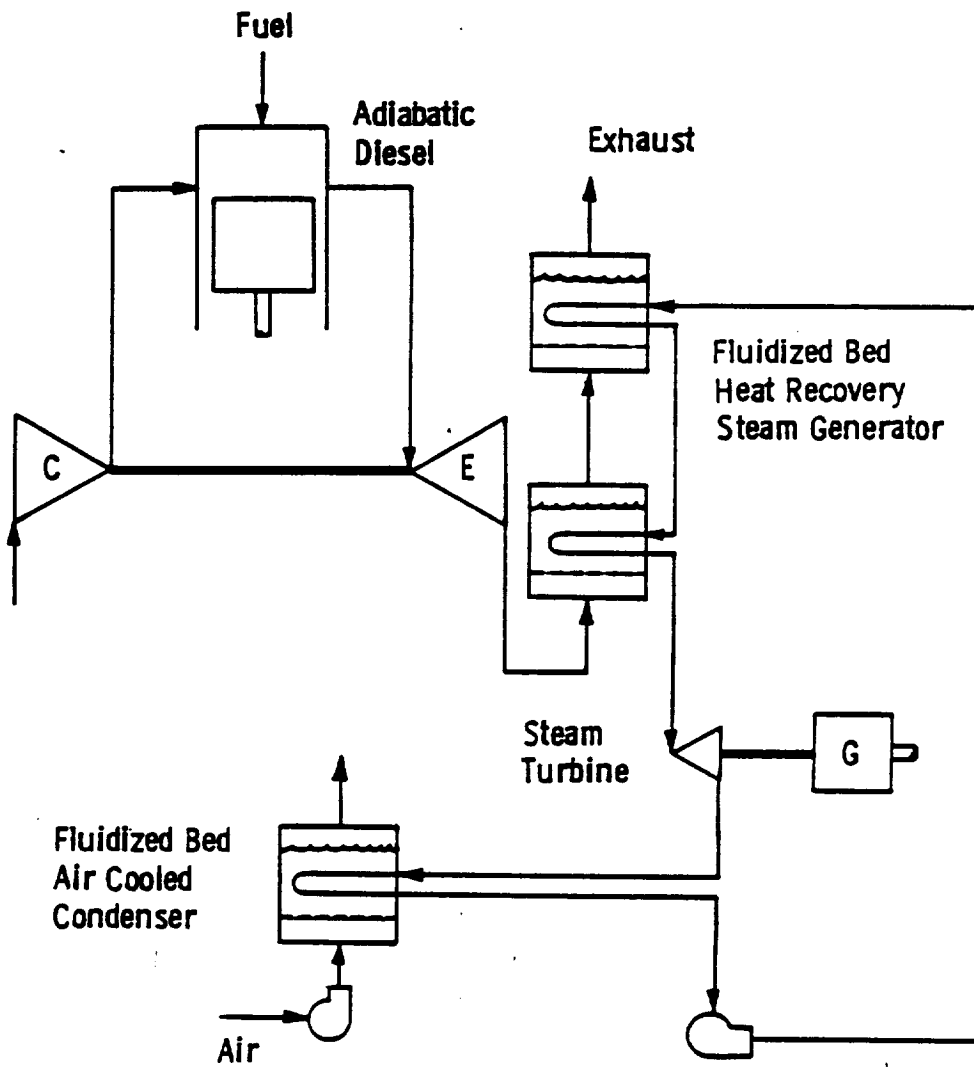


Fig. 4. 6—Turbocharged diesel with subposed steam Rankine cycle.

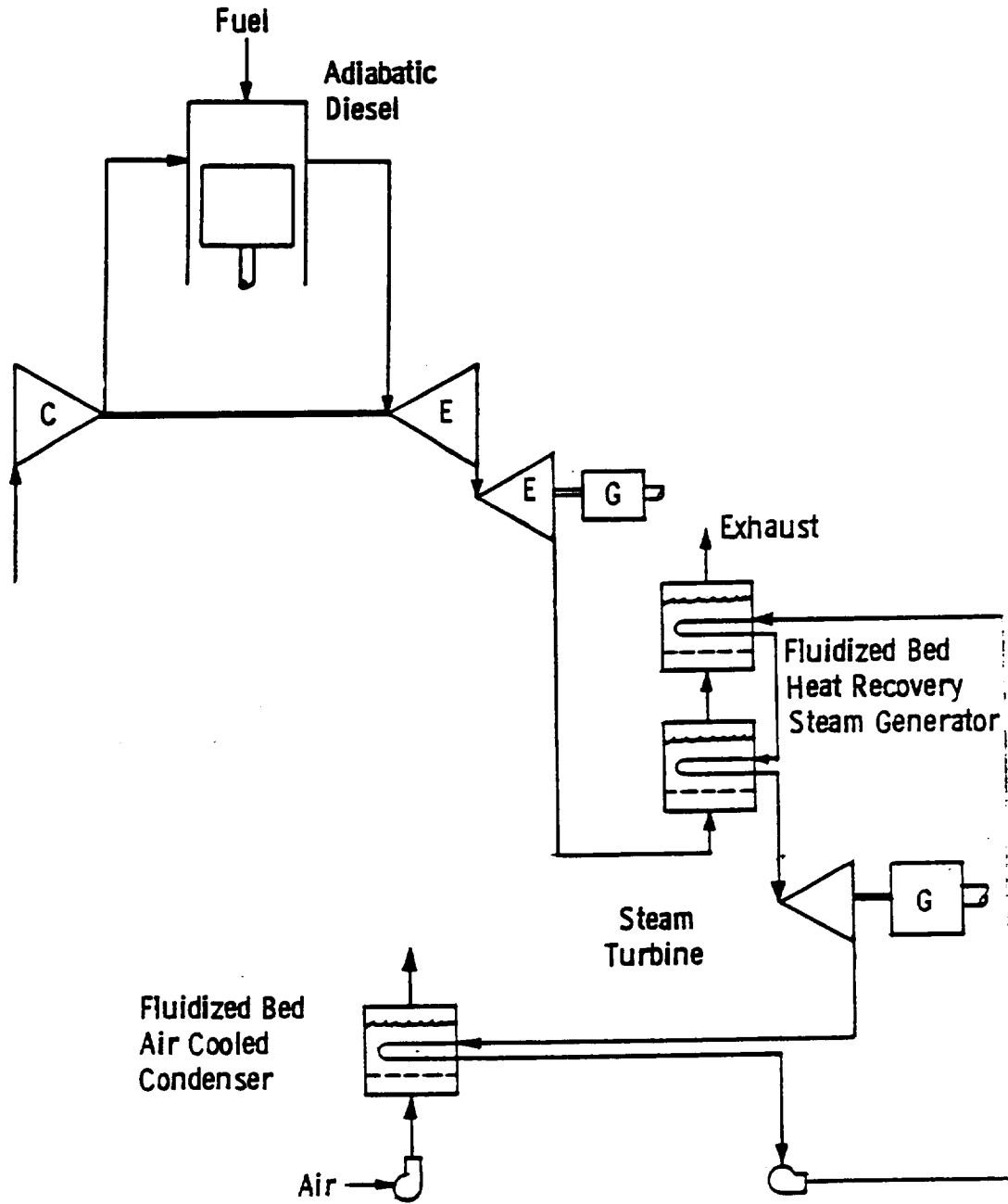


Fig. 4. 7— Turbocompound diesel with subposed steam Rankine cycle.

Table 4.2
 PERFORMANCE SUMMARY OF ADIABATIC DIESEL ENGINE WITH
 STEAM RANKINE BOTTOMING CYCLE

Case	1	2	3	4	5
Engine Configuration	ATCD/A	—————>	—————>	—————>	ATCPD/A
$(\Delta P/P)_{hx}$	0.05	—————>	—————>	—————>	—————>
$(T_{exh})_{ad} - ^\circ F$	1126.5	—————>	—————>	—————>	1061.5
Corr. Eng. Power - hp	318.0	—————>	—————>	—————>	338.0
Corr. Eng. SFC - lb/hp hr	0.312	—————>	—————>	—————>	0.295
$P_{throt} - psia$	200	300	—————>	400	300
$T_{throt} - ^\circ F$	900	800	—————>	700	800
$T_{cond} - ^\circ F$	160	160	—————>	—————>	—————>
$(\Delta T_{pinch})_{hx} - ^\circ F$	150	150	100	—————>	150
Approach - $^\circ F$	50	—————>	—————>	—————>	—————>
$T_{stack} - ^\circ F$	532	567	517	545	567
Steam Flow Rate - lb/s	0.0934	0.0933	0.0998	0.1000	0.0819
Gross Power - hp	33.5	33.1	35.4	34.8	29.1
Pump Power - hp	0.2	0.2	0.2	0.3	0.2
Net Power - hp	33.3	32.9	35.2	34.5	28.9
System Performance					
Power - hp	351.3	350.9	353.2	352.5	366.0
SFC - lb/hp hr	0.282	0.283	0.281	0.282	0.272
PIF, Note 1	1.105	1.104	1.111	1.109	1.0792

(1) Relative to ATCPD/A Engine Configuration, PIF is Performance Improvement Factor

Curve 749106-A

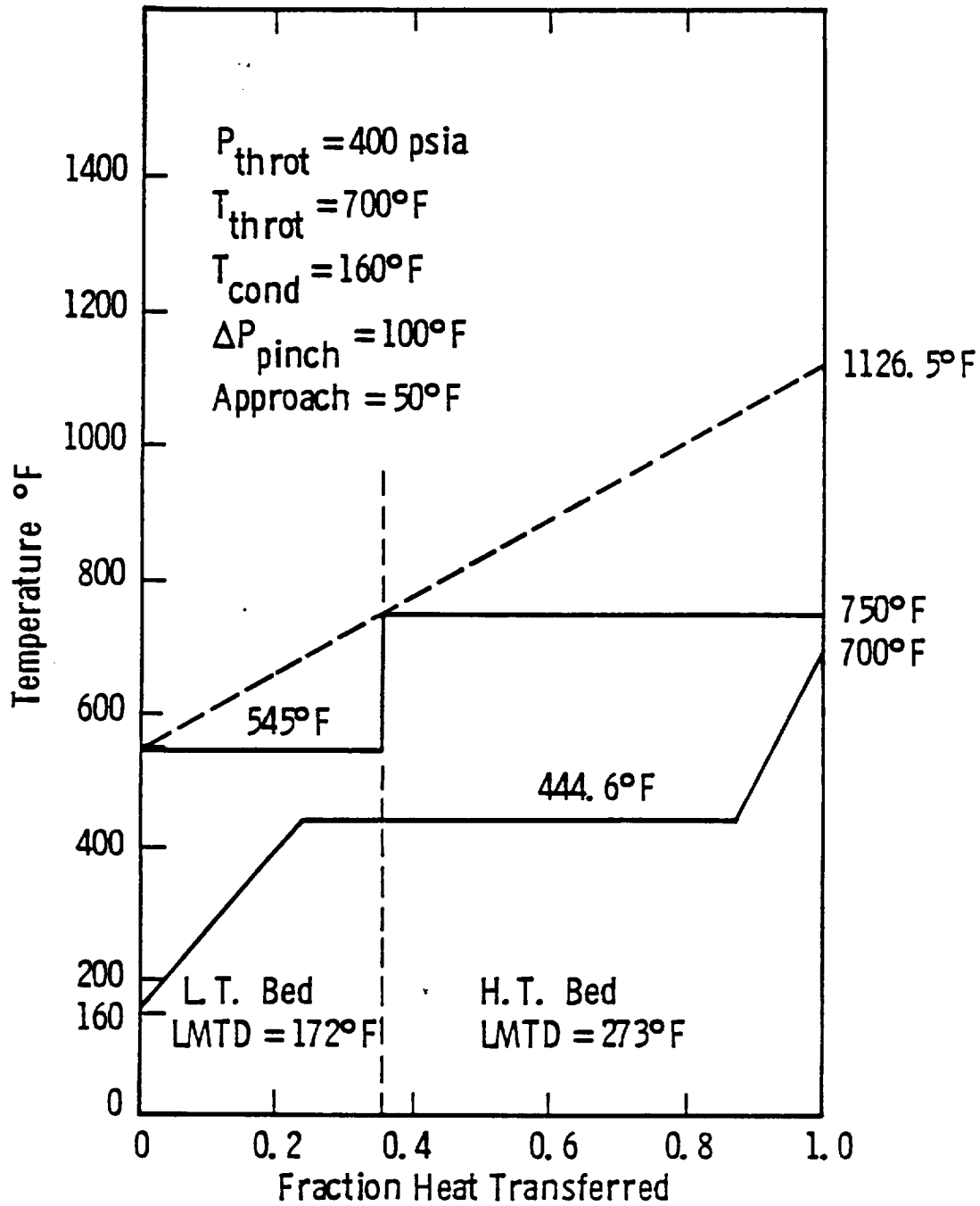


Fig. 4. 8—Fluidized bed heat exchanger temperature profile, steam Rankine cycle

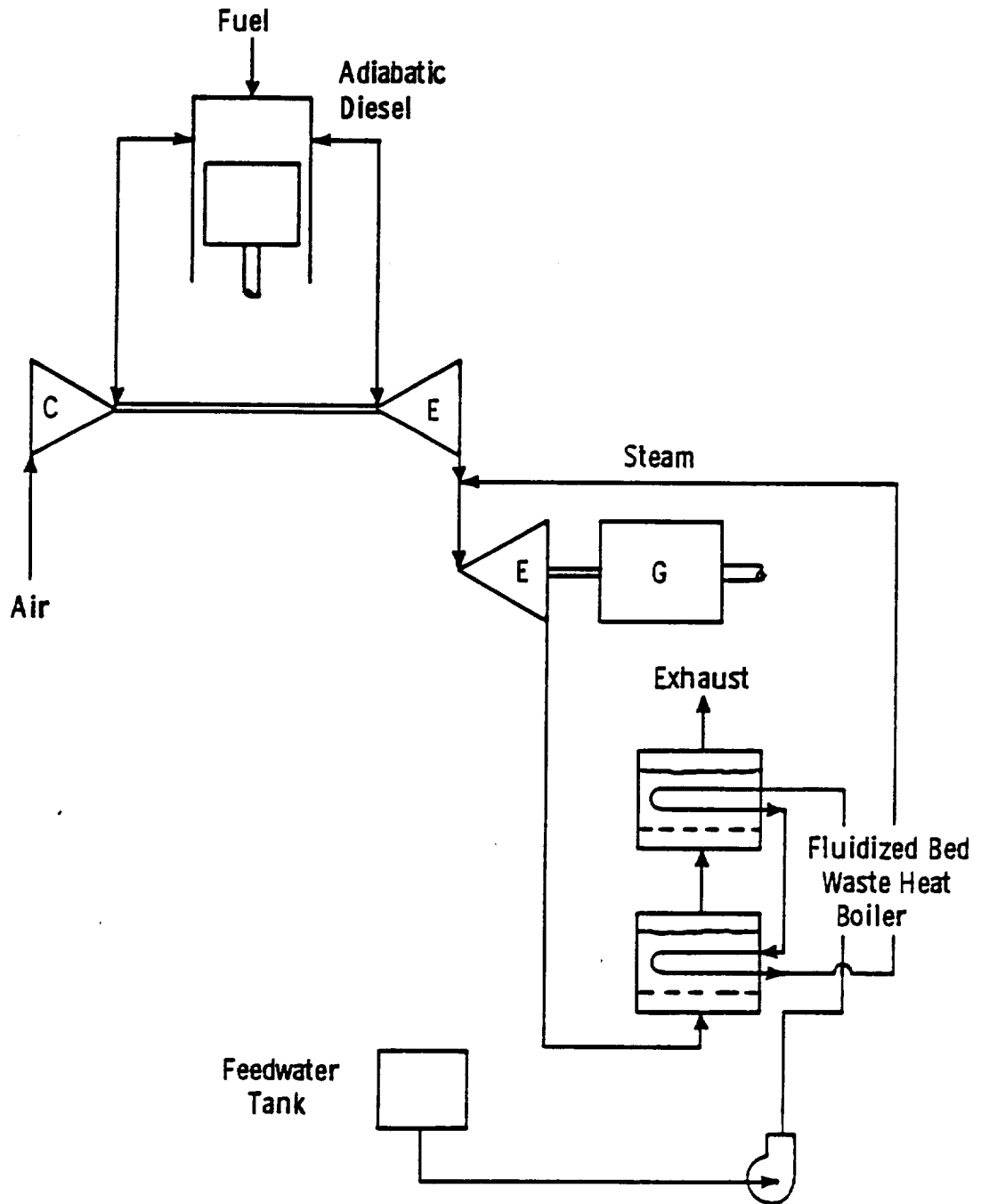


Fig. 4. 9—Turbocompound diesel with steam injection between compressor drive expander and power expander

Table 4.3

PERFORMANCE SUMMARY OF ADIABATIC TURBOCOMPOUND
DIESEL ENGINE WITH STEAM INJECTION BETWEEN
COMPRESSOR DRIVE AND POWER EXPANDERS

Case	1	2	3	4
Engine Configuration	ATCD/A	>		ATCD
Injection Pressure - psia	30	40	50	30
Corr. T_{exh} - °F	1240	1305	1361	1360
Corr. Power - hp	282.3	262.1	244.5	280.4
Corr. SFC - lb/hp hr	0.351	0.379	0.406	0.356
$(\Delta P/P)_{\text{hx}}$	0.05	>		
ΔT_{pinch} - °F	40	>		
Approach - °F	100	>		
Expander Power - hp	76.8	110.1	136.2	83.1
System Performance				
Power - hp	359.1	372.2	380.7	363.5
SFC - lb/hp hr	0.276	0.267	0.261	0.275
PIF, Note 1	1.122	1.163	1.190	1.141

(1) Relative to ATCD/A Engine Configuration, PIF is Performance Improvement Factor

after cooler on the turbocompound engine has a negligible effect on the performance.

The heat exchanger temperature distribution for Case 1 is shown in Figure 4.10. It should be noted that the exhaust temperature from the power expander is somewhat below the recommended minimum value (900°F) for the first fluidized bed and the first bed temperature is substantially below that value. It was found, however, that the system performance was not significantly affected by either the Δt pinch or the Δt approach of the heat exchanger.

A series of calculations were also made for the system shown in Figure 4.11 where the steam is injected ahead of the compressor drive expander of the turbocompound engine. The performance model of the turbocompound engine without steam injection shown in Figure 4.12 was used as the basis for these calculations. The exhaust conditions from the adiabatic diesel cylinder were held constant and the compressor drive expander outlet pressure was varied to match the compressor power requirements. The results of these calculations are summarized in Table 4.4. Comparison of Cases 1 and 2 show that the system performance is a moderate function of the compressor-drive and power expander's efficiency. Comparing Cases 1 and 3 shows that the performance is a weak function of the Δt pinch.

4.4 Open Brayton Cycle

A series of preliminary performance calculations were made for a variety of open Brayton bottoming cycle configurations. Figure 4.13 shows the simple open Brayton cycle without intercooling or recuperation and Table 4.5 summarizes its performance. Parameters evaluated include compressor pressure ratio, expander inlet temperature, adiabatic engine configuration, and heat exchanger temperature differences. None of these parameters over the range evaluated were found to have significant effects on performance.

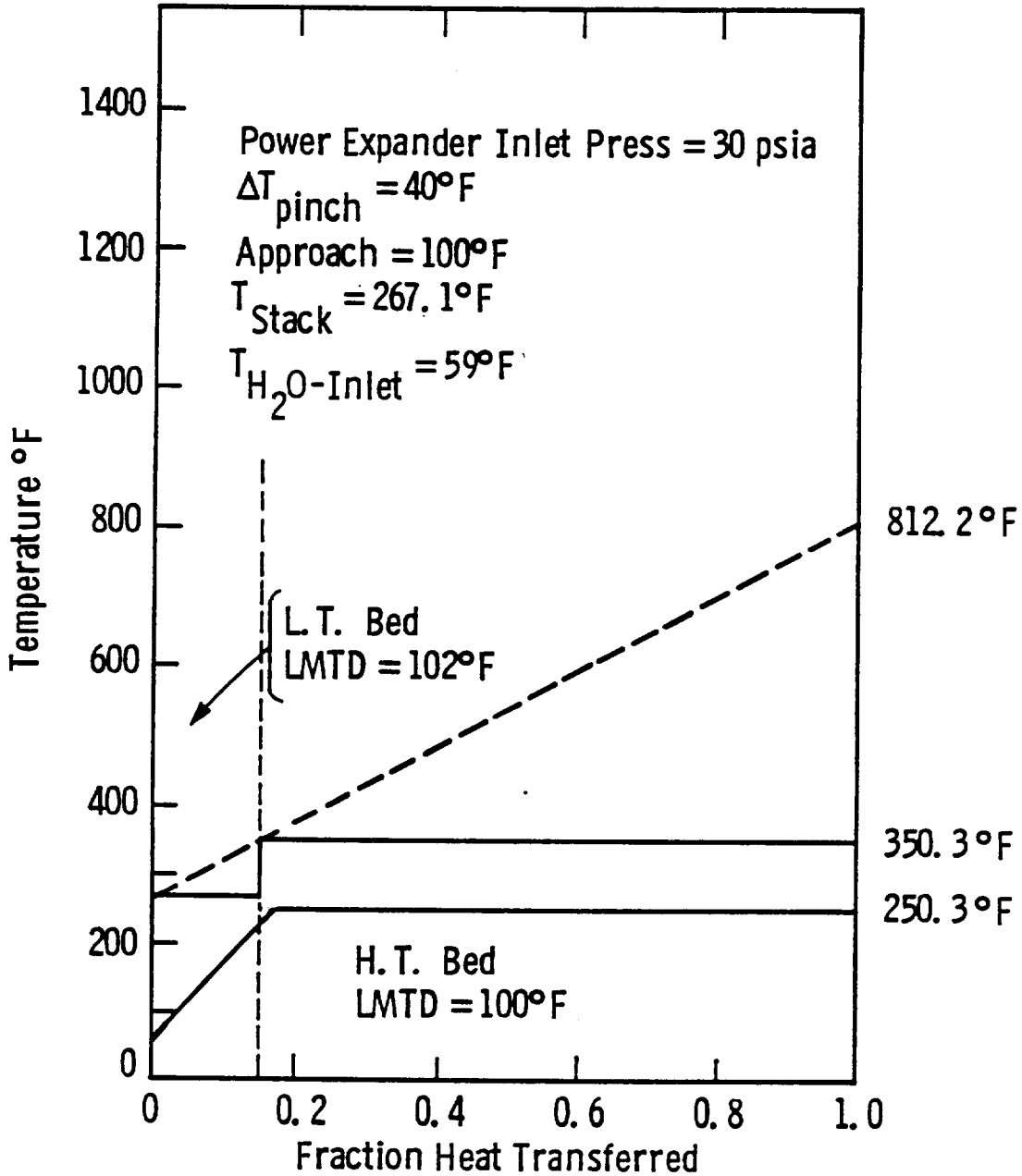


Fig. 4. 10—Fluidized bed heat exchanger temperature profile. Turbocompound engine with steam injection between compressor drive and power expanders

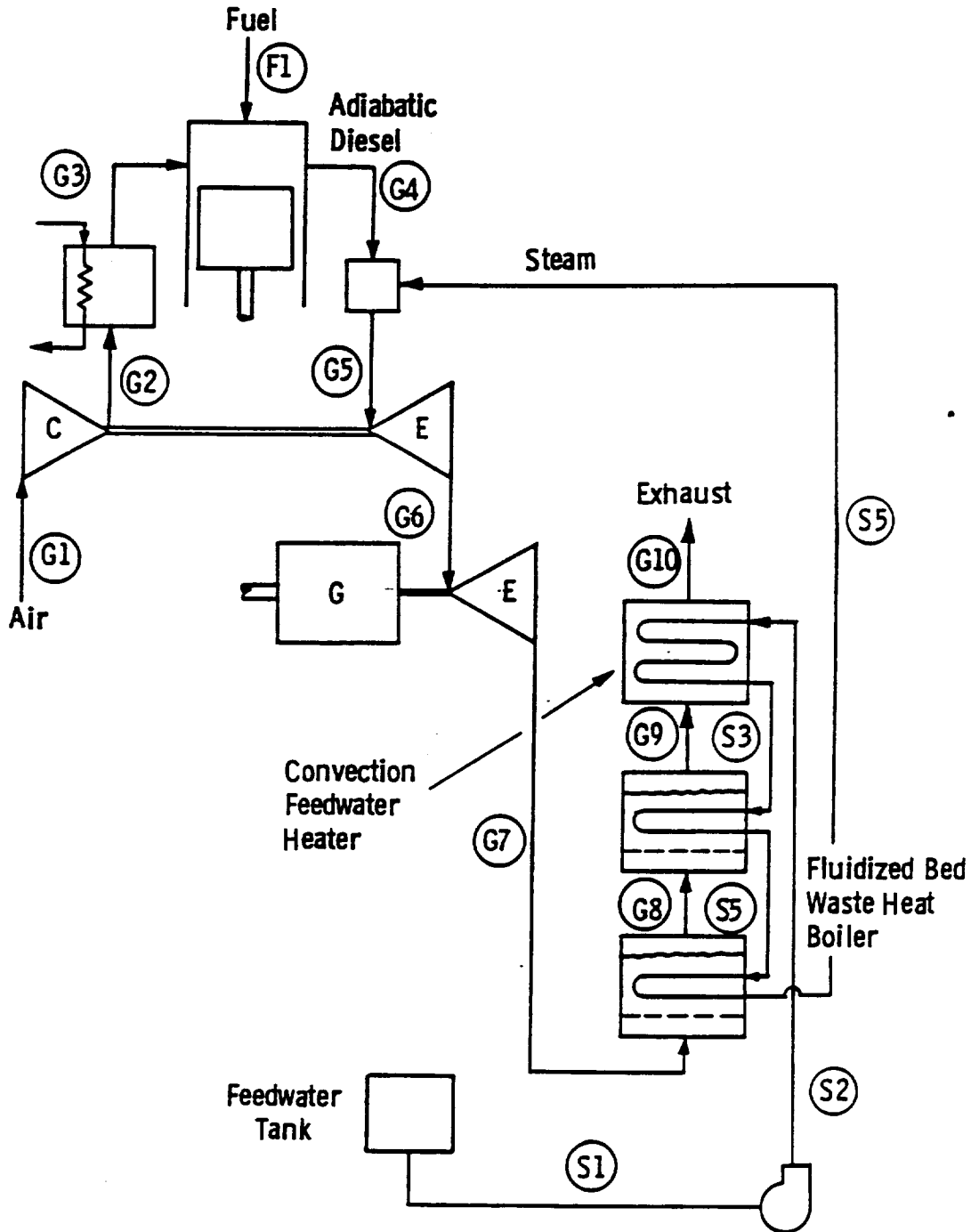
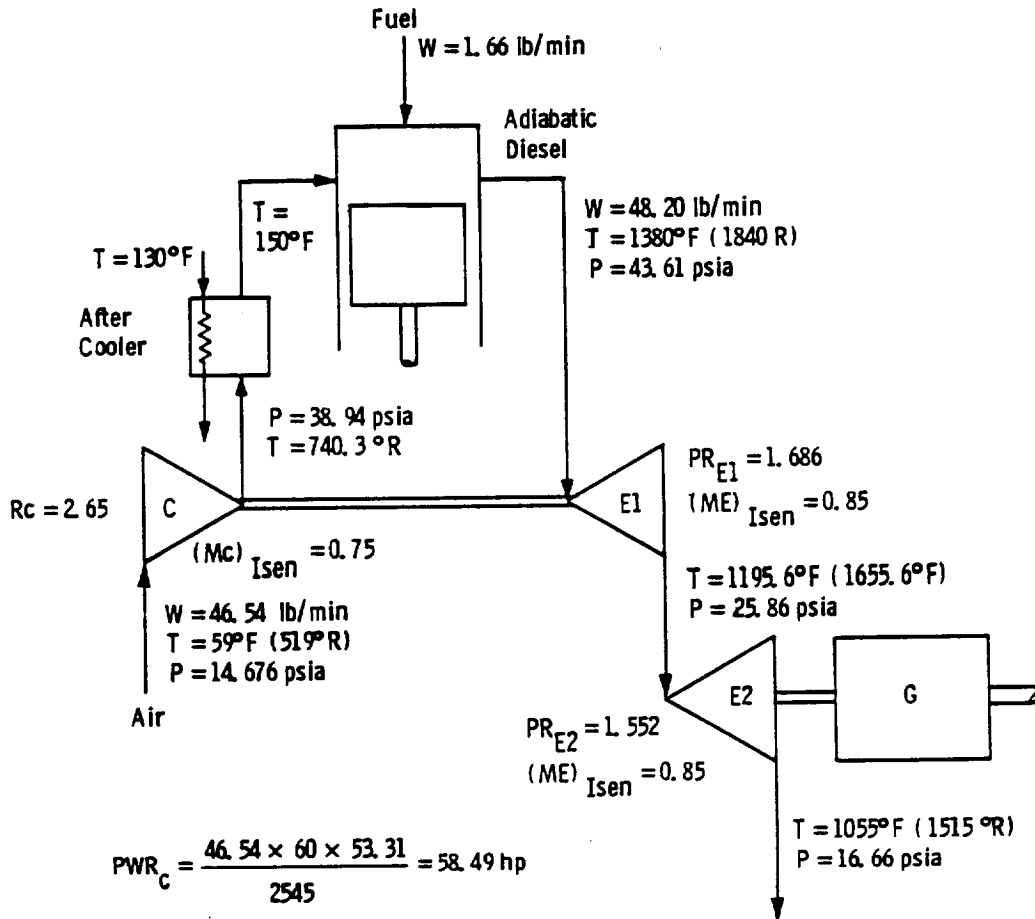


Fig. 4. 11—Turbocompound diesel with steam injection ahead of compressor drive expander



$$PWR_C = \frac{46.54 \times 60 \times 53.31}{2545} = 58.49 \text{ hp}$$

$$PWR_E = PWR_C / M_{Mech} = 58.49 / 0.98 = 59.69 \text{ hp}$$

$$\Delta H_{E1} = (59.69 \times 2545) / (60 \times 48.20) = 52.53 \text{ Btu/lb}$$

$$\Delta H_{E2} = (91.70 - 52.53) = 39.17 \text{ Btu/lb}$$

$$PWR_{E2} = 43.61 \times 60 \times 39.17 / 2547 = 40.24 \text{ hp}$$

$$\text{Basic Engine Power} = 340 - 40.2 = 299.8 \text{ hp}$$

Fig. 4.12-ATCPD/A model for steam injection system

Table 4.4
 PERFORMANCE SUMMARY OF ADIABATIC TURBOCOMPOUND
 DIESEL ENGINE WITH STEAM INJECTION AHEAD OF
 THE POWER EXPANDER

Case	1	2	3
Engine Configuration	ATCPD/A	>	
Compressor Efficiency - %	75.0	>	
Compressor-Drive Expander Efficiency - %	85.0	87.5	85.0
Turbocharger Mechanical Efficiency - %	98.0	>	
No. of HX Stages	2	>	
Δt (pinch) - ^o F	40.0	>	100.0
Δt (approach) - ^o F	100.0	>	
HX Efficiency - %	99.0	>	
Injection Pressure - psia	43.61	>	
Power Expander Inlet Pressure- psia	26.85	27.21	26.80
HX Pressure Drop - %	11.95	>	
Power Expander Efficiency - %	85.0	87.5	85.0
Thermodynamic Power - kW	47.59	49.92	47.27
Power Expander Mechanical Efficiency - %	99.0	>	
Gear Efficiency - %	99.0	>	
Gross Shaft Power - kW	46.64	48.93	46.33
Feed Pump Efficiency - %	70.0	>	
Auxiliary Power - kW	0.21	>	
Net Shaft Power - kW	46.43	48.72	46.12
- hp	62.24	65.31	61.82
Basic Engine Power - hp	299.8	>	
System Performance			
Power - hp	362.0	365.1	361.6
SFC - lb/hp hr	0.275	0.273	0.275
PIF, Note 1	1.065	1.074	1.064

(1) Relative to ATCPD/A Engine Configuration, PIF is Performance Improvement Factor

Dwg. 9354A05

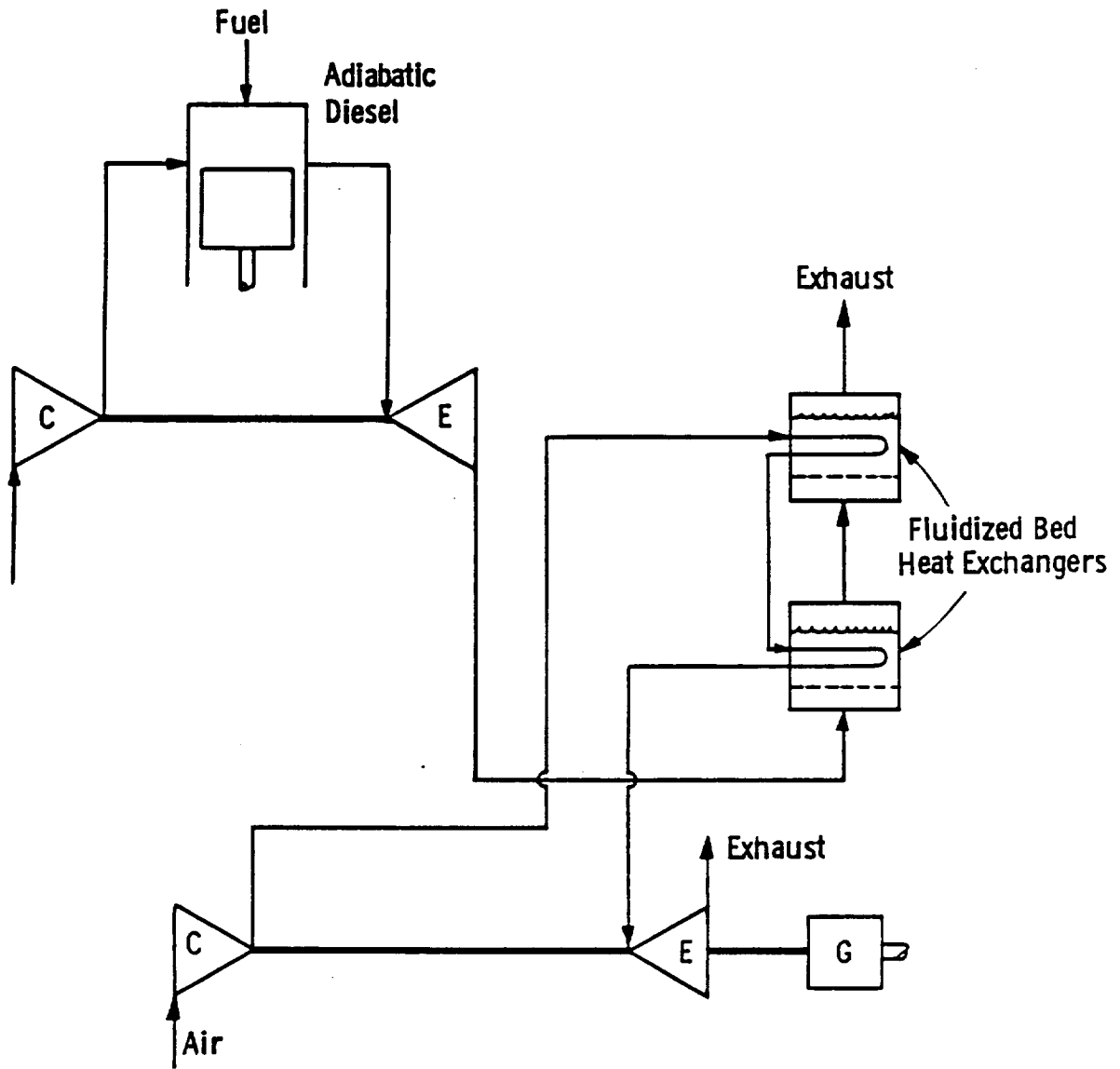


Fig. 4.13 – Turbocharged diesel with subposed open Brayton cycle

Table 4.5
 PERFORMANCE SUMMARY OF ADIABATIC DIESEL ENGINE
 WITH SUBPOSED OPEN BRAYTON CYCLE

Case	1	2	3	4
Engine Configuration	ATCD/A			ATCD
$(\Delta P/P)_{hx}$	0.05	_____>		
Corr. T_{exh} - °F	1127	_____> 1247		
Corr. Power - hp	318	_____> 316.5		
Corr. SFC - lb/hp hr	0.312	_____> 0.317		
Compressor Press. Ratio	3.0	3.5	_____>	
Compressor Efficiency - %	85	_____>		
Expander Inlet Temp. - °F	800	_____>	850	_____>
Expander Efficiency - %	85	_____>		
ΔT_{pinch} - °F	100	_____>	50	_____>
$\Delta t_{approach}$ - °F	100	100	50	50
T_{stack} - °F	650	662	650	610
Heat Recovered - Btu/hr	369720	362160	369720	503280
Air Flow Rate - lb/s	0.786	0.827	0.762	1.037
Net Power Output - hp	16.4	16.4	18.2	24.7
System Performance				
Power - hp	334.4	334.4	336.2	341.2
SFC - lb/hr hr	0.297	0.297	0.295	0.294
PIF, Note 1	1.045	1.045	1.051	1.078

(1) Relative to ATCD/A Engine Configuration, PIF is Performance Improvement Factor

Additional performance calculations were made for the open Brayton cycle with intercooling (see Figure 4.14) and recuperation (see Figure 4.15). The heat exchanger temperature profile for several of the intercooled cases is shown in Figure 4.16. The results of these performance calculations are summarized in Cases 1 and 2 of Table 4.6. Comparing Case 1 with Case 3 of Table 4.5 shows that intercooling improves the system performance about 1%. Comparing Cases 1 and 2 shows that increasing the expander efficiency from 85 to 90% improves the SFC by about 2%.

Case 3 in Table 4.6 represents to optimum version of the recuperative cycle shown in Figure 4.15. Comparing this with the performance of the simple open cycle in Table 4.5 shows that the use of recuperation in combination with the two stage fluidized bed heat exchanger has a detrimental effect on the system performance.

It was concluded that the potential for the supposed open Brayton cycle with fluidized bed heat recovery is substantially poorer than it is with convective heat recovery as reported by United Technologies in Reference 17. This occurs because the attainable stack gas temperature with two stages of fluidized bed (see Figure 4.16) is considerably higher than that for a counterflow convective heat exchanger.

4.5 Closed Brayton Cycle

A series of preliminary performance calculations were made for closed Brayton bottoming cycles to determine the effect of cycle pressure ratio and expander inlet temperature using helium as the working fluid. Figure 4.17 shows the cycle schematic. Typical temperature profiles for the heat exchangers for the closed Brayton cycle are shown in Figure 4.18. Two fluidized beds are used for heat recovery while only one is used for heat rejection.

The results of the performance calculations are shown plotted in Figures 4.19, 4.20 and 4.21. These plots show that the optimum cycle

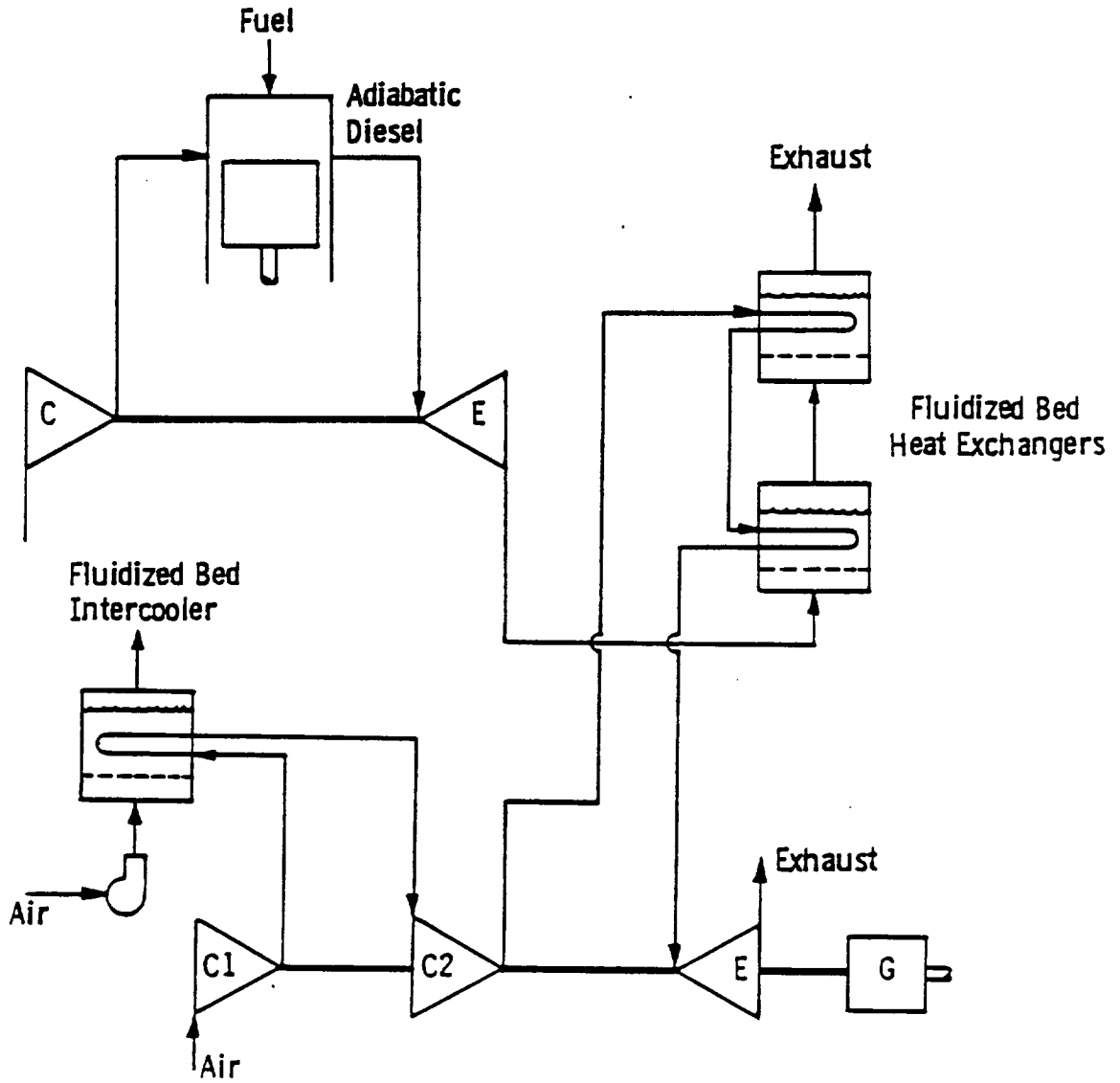


Fig. 4. 14—Turbocharged diesel with subposed intercooled open Brayton cycle

Dwg. 9354A06

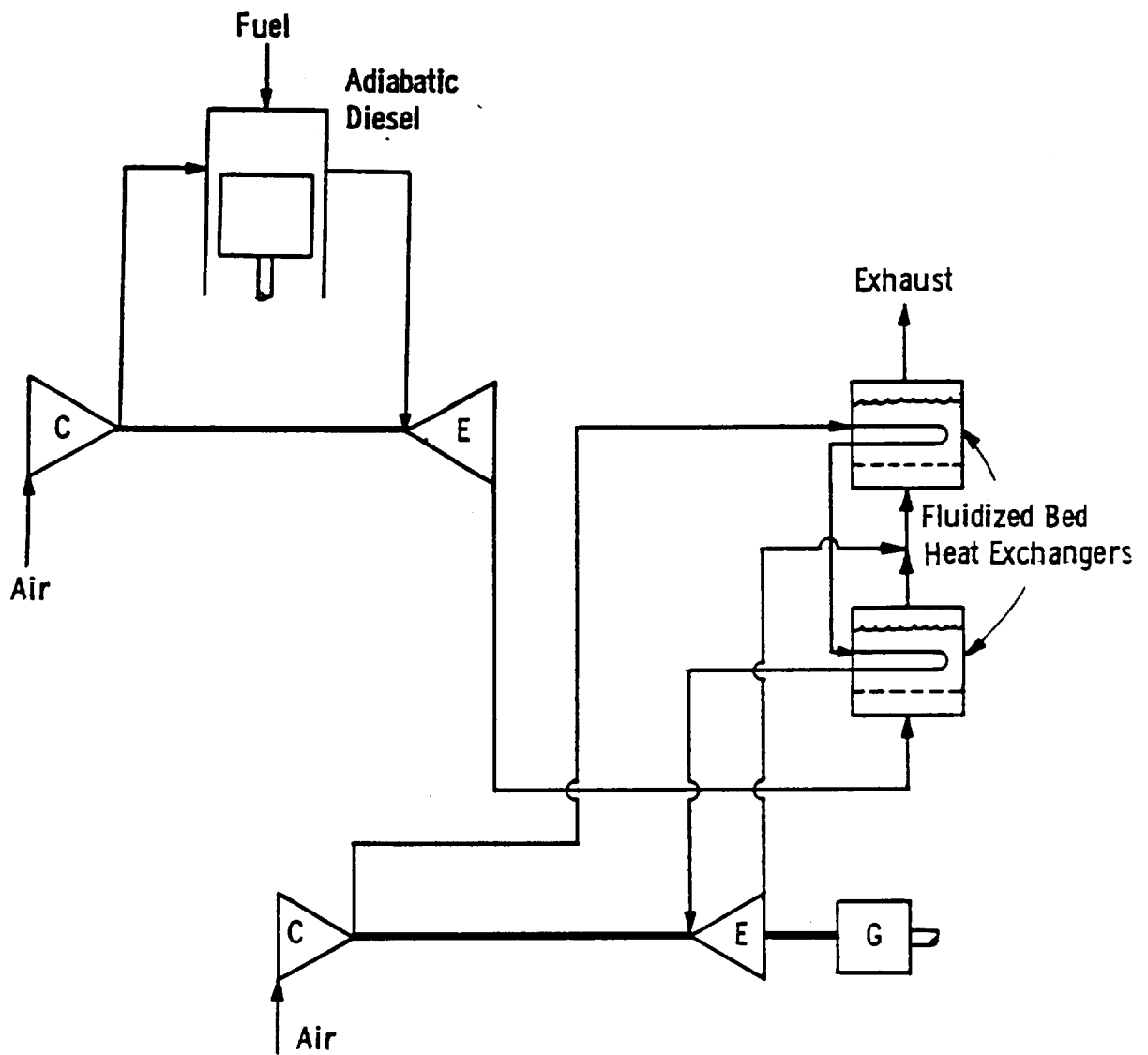


Fig. 4.15 – Turbocharged diesel with subposed recuperated open Brayton cycle.

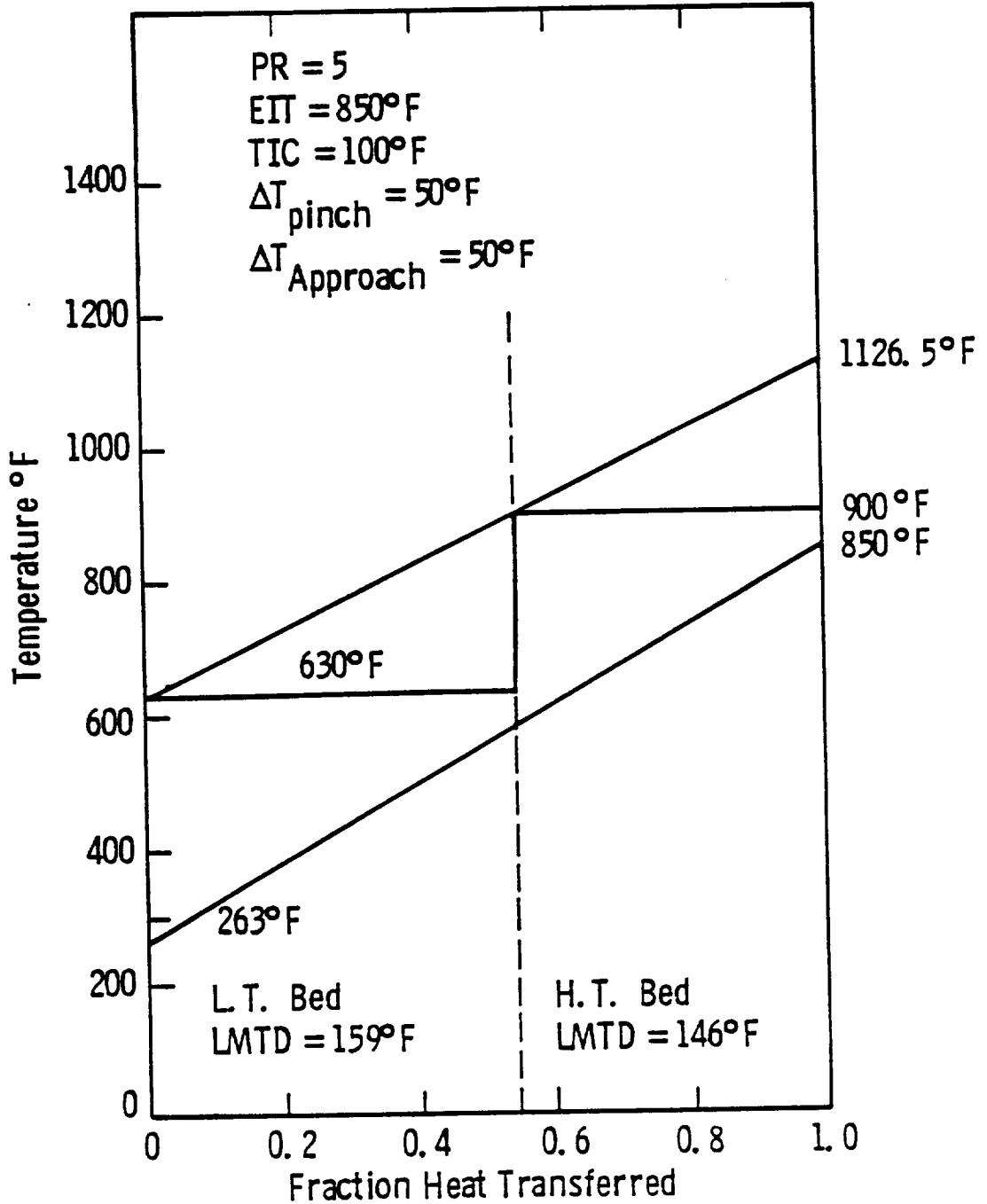


Fig. 4. 16—Fluidized bed heat exchanger temperature profile intercooled open Brayton cycle

Table 4.6

PERFORMANCE SUMMARY OF ADIABATIC DIESEL ENGINE
WITH SUBPOSED OPEN BRAYTON CYCLE

Case	1	2	3
Engine Conf.	ATCD/A	—————>	—————>
Cycle	Intercooled	—————>	Recuperated
$(\Delta P/P)_{hx}$	0.05	—————>	—————>
Corr. T_{exh} - °F	1127	—————>	—————>
Corr. Power - hp	318	—————>	—————>
Corr. SFC - lb/hphr	0.312	—————>	—————>
Compressor Pressure Ratio	5.0	—————>	3.0
Compressor Efficiency - %	86	88	85
Expander Inlet Temp. - F	850	—————>	800
Expander Efficiency - %	85	90	85
ΔT_{pinch} - °F	50	—————>	100
$\Delta T_{approach}$ - °F	50	50	100
T_{stack} - °F	630	630	625
Heat Recovered - Btu/hr	382680	—————>	
Air Flow Rate - lb/s	0.722	—————>	0.706
Net Power Output - hp	21.9	27.7	13.6
System Performance			
Power - hp	339.7	345.7	331.6
SFC - lb/hphr	0.292	0.287	0.299
PIF, Note 1	1.063	1.081	1.036

(1) Relative to ATCD/A Engine Configuration, PIF is Performance Improvement Factor

Curve 749105-A

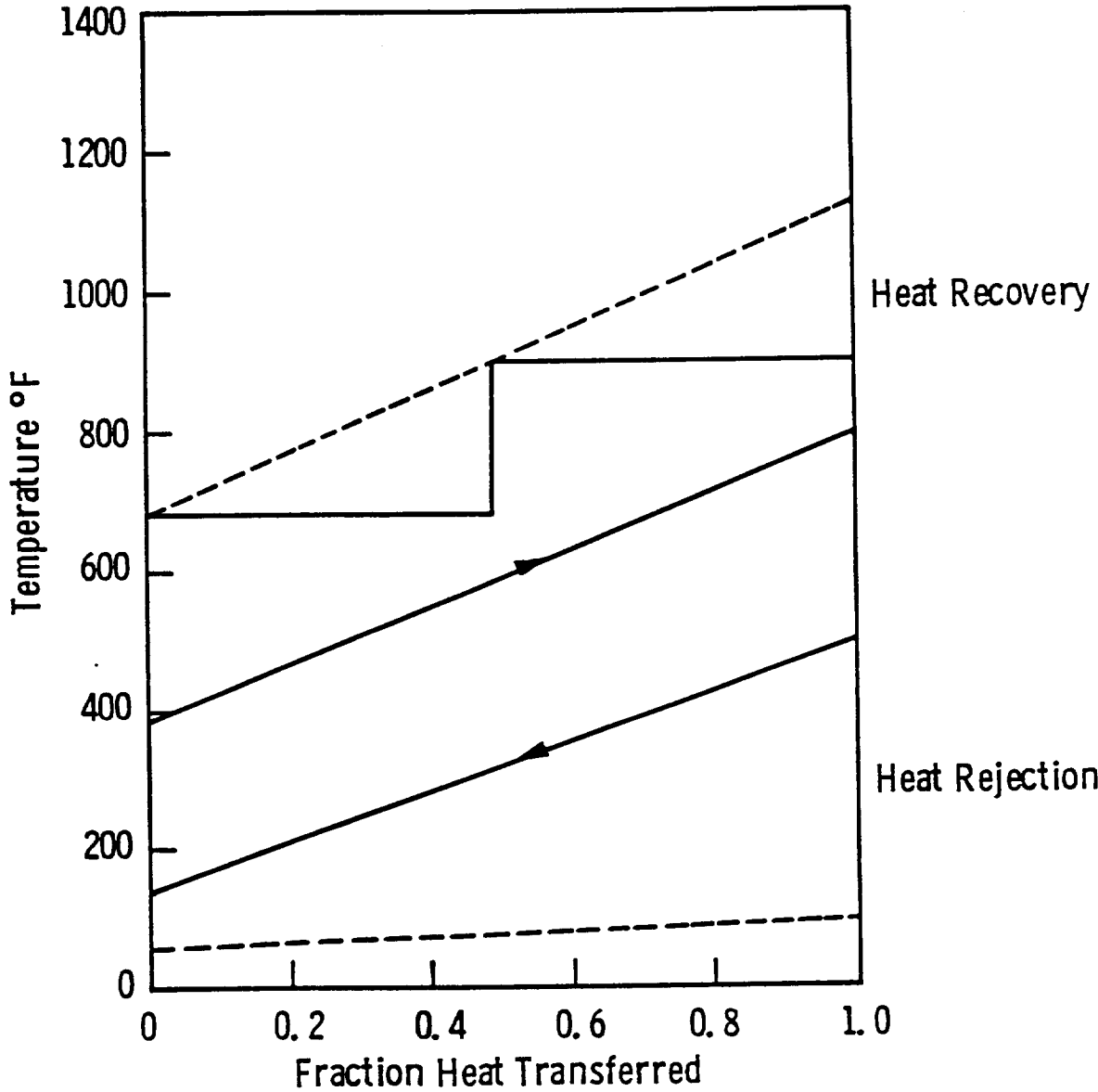


Fig. 4. 18—Fluidized bed heat exchanger temperature profiles for closed Brayton cycle

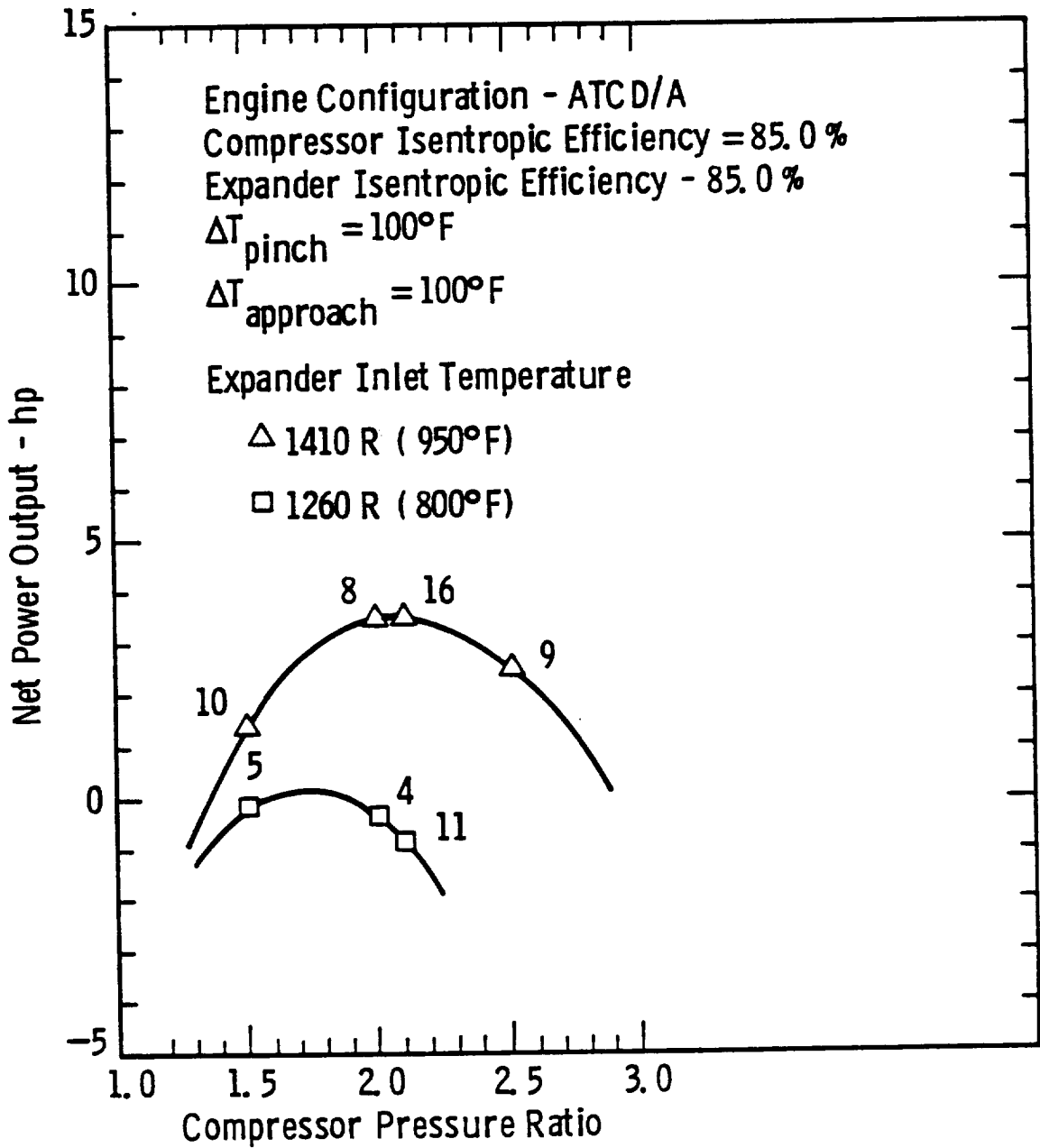


Fig. 4.19—Adiabatic diesel engine with subposed closed Brayton cycle

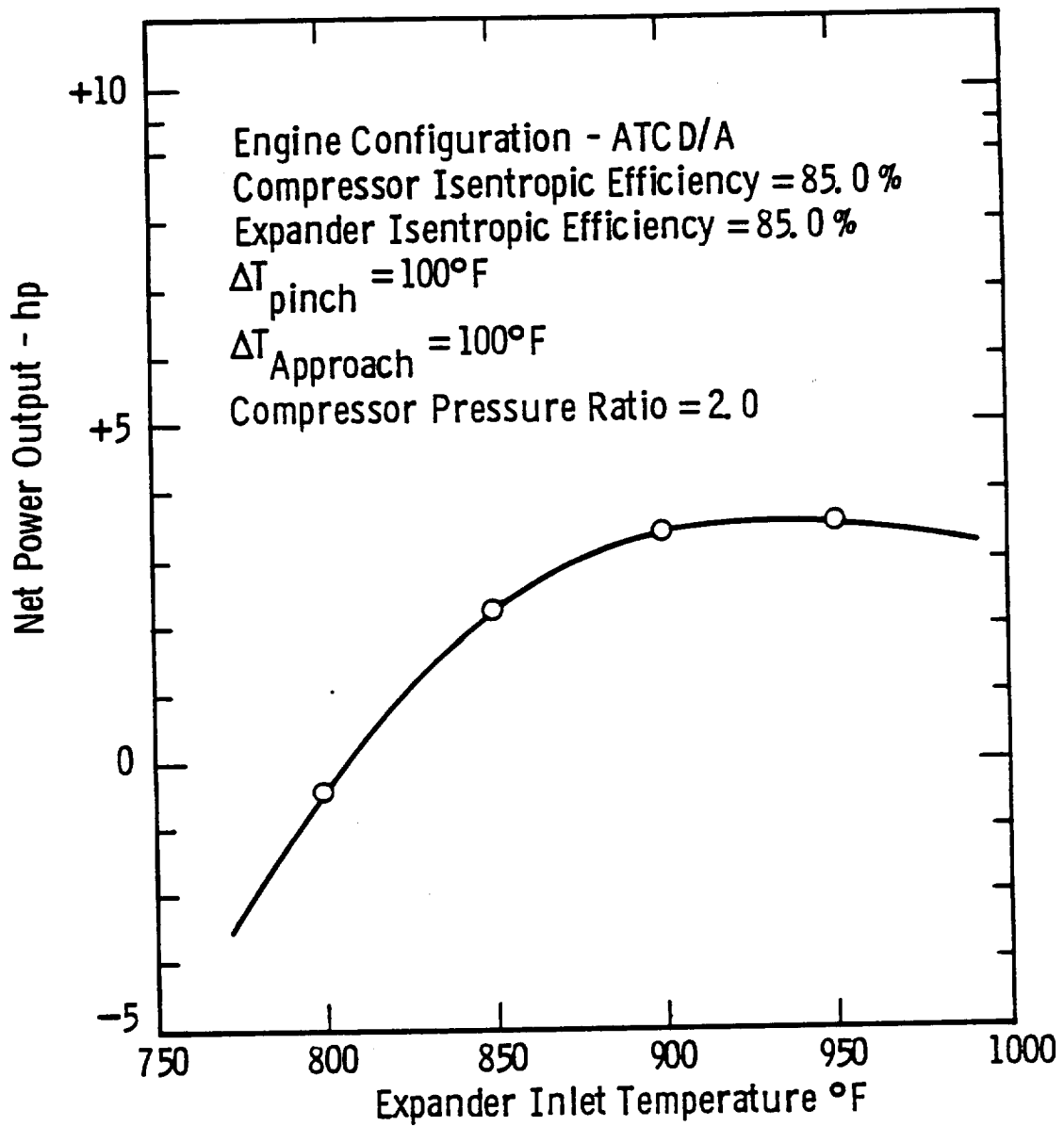


Fig. 4. 20—Adiabatic diesel engine with closed Brayton bottoming cycle

Curve 749109-A

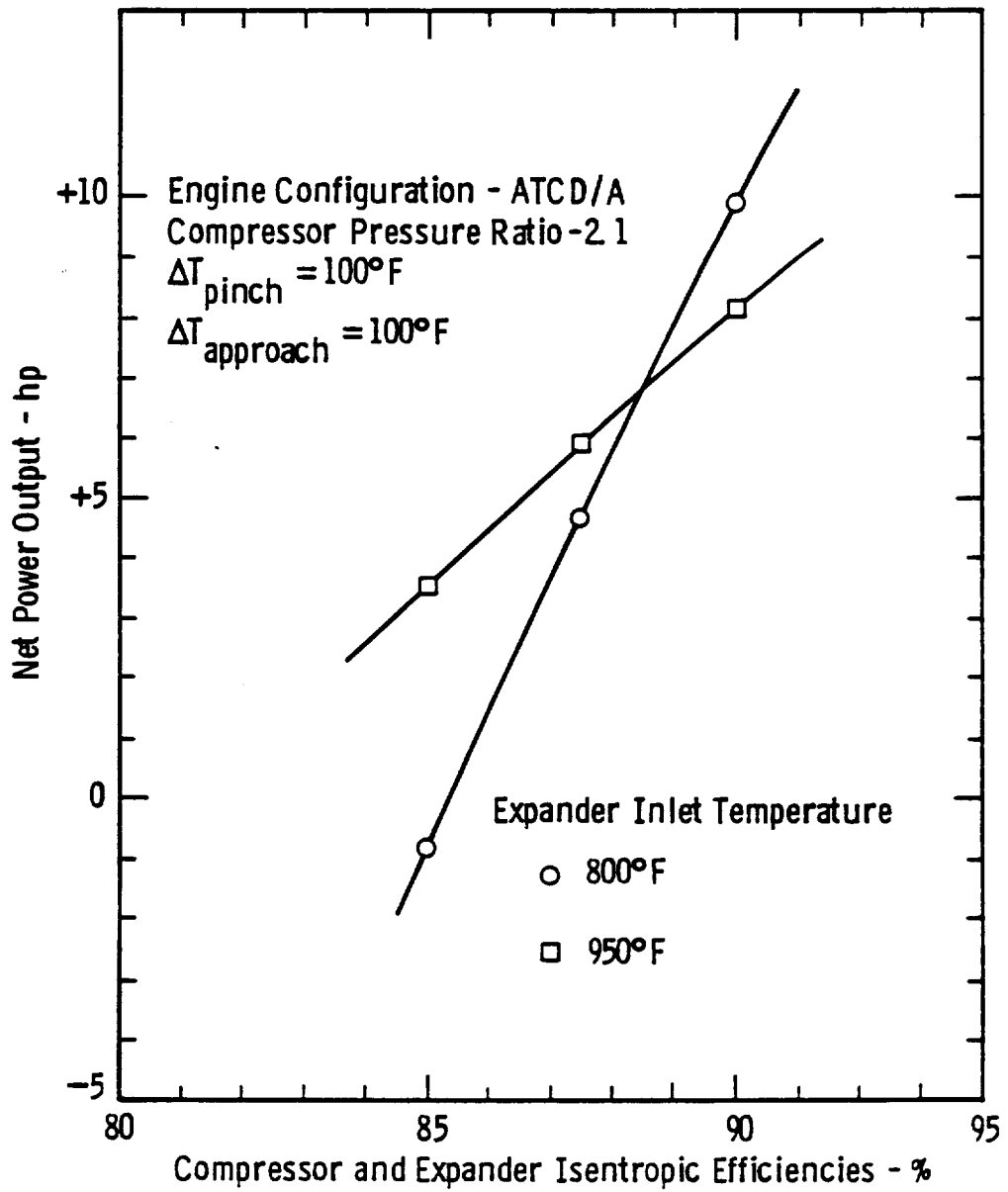


Fig. 4. 21—Adiabatic diesel engine with closed Brayton bottoming cycle

has a compressor pressure ratio of about 2 and an expander inlet temperature of about 950°F. The net power output is a product of the heat recovered and the cycle efficiency which have opposing characteristics. Figure 4.21 shows that the subsystem performance is a strong function of the compressor and expander isentropic efficiencies and, that for isentropic efficiency values greater than 88.5%, the optimum value of expander inlet temperature is less than 950°F.

The cycle operating conditions which are thought to represent the maximum possible potential of this bottoming cycle are given in Table 4.7.

Table 4.7
CONDITIONS FOR MAXIMUM PERFORMANCE OF CLOSED BRAYTON BOTTOMING
CYCLE FOR ADIABATIC DIESEL ENGINE

Compressor Pressure Ratio	- 2.1
Working Fluid	- He
Compressor Isentropic Efficiency	- 90.0%
Compressor Inlet Temperature	- 600°F
Expander Inlet Temperature	- 1260°F
Expander Isentropic Efficiency	- 90.0%
$(\Delta P/P)_{HXIC}$	- 1.0%
$(\Delta P/P)_{HXIH}$	- 2.5%
$(\Delta P/P)_{HX2C}$	- 1.0%
$(\Delta P/P)_{HX2H}$	- 2.5%
ΔT_{PINCH}	- 100°F
$\Delta T_{APPROACH}$	- 100°F
Net Subsystem Power	- 9.92 hp
Corrected Engine Power	- 318.0 hp
Corrected Engine SPC	- 0.312 lb/hphr
System Performance Power	- 327.9 hp
SFC	- 0.303 lb/hphr
PIF, Note 1	- 1.025

(1) Relative to ATCD/A Engine Configuration, PIF is Performance Improvement Factor.

4.6 Stirling Engine

A series of preliminary performance calculations were made for the Stirling engine subsystem configuration shown in Figure 4.22. This subsystem uses an intermediate heat transfer loop between an external fluidized bed heat exchanger and the Stirling engine and is based on the system evaluated by General Electric in the Cogeneration Technology Alternatives Study (Reference 18). A two-stage fluidized bed heat exchanger was assumed with a typical temperature profile as shown in Figure 4.23.

The Stirling engine performance was derived from data tabulated in Martiri's Stirling Engine Design Manual (Reference 19) for a cold end temperature of 100°C (212°F). The results of these calculations are summarized in Table 4.8. Two adiabatic diesel engine configurations were evaluated over a range of Stirling engine peak cycle temperatures. The system performance is shown to be a weak function of both the engine configuration and the peak cycle temperature.

Since the use of the intermediate heat transfer loop gave high stack gas temperatures and marginal system performance relative to other bottoming cycles evaluated, optional heat transfer configurations were investigated. These results are summarized in Table 4.9. Integrated fluidized bed heat exchangers as shown in Figure 4.24 were found to have a potential for significantly better performance than the external heat exchangers with an intermediate heat transfer loop (see Table 4.9); but, were judged to be physically impractical.

A configuration using a single external fluidized bed heat exchanger with heat pipes for transporting the heat to the Stirling engine as illustrated in Figure 4.25 was found to give system performance comparable with that of the integrated arrangement. Performance calculations for these cases are given in Table 4.10.

Dwg. 9354A11

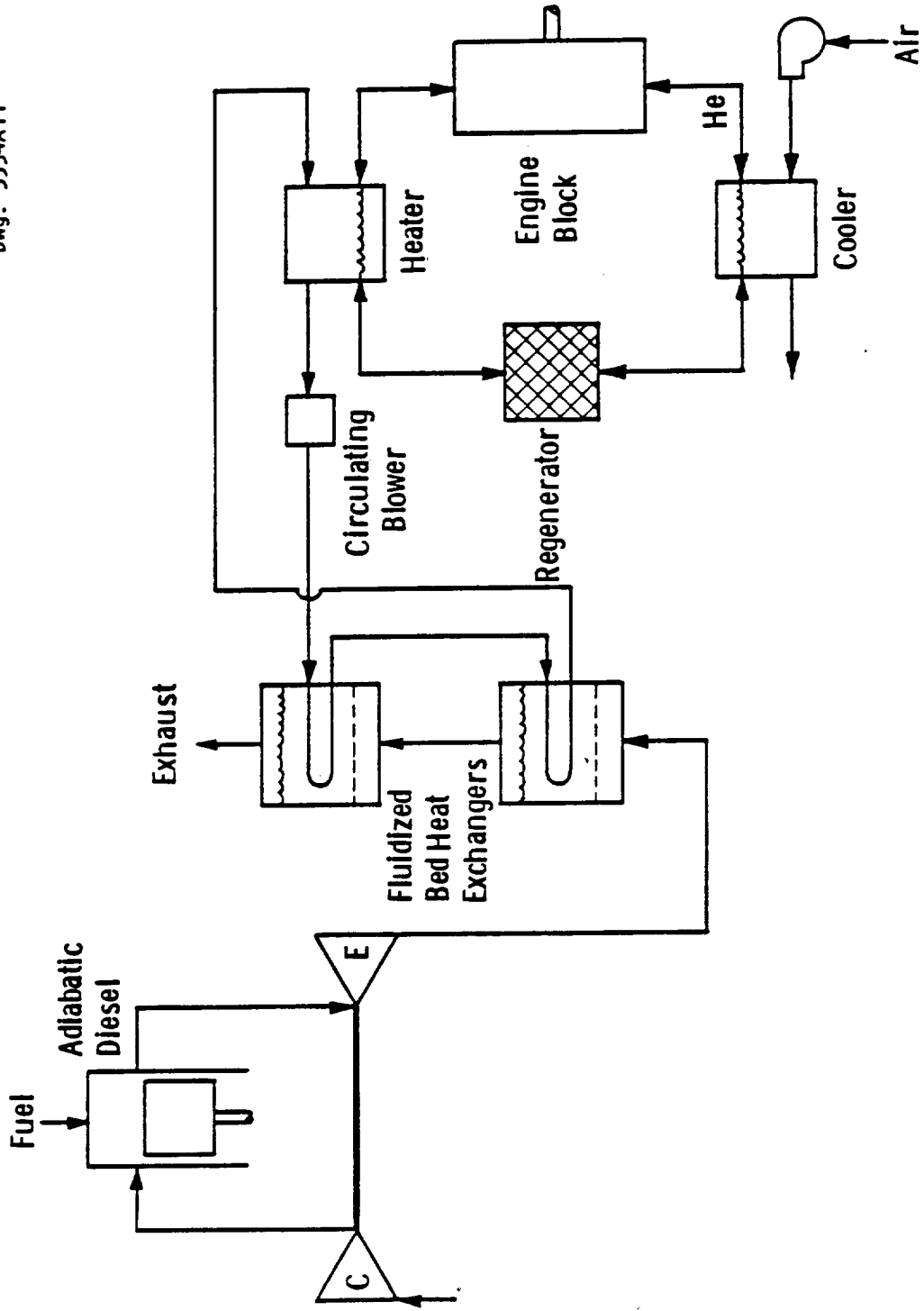


Fig. 4. 22—Adiabatic diesel with subposed Stirling cycle

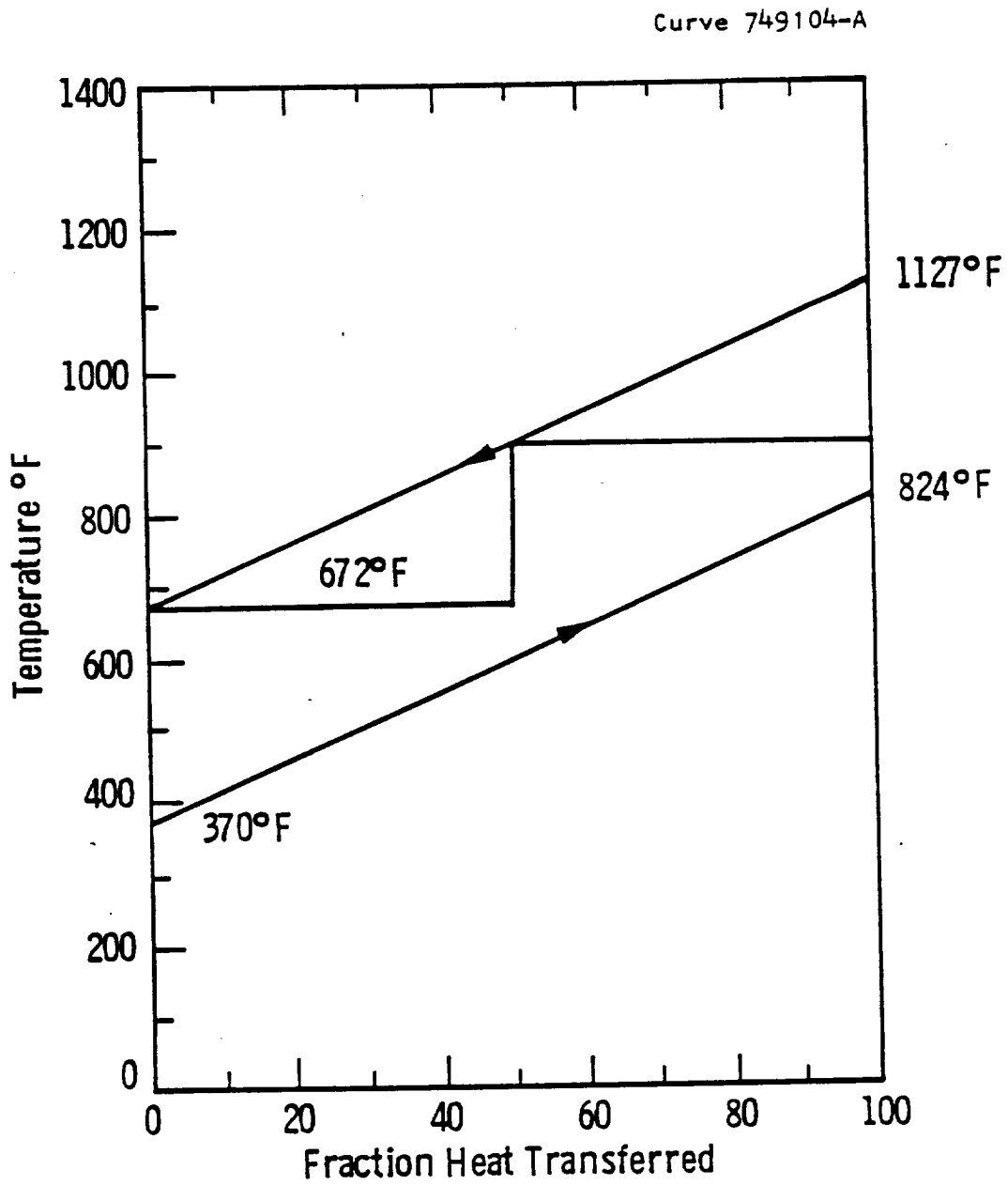


Fig. 4. 23—Temperature profile of fluidized bed heat exchanger for stirling engine subsystem with intermediate heat transfer loop

Table 4.8
 PERFORMANCE SUMMARY OF ADIABATIC DIESEL ENGINE
 WITH SUBPOSED STIRLING CYCLE

Case	1	2	3	4
Engine Configuration	ATCD/A		ATCD	
$(\Delta P/P)_{hx}$	0.05			
Corr. T_{exh} - °F	1127		1247	
Corr. Power - hp	318		316.5	
Corr. SFC - lb/hp hr	0.312		0.317	
Working Fluid	He			
T_{stack} - °F	925	825	950	850
Approach - °F	25			
FBHX ΔT_{pinch} - °F	75			
Peak Cycle Temp. °F	725	575	700	550
Cooler Temp. - °F	212			
Heat Recovered - Btu/hr	158337	235384	239714	317713
ETA _{stir} - %	27.4	20.9	26.2	19.4
Power Output - hp	17.1	19.4	24.7	24.2
System Performance				
Power - hp	335.1	337.4	341.2	340.7
SFC - lb/hp hr	0.296	0.294	0.294	0.295
PIF, Note 1	1.047	1.054	1.071	1.070

(1) Relative to ATCD/A Engine Configuration, PIF is Performance Improvement Factor

Table 4.9
 PERFORMANCE SUMMARY OF ADIABATIC DIESEL ENGINE
 WITH SUBPOSED STIRLING CYCLE

<u>Case</u>	<u>1</u>	<u>2</u>
Engine Configuration	ATCD	
$(\Delta P/P)_{hx}$	0.05	
Corr. T_{exh} - °F	1246.5	
Corr. Engine Pwr. - hp	316.5	
Corr. SFC - lb/hp hr	0.317	
FBHX Configuration	Internal	
Working Fluid	He	
T_{stack} - °F	775	775
Approach - °F	100	200
Peak Cycle Temp. °F	675	575
Cooler Temp. - °F	212	212
Heat Recovered - Btu/hr	372860	372860
ETA _{stir} - %	25.4	20.9
Power - hp	37.2	30.6
System Performance		
Power - hp	353.7	347.1
SFC - lb/hp hr	0.284	0.289
PIF (Performance Improvement Factor)		
ATCD	1.111	1.090
ATCD/A	1.105	1.085

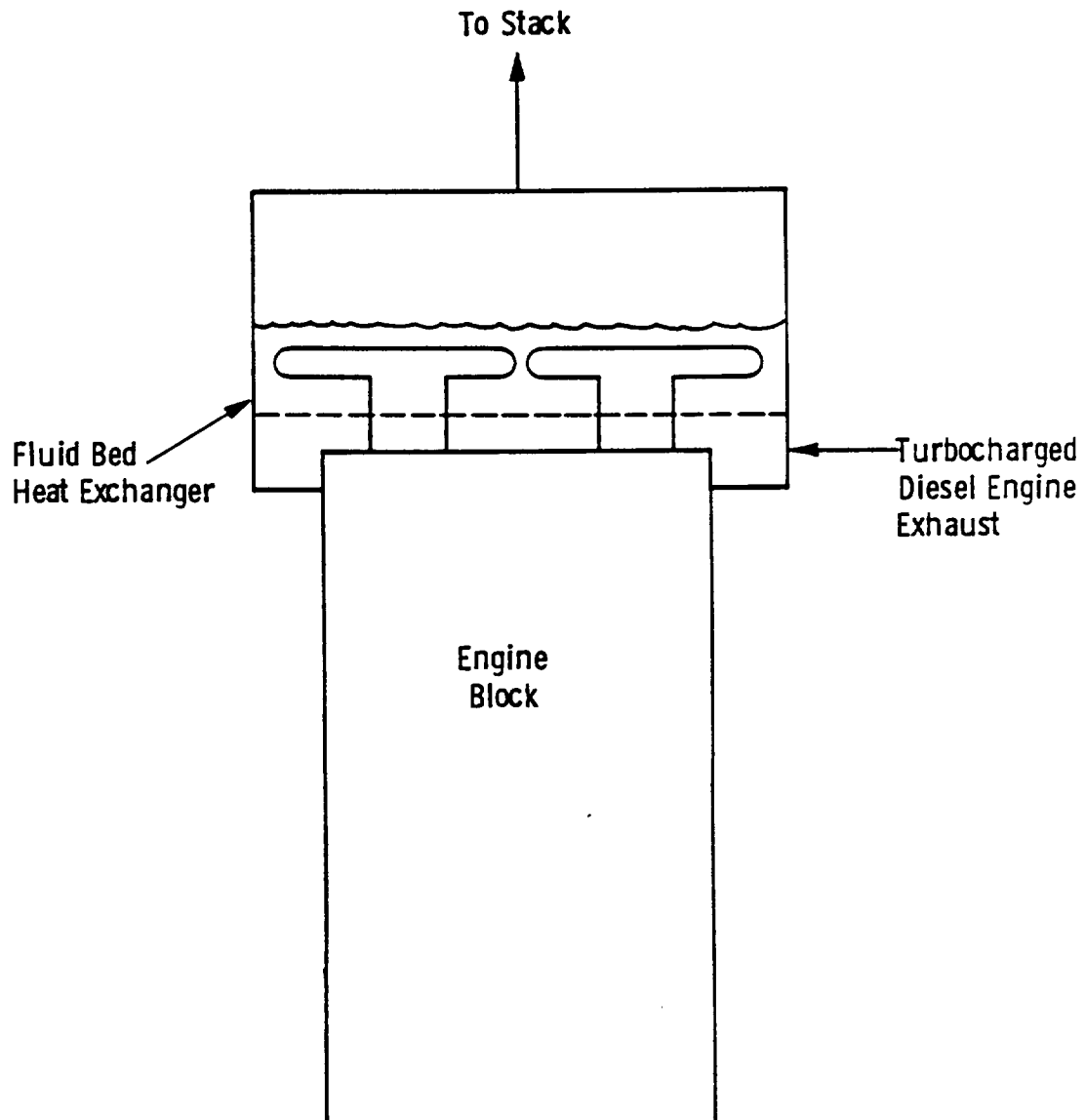


Fig. 4. 24—Single stage FBHX heater integrated with Stirling engine

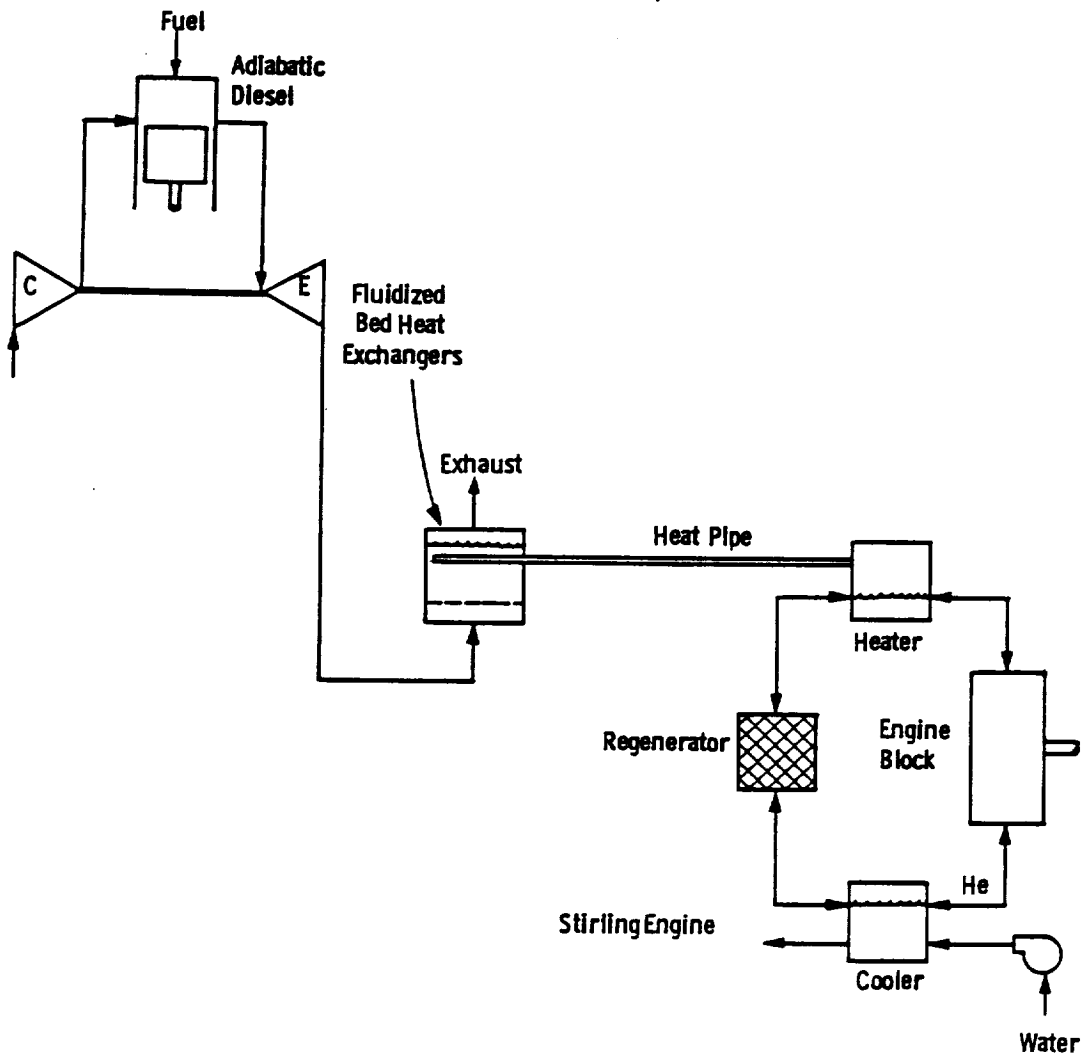


Fig. 4. 25—Adiabatic diesel with subposed stirling engine using heat pipes

Table 4.10
 PERFORMANCE SUMMARY OF ADIABATIC DIESEL ENGINE
 WITH SUBPOSED STIRLING CYCLE

Case	1	2	3	4
Engine Configuration	ATCD	—————>		
$(\Delta P/P)_{hx}$	0.05	—————>		
Corr. T_{exh} - °F	1246.5	—————>		
Corr. Engine Pwr. - hp	316.5	—————>		
Corr. SFC - lb/hp hr	0.317	—————>		
FBHX Conf.	External with heat pipes ———>			
Working Fluid	He	—————>		
T_{stack} - °F	775	—————>		
Approach - °F	100	—————>		
ΔT_{hp} - °F	0	25	50	75
Peak Cycle Temp. °F	675	650	625	600
Cooler Temp. - °F	212	—————>		
Heat Recovered - Btu/hr	372860	—————>		
ETA _{stir} - %	25.4	24.4	23.3	22.1
Power - hp	37.2	35.8	34.1	32.4
System Performance				
Power - hp	353.7	352.3	350.6	348.9
SFC - lb/hp hr	0.284	0.285	0.286	0.288
PIF (Performance Improvement Factor)				
ATCD	1.111	1.106	1.101	1.095
ATCD/A	1.105	1.101	1.096	1.090

4.7 Analysis of Screening Evaluations

Table 4.11 summarizes the results of the screening evaluations made on the six candidate bottoming cycles. The projected specific fuel consumption is quantitative whereas the volume and weight are qualitative. The projected SFC's for the organic Rankine, steam Rankine, and steam injection cycles are within a $\pm 1\%$ band. The organic Rankine cycle was selected for further evaluation. While the performance of the steam Rankine cycle is about equal to that of the organic Rankine cycle, it was decided to select only one Rankine cycle for further evaluation.

The steam injection cycle was selected for further evaluation because of its uniqueness despite the negative volume and weight factors associated with the feedwater requirements.

It was concluded that the use of a fluid bed heat exchanger in combination with Brayton cycles did not have a high potential so neither of these cycles were selected for further evaluation.

The subposed Stirling engine was also selected for further evaluation to provide basis for comparing ongoing NASA Stirling engine and cycle evaluations.

Table 4.11
EVALUATION OF CANDIDATE BOTTOMING CYCLES

<u>Bottoming Cycle</u>	<u>Projected SFC (lb/hp hr)</u>	<u>Volume</u>	<u>Weight</u>
Organic Rankine	0.269 (Table 4.1, Case 5)	+	+
Steam Rankine	0.272 (Table 4.2, Case 5)	+	+
Steam Injection	0.273 (Table 4.4, Case 2)	-	-
Open Brayton	0.287 (Table 4.6, Case 2)	+	+
Closed Brayton	0.303 (Table 4.7)	+	+
Stirling	0.284 (Table 4.10, Case 1)	+	+

5. EVALUATION OF SELECTED HEAT RECOVERY SYSTEMS

The bottoming systems selected for further evaluation in the screening phase were:

- o Organic Rankine cycle
- o Steam injection cycle
- o Stirling engine

These systems were first defined more comprehensively than had been done in the screening phase, secondly, performance calculations were made for the truck applications at reference conditions, thirdly, sensitivity analyses were made relative to the adiabatic diesel exhaust temperature, and, finally performance calculations were made for the alternate applications - locomotive and marine.

5.1 Organic Rankine Cycle

5.1.1 Truck Applications

The RC-1 cycle conditions used by the Thermo Electron Corporation (TECO) in Reference 1 were used as the reference conditions in the organic Rankine cycle evaluation. This was done to provide a comparison between the fluidized bed heat exchanger and the conventional heat exchanger for an organic Rankine bottoming cycle.

A schematic drawing of this system is shown in Figure 5.1. The heat recovery apparatus consists of two fluidized beds and one convective heat exchanger. The feed fluid is regeneratively heated and the condenser is air cooled.

The state points for the reference conditions for the truck application are given in Table 5.1. State points for $\pm 45^{\circ}\text{F}$ adiabatic

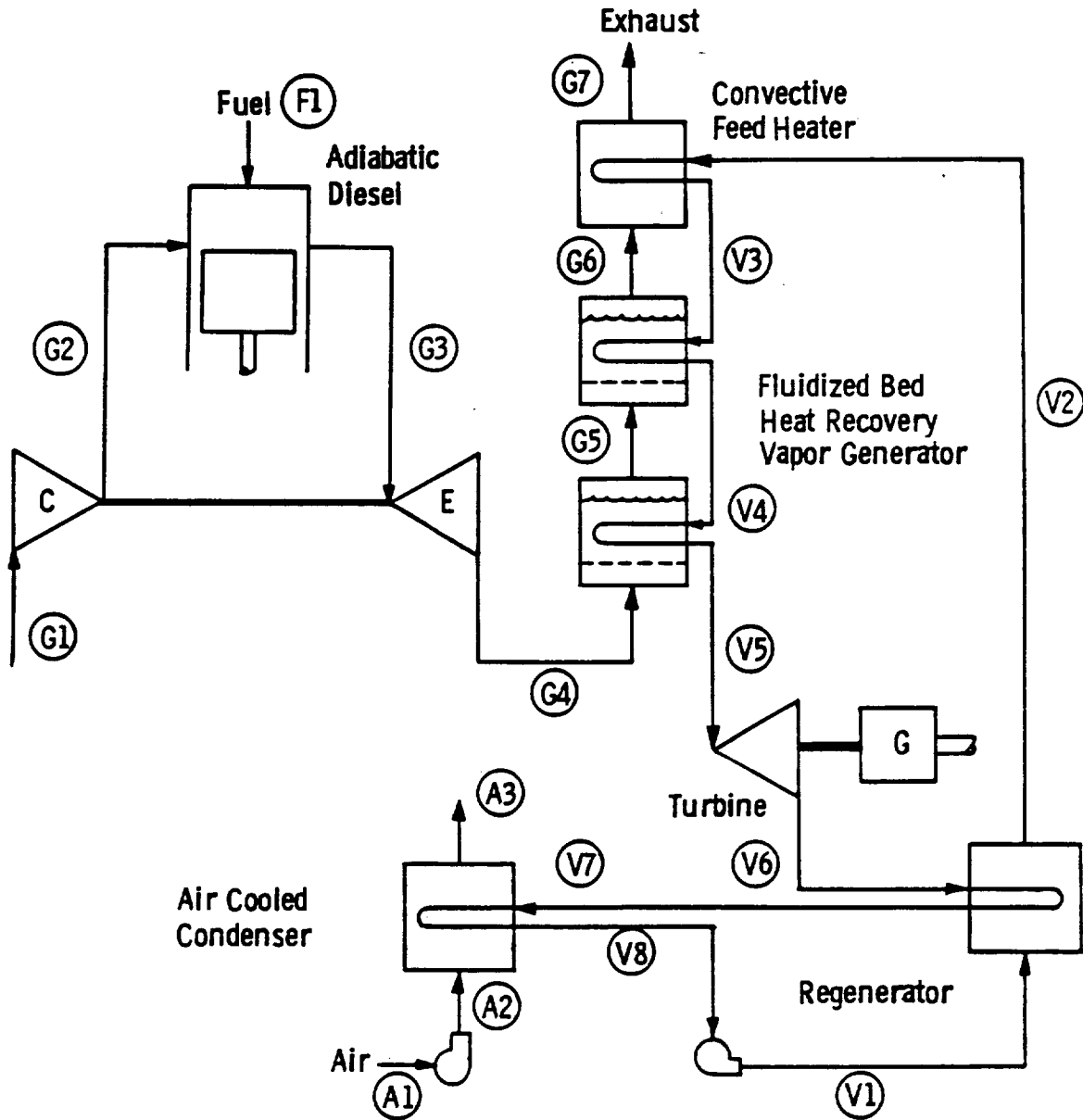


Fig. 5. 1—Turbocharged diesel with subposed organic Rankine cycle.

TABLE 5.1--ATCD WITH ORGANIC RANKINE CYCLE USING RC-1 (REFERENCE CONDITIONS TRUCK APPLICATION)

Station	Pressure (Psia)	Temperature (°F)	Enthalpy (Btu/lb)	Flow Rate (lb/s)	Composition
G1	14.7	59	28.6	0.774	Air
G2	-	-	-	0.774	Air
G3	-	1445	-	0.802	(1)
G4	17.18	1245	343.3	0.802	(1)
G5	-	900	247.0	0.802	(1)
G6	-	587	163.2	0.802	(1)
G7	≤ 16.66	347	101.3	0.802	(1)
F1	-	59	-	0.0278	No. 2 Dist.
V1	880	148	28.6	1.216	RC-1
V2	870	317	78.7	1.216	RC-1
V3	852	422	120.8	1.216	RC-1
V4	828	557	176.0	1.216	RC-1
V5	800	750	232.7	1.216	RC-1
V6	8.0	542	193.5	1.216	RC-1
V7	-	320	143.4	1.216	RC-1
V8	7.0	135	25.1	1.216	RC-1
A1	14.7	59	28.6	9.79	Air
A2	14.7+	59	28.6	"	Air
A3	14.7	120	43.3	"	Air

(1) Air - 0.4663
 CO₂ - 0.0721
 H₂O - 0.0725
 N₂ - 0.3843
 A - 0.0048

diesel engine exhaust temperatures are given in Tables 5.2 and 5.3. The calculated performance for these three cases are summarized in Table 5.4. These results show that the specific fuel consumption of the compound system varies about 1.7% for a 100°F change in diesel engine exhaust temperature.

5.1.2 Locomotive Application

The state points for the reference conditions for the locomotive application are shown in Table 5.5. All parameters except flow rate are the same as for the truck application. The capacity multiplier is 9.64 and the flow rate is proportionally greater for the truck application.

5.1.3 Marine Application

The state points for the reference conditions for the marine application are shown in Table 5.6. In the marine application the condenser is water cooled rather than air cooled so several of the temperature and pressure values are different from those for the truck and locomotive applications. The capacity multiplier is 15.0 but the flow rate multiplier is only 14.8. The use of the water cooled condenser also affects the system performance as shown in Table 5.7.

5.2 Steam Injection Cycle

The flow sheet for the turbocompound adiabatic diesel engine with integrated steam injection was modified as shown in Figure 5.2. A steam-heated feedwater heater was added to avoid cold end corrosion problems in the convection feedwater heater. This change does not affect the system performance. It does, however, affect the size and cost of the fluidized bed boiler.

The heat recovery train temperature profile for the steam injection cycle is shown in Figure 5.3.

TABLE 5.2-ATCD WITH ORGANIC RANKINE CYCLE USING RC-1 (HIGH TEMPERATURE CONDITIONS-TRUCK APPLICATION)

Station	Pressure (Psia)	Temperature (°F)	Enthalpy (Btu/lb)	Flow Rate (lb/s)	Composition
G1	14.7	59	28.6	0.774	Air
G2	-	-	-	0.774	Air
G3	-	1490	-	0.802	(1)
G4	17.18	1290	356.3	0.802	(1)
G5	-	900	247.0	0.802	(1)
G6	-	575	160.0	0.802	(1)
G7	≤ 16.66	347	101.3	0.802	(1)
F1	-	59	-	0.0278	No. 2 Dist.
V1	880	148	28.6	1.281	RC-1
V2	870	317	78.7	1.281	RC-1
V3	~ 852	413	117.3	1.281	RC-1
V4	~ 828	545	171.9	1.281	RC-1
V5	800	750	232.7	1.281	RC-1
V6	8.0	542	193.5	1.281	RC-1
V7	-	320	143.4	1.281	RC-1
V8	7.0	135	25.1	1.281	RC-1
A1	14.7	59	28.6	10.31	Air
A2	14.7+	~ 59	28.6	"	Air
A3	14.7	120	43.3	"	Air

(1) Air - 0.4663
 CO₂ - 0.0721
 H₂O - 0.0725
 N₂ - 0.3843
 A - 0.0048

TABLE 5.3—ATCD WITH ORGANIC RANKINE CYCLE USING RC-1 (LOW TEMPERATURE CONDITIONS - TRUCK APPLICATION)

Station	Pressure (Psia)	Temperature (°F)	Enthalpy (Btu/lb)	Flow Rate (Lb/s)	Composition
G1	14.7	59	28.6	0.774	Air
G2	-	-	-	0.774	Air
G3	-	1400	-	0.802	(1)
G4	17.18	1200	330.6	0.802	(1)
G5	-	900	247.0	0.802	(1)
G6	-	607	168.4	0.802	(1)
G7	≤16.66	347	101.3	0.802	(1)
F1	-	59	-	0.0278	No. 2Dist.
V1	880	148	28.6	1.152	RC-1
V2	870	317	78.7	1.152	RC-1
V3	~ 852	439	128.0	1.152	RC-1
V4	~ 828	577	182.1	1.152	RC-1
V5	800	750	232.7	1.152	RC-1
V6	8.0	542	193.5	1.152	RC-1
V7	-	320	143.4	1.152	RC-1
V8	7.0	135	25.1	1.152	RC-1
A1	14.7	59	28.6	9.28	Air
A2	14.7 +	~59	~28.6	"	Air
A3	14.7	120	43.3	"	Air

(1) Air - 0.4663
 CO₂ - 0.0721
 H₂O - 0.0725
 N₂ - 0.3843
 A - 0.0048

Table 5.4

ADIABATIC DIESEL EXHAUST GAS TEMPERATURE SENSITIVITY ANALYSIS
FOR THE TURBOCHARGED ENGINE WITH ORGANIC RANKINE BOTTOMING CYCLE

Case	1	2	3
Engine Type	ATCD	_____>	
Working Fluid	RCI	_____>	
Exhaust Temp. - °F	1245, Note 1	1290	1200
Stack Temp. - °F	347	347	347
Heat Recovered - Btu/hr	673,940	710,200	638,743
Turbine Power - hp	62.4	65.8	59.2
Pump Power - hp	6.2	6.5	5.9
Net Power - hp	56.2	59.3	53.3
System			
Power - hp	373.3	376.4	370.4
SFC - lb/hp hr	0.269	0.267	0.271
PIF, Note 2	1.098	1.107	1.089

(1) Reference Case

(2) Relative to ATCPD/A Engine Configuration, PIF is Performance Improvement Factor

TABLE 5.5-ATCD WITH ORGANIC RANKINE CYCLE USING RC-1
(REFERENCE CONDITIONS-LOCOMOTIVE APPLICATION)

Station	Pressure (Psia)	Temperature (°F)	Enthalpy (Btu/lb)	Flow Rate (lb/s)	Composition
G1	14.7	59	28.6	7.46	Air
G2	-	-	-	7.46	Air
G3	-	1445	-	7.73	(1)
G4	17.18	1245	343.3	7.73	(1)
G5	-	900	247.0	7.73	(1)
G6	-	587	163.2	7.73	(1)
G7	≤ 16.66	347	101.3	7.73	(1)
F1	-	59	-	0.268	No. 2 Dist.
V1	880	148	28.6	11.73	RC-1
V2	870	317	78.7	11.73	RC-1
V3	852	422	120.8	11.73	RC-1
V4	828	557	176.0	11.73	RC-1
V5	800	750	232.7	11.73	RC-1
V6	8.0	542	193.5	11.73	RC-1
V7	-	320	143.4	11.73	RC-1
V8	7.0	135	25.1	11.73	RC-1
A1	14.7	59	28.6	94.4	Air
A2	14.7+	59	28.6	94.4	Air
A3	14.7	120	43.3	94.4	Air

(1) Air - 0.4663
 CO₂ - 0.0721
 H₂O - 0.0725
 N₂ - 0.3843
 A - 0.0048

TABLE 5.6-ATCD WITH ORGANIC RANKINE CYCLE USING RC-1
(REFERENCE CONDITIONS-MARINE APPLICATION)

Station	Pressure (Psia)	Temperature (°F)	Enthalpy (Btu/lb)	Flow Rate (lb/s)	Composition
G1	14.7	59	28.6	11.43	Air
G2	-	-	-	11.43	Air
G3	-	1445	-	11.84	(1)
G4	17.18	1245	343.3	11.84	(1)
G5	-	900	247.0	11.84	(1)
G6	-	587	163.2	11.84	(1)
G7	≤ 16.66	347	101.3	11.84	(1)
F1	-	59	-	0.410	No. 2 Dist.
V1	800	104	17.2	17.88	RC-1
V2	870	298	72.4	17.88	RC-1
V3	852	422	120.8	17.88	RC-1
V4	828	557	176.0	17.88	RC-1
V5	800	750	232.7	17.88	RC-1
V6	5.0	528	190.1	17.88	RC-1
V7	+4.0	289	134.9	17.88	RC-1
V8	2.7	90	13.6	17.88	RC-1
W1	14.7	59	59	35.5	Water
W2	14.7 +	59	59	35.5	Water
W3	14.7	120	120	35.5	Water

(1) Air - 0.4663
CO₂ - 0.0721
H₂O - 0.0725
N₂ - 0.3843
A - 0.0048

Table 5.7

PERFORMANCE OF RC-1 ORGANIC RANKINE CYCLE
IN MARINE APPLICATION

Engine Type	ATCD
Cycle Type	Organic Rankine
Working Fluid	RCI
Exhaust Temp. - °F	1245, Note 1
Stack Temp. - °F	347
Heat Recovered - Btu/hr	9.955×10^6
Turbine Power - hp	997.1
Pump Power - hp	92.7
Net Power - hp	904.4
System	
Power - hp	5600
SFC - lb/hp hr	0.264
PIF, Note 2	1.110

-
- (1) Reference Case
(2) Relative to ATCPD/A Engine Configuration, PIF is Performance Improvement Factor

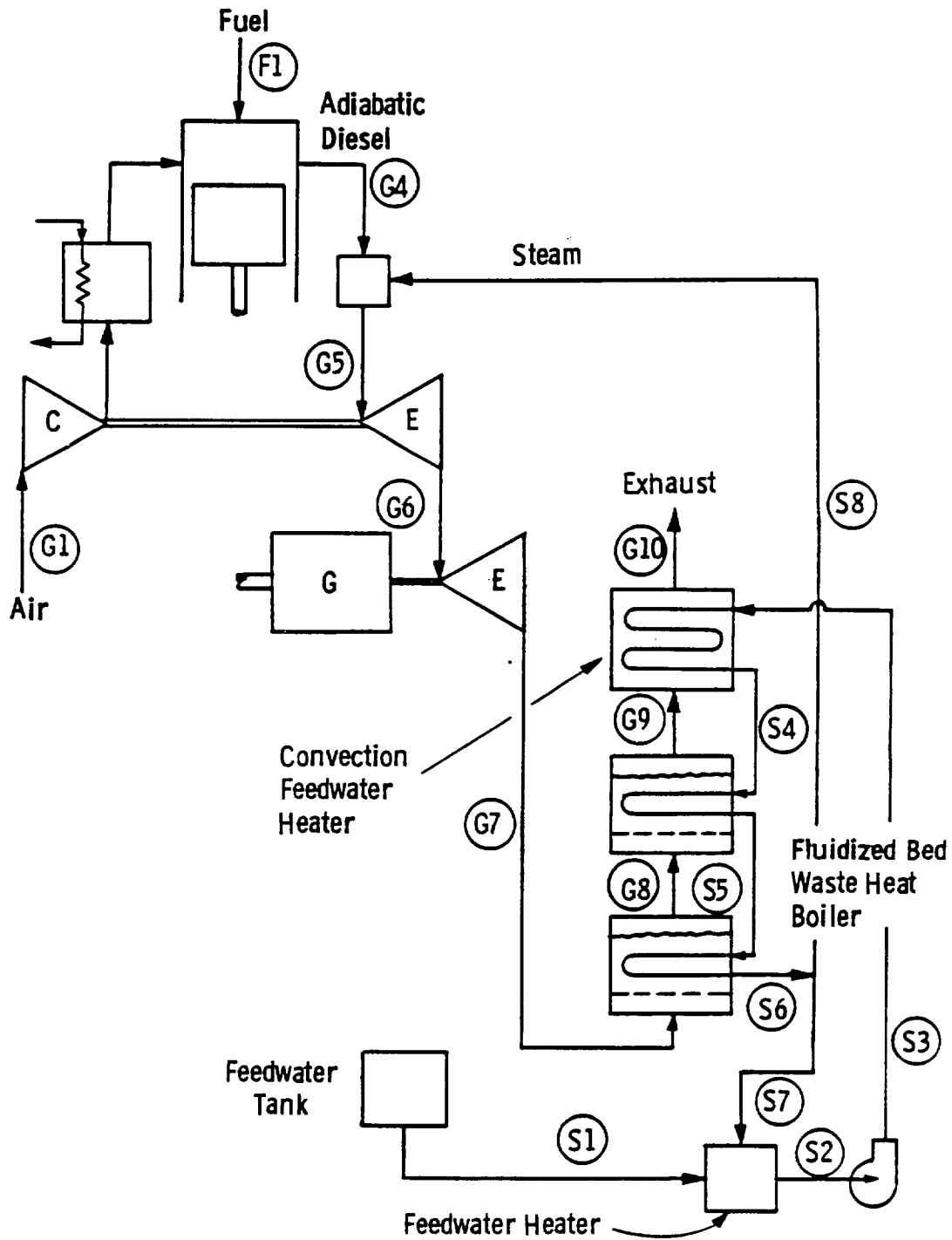


Fig. 5. 2—Turbocompound diesel with steam injection ahead of compressor drive expander.

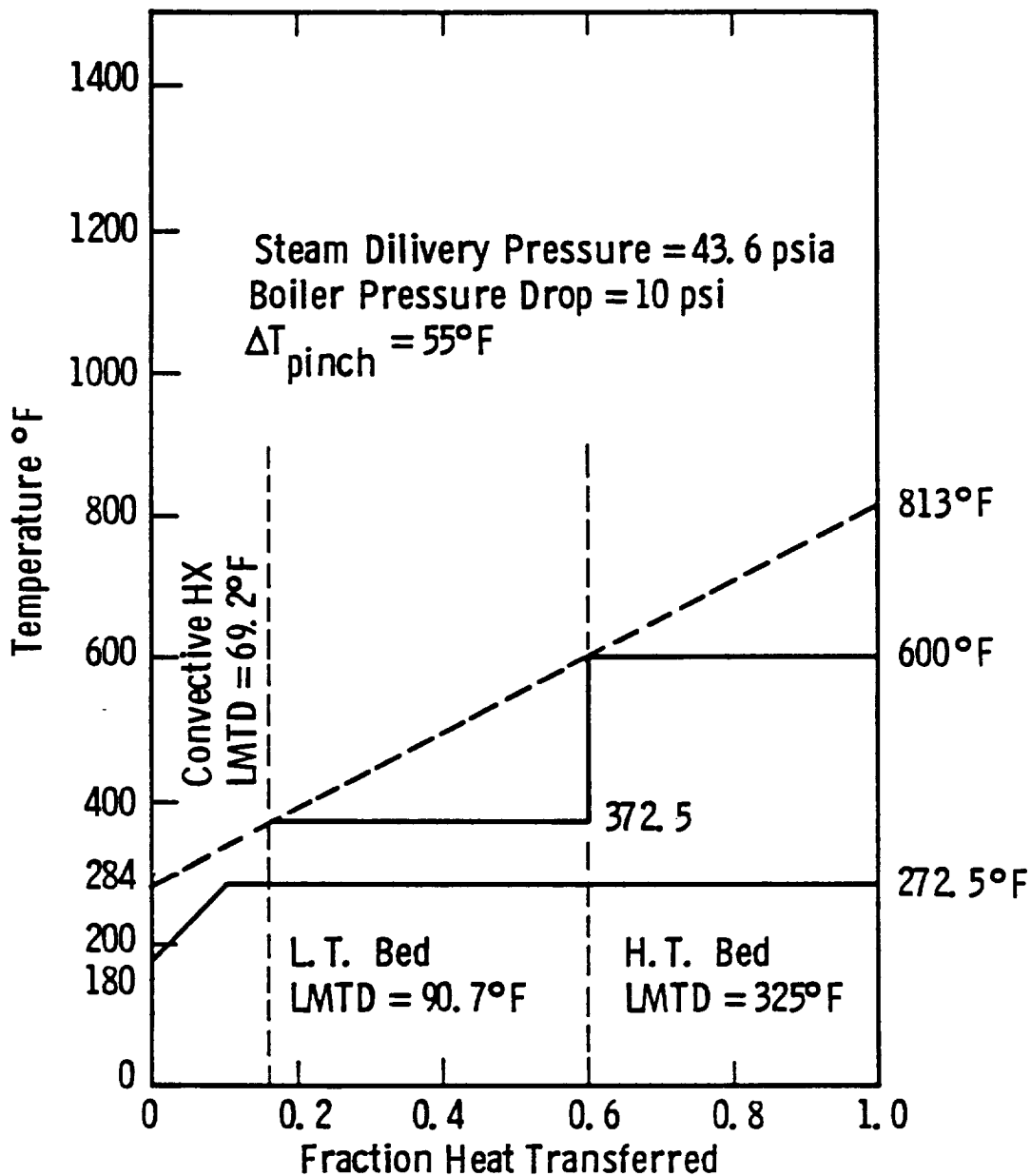


Fig. 5.3—Fluidized bed heat exchanger temperature profile. Turbocompound engine with steam injection ahead of compressor drive expander

5.2.1 Truck Application

The reference case state point conditions for the truck application are listed in Table 5.8. Calculations were made for $\pm 40^\circ\text{F}$ variations in the cylinder exhaust temperature of the turbocompound engine compressor-drive expander to determine the sensitivity of the system performance. State points conditions for these two cases are listed in Tables 5.9 and 5.10.

The system performances for the three cases for the truck application are summarized in Table 5.11. This indicates that there is a 2.3% change in the system specific fuel consumption for a 100°F variation in cylinder exhaust temperature.

5.2.2 Locomotive and Marine Applications

The state point conditions for the steam injection cycle in the locomotive application are given in Table 5.12 and those for the marine application are given in Table 5.13. Since there is no heat rejection in this cycle, the performances for all applications, including the marine, are the same and the only parameter which varies with application is flow rate. The flow rate multiplier for the locomotive and marine applications are 9.64 and 15.48 respectively.

5.3 Stirling Engine

The final configuration of the Stirling engine bottoming cycle with heat pipes is shown in Figure 5.4. The heat recovery temperature profile for this system is shown in Figure 5.5. Two subposed Stirling engines are used -- one high temperature and one low temperature. Each engine has a dedicated fluidized bed that operates at the respective temperature but are integrated into one heat exchanger unit. Mercury is used as the working fluid in the high temperature heat pipes and toluene is used in the low temperature ones. Hydrogen is used as the working fluid in the Stirling engines.

TABLE 5.8--ATC PD/A WITH STEAM INJECTION (REFERENCE CASE) FOR TRUCK APPLICATION

Station	Pressure psia	Temperature deg F	Flow Rate lb/s	Composition
G1	14.7	59	0.776	1
G2	39.0	291	0.776	1
G3	-	-	0.776	1
G4	43.6	1380	0.804	2
G5	43.6	1127	0.927	3
G6	26.9	974	0.927	3
G7	15.5	813	0.927	3
G8	15.2	600	0.927	3
G9	14.9	373	0.927	3
G10	14.7	284	0.927	3
S1	14.7	59	0.1228	
S2	14.7	180	0.1373	
S3	53.6	180	0.1373	
S4	50.3	281	0.1373	
S5	46.9	277	0.1373	
S6	43.6	273	0.1373	
S7	43.6	273	0.0145	
S8	43.6	273	0.1228	
F1	-	59	0.0277	

Gas Compositions

Gas Comp. No	1	2	3
Exc. Dry Air	1.0000	.46631	.37440
(CO ₂)	.00000	.72046-001	.57847-001
Water Vapor	.00000	.72516-001	.25531
(SO ₂)	.00000	.00000	.00000
Nitrogen	.00000	.38431	.30856
Argon	.00000	.48259-002	.38748-002
Mol. Weight	28.969	28.945	26.791
Gas Constant	53.320	53.388	59.771

TABLE 5.9—ATCPD/A WITH STEAM INJECTION (HIGH TEMPERATURE CASE) FOR TRUCK APPLICATION

Station	Pressure psia	Temperature deg F	Flow Rate lb/s	Composition
G1	14.7	59	0.776	1
G2	39.0	291	0.776	1
G3	—	—	0.776	1
G4	43.6	1420	0.804	2
G5	43.6	1149	0.933	3
G6	27.2	998	0.933	3
G7	15.5	832	0.933	3
G8	15.2	600	0.933	3
G9	14.9	373	0.933	3
G10	14.7	282	0.933	3
S1	14.7	59	0.1292	
S2	14.7	180	0.1445	
S3	53.6	180	0.1445	
S4	50.3	281	0.1445	
S5	46.9	277	0.1445	
S6	43.6	273	0.1445	
S7	43.6	273	0.0153	
S8	43.6	273	0.1292	
F1	—	59	0.0277	

Gas Compositions

Gas Comp. No	1	2	3
Exc. Dry Air	1.0000	.46631	.37062
(CO ₂)	.00000	.72045-001	.57263-001
Water Vapor	.00000	.72516-001	.26283
(SO ₂)	.00000	.00000	.00000
Nitrogen	.00000	.38431	.30545
Argon	.00000	.48259-002	.38357-002
Mol. Weight	28.969	28.945	26.703
Gas Constant	53.320	53.388	60.033

TABLE 5.10-ATCPD/A WITH STEAM INJECTION (LOW TEMPERATURE CASE) FOR TRUCK APPLICATION

Station	Pressure psia	Temperature deg F	Flow Rate lb/s	Composition
G1	14.7	59	0.776	1
G2	39.0	291	0.776	1
G3	-	-	0.776	1
G4	43.6	1340	0.804	2
G5	43.6	1105	0.920	3
G6	26.5	949	0.920	3
G7	15.5	796	0.920	3
G8	15.2	600	0.920	3
G9	14.9	373	0.920	3
G10	14.7	287	0.920	3
S1	14.7	59	0.1165	
S2	14.7	180	0.1303	
S3	53.6	180	0.1303	
S4	50.3	281	0.1303	
S5	46.9	277	0.1303	
S6	43.6	273	0.1303	
S7	43.6	273	0.0138	
S8	43.6	273	0.1165	
F1	-	59	0.0277	

Gas Compositions

Gas Comp. No	1	2	3
Exc. Dry Air	1.0000	.46631	.37825
(CO ₂)	.00000	.72046-001	.58441-001
Water Vapor	.00000	.72516-001	.24766
(SO ₂)	.00000	.00000	.00000
Nitrogen	.00000	.38431	.31173
Argon	.00000	.48259-002	.39146-002
Mol. Weight	28.969	28.945	26.881
Gas Constant	53.320	53.388	59.504

Table 5.11

ADIABATIC DIESEL EXHAUST GAS TEMPERATURE SENSITIVITY ANALYSIS FOR
TURBOCOMPOUND ENGINE WITH STEAM INJECTION AHEAD OF
COMPRESSOR-DRIVE EXPANDER

Engine Type	ATCPD/A	_____>	
Cylinder Temp. - °F	1380, Note 1	1420	1340
Stack Temp. - °F	284	282	287
Heat Recovered - Btu/hr	510,912	537,350	484,320
Basic Engine Pwr. - hp	299.8	_____>	
Net Expander Pwr. - hp	62.2	65.4	59.1
System			
Power - hp	362.0	365.2	358.9
SFC - lb/hp hr	0.275	0.273	0.278
PIF, Note 2	1.065	1.074	1.056

(1) Reference Case

(2) Relative to ATCPD/A Engine Configuration, PIF is Performance Improvement Factor

TABLE 5. 12--ATCPD/A WITH STEAM INJECTION (REFERENCE CASE) FOR LOCOMOTIVE APPLICATION

Station	Pressure psia	Temperature deg F	Flow Rate lb/s	Composition
G1	14.7	59	7.48	1
G2	39.0	291	7.48	1
G3	-	-	7.48	1
G4	43.6	1380	7.75	2
G5	43.6	1127	8.94	3
G6	26.9	974	8.94	3
G7	15.5	813	8.94	3
G8	15.2	600	8.94	3
G9	14.9	373	8.94	3
G10	14.7	284	8.94	3
S1	14.7	59	1.184	
S2	14.7	180	1.324	
S3	53.6	180	1.324	
S4	50.3	281	1.324	
S5	46.9	277	1.324	
S6	43.6	273	1.324	
S7	43.6	273	0.140	
S8	43.6	273	1.184	
F1	-	59	0.2670	

Gas Compositions

Gas Comp. No	1	2	3
Exc. Dry Air	1.0000	.46631	.37440
(CO ₂)	.00000	.72046-001	.57847-001
Water Vapor	.00000	.72516-001	.25531
(SO ₂)	.00000	.00000	.00000
Nitrogen	.00000	.38431	.30856
Argon	.00000	.48259-002	.38748-002
Mol. Weight	28.969	28.945	26.791
Gas Constant	53.320	53.388	59.771

TABLE 5.13—ATC PD/A WITH STEAM INJECTION (REFERENCE CASE) FOR MARINE APPLICATION

Station	Pressure psia	Temperature deg F	Flow Rate lb/s	Composition
G1	14.7	59	12.01	1
G2	39.0	291	12.01	1
G3	-	-	12.01	1
G4	43.6	1380	12.44	2
G5	43.6	1127	14.34	3
G6	26.9	974	14.34	3
G7	15.5	813	14.34	3
G8	15.2	600	14.34	3
G9	14.9	373	14.34	3
G10	14.7	284	14.34	3
S1	14.7	59	1.900	
S2	14.7	180	2.124	
S3	53.6	180	2.124	
S4	50.3	281	2.124	
S5	46.9	277	2.124	
S6	43.6	273	2.124	
S7	43.6	273	0.2243	
S8	43.6	273	1.900	
F1	-	59	0.4285	

Gas Compositions

Gas Comp. No	1	2	3
Exc. Dry Air	1.0000	.46631	.37440
(CO ₂)	.00000	.72046-001	.57847-001
Water Vapor	.00000	.72516-001	.25531
(SO ₂)	.00000	.00000	.00000
Nitrogen	.00000	.38431	.30856
Argon	.00000	.48259-002	.38748-002
Mol. Weight	28.969	28.945	26.791
Gas Constant	53.320	53.388	59.771

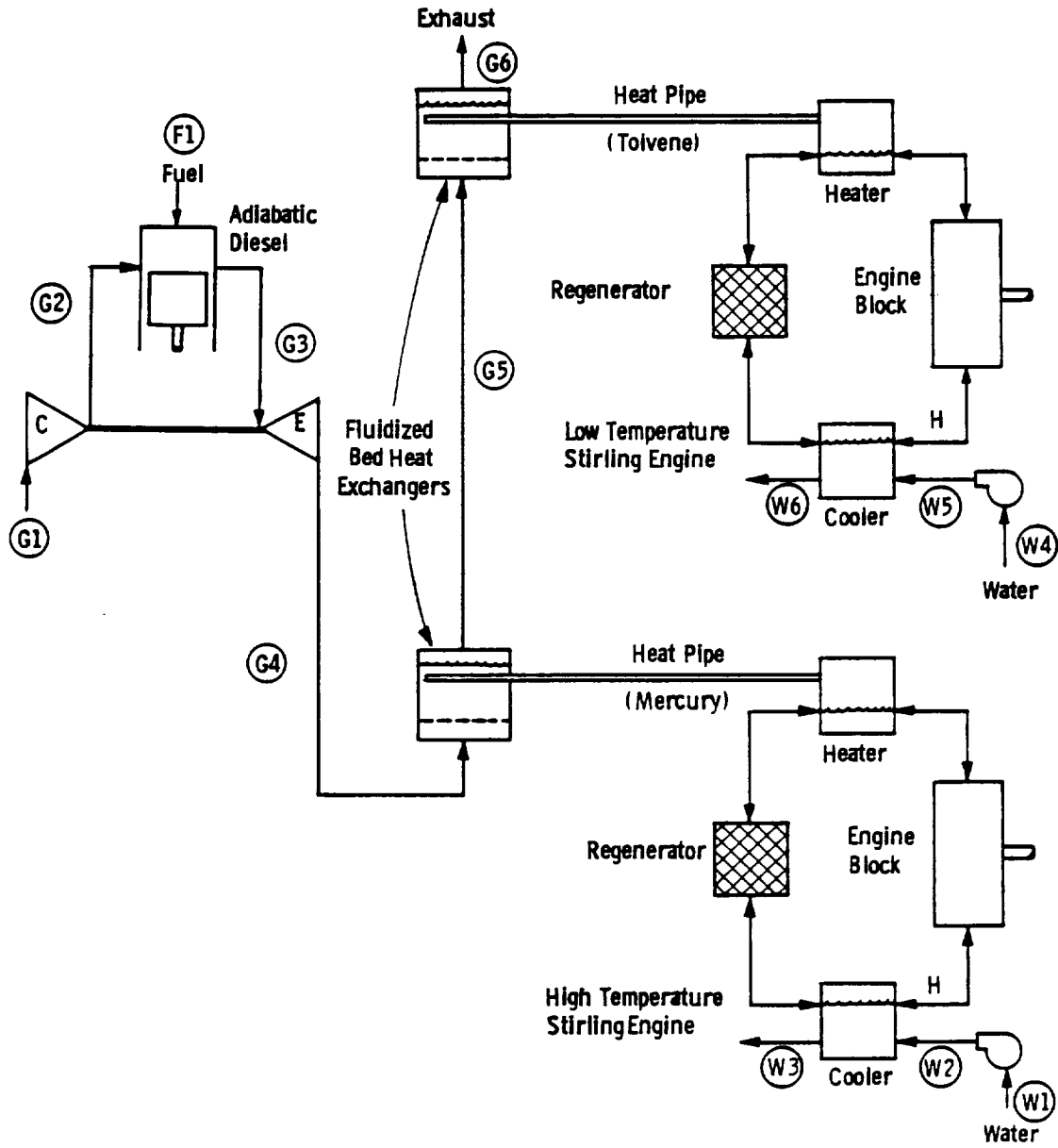


Fig. 5.4—Adiabatic diesel with subposed stirling engines using heat pipes

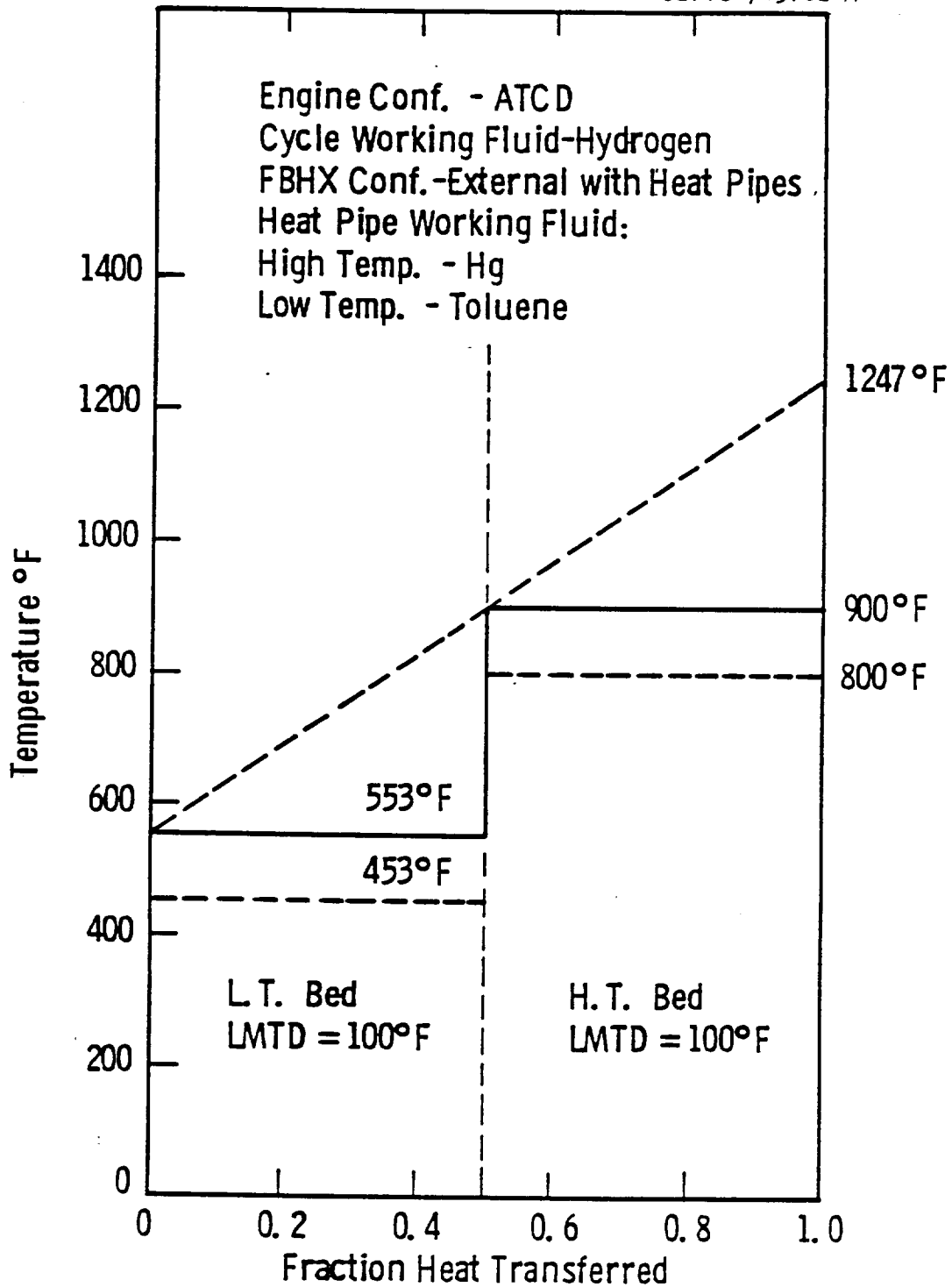


Fig. 5.5—Fluidized bed heat exchanger temperature profile, Stirling engine

5.3.1 Truck Application

The MOD1 Stirling engine configuration shown in Figure 5.6 and described in Reference 20 was used as a model for the performance calculations. The Carlquist formula described in Reference 21 was used for estimating the Stirling engine performance as a function of design parameters;

$$\eta_{net} = (1-T_c/TH) \times C \times \eta_H \times \eta_m \times fa$$

where

- C = Carnot efficiency ratio
- η_H = heater efficiency
- η_m = engine mechanical efficiency
- fa = auxiliary power ratio
- Tc = cold end temperature
- TH = hot end temperature
- η_{net} = net engine efficiency

Values for some of these parameters for the MOD1 engine configuration are as follows:

$$\begin{aligned}\eta_H &= 0.92 \\ T_c &= 50C (323^\circ F) \\ TH &= 720C (993^\circ F) \\ \eta_{net} &= 0.277\end{aligned}$$

The lumped value for the other parameters is therefore:

$$\begin{aligned}C \times \eta_m \times fa &= \eta_{net} / ((1-T_c/TH) \times \eta_H) \\ &= 0.277 / ((1-323/993) \times 0.92) = 0.446\end{aligned}$$

Assuming 1% heat loss in the heat pipes gives:

$$\begin{aligned}\eta_{net} &= (1-T_c/TH) \times 0.446 \times 0.99 \\ &= (1-T_c/TH) \times 0.442\end{aligned}$$

ORIGINAL PAGE IS
OF POOR QUALITY

Dwg. 9370A34

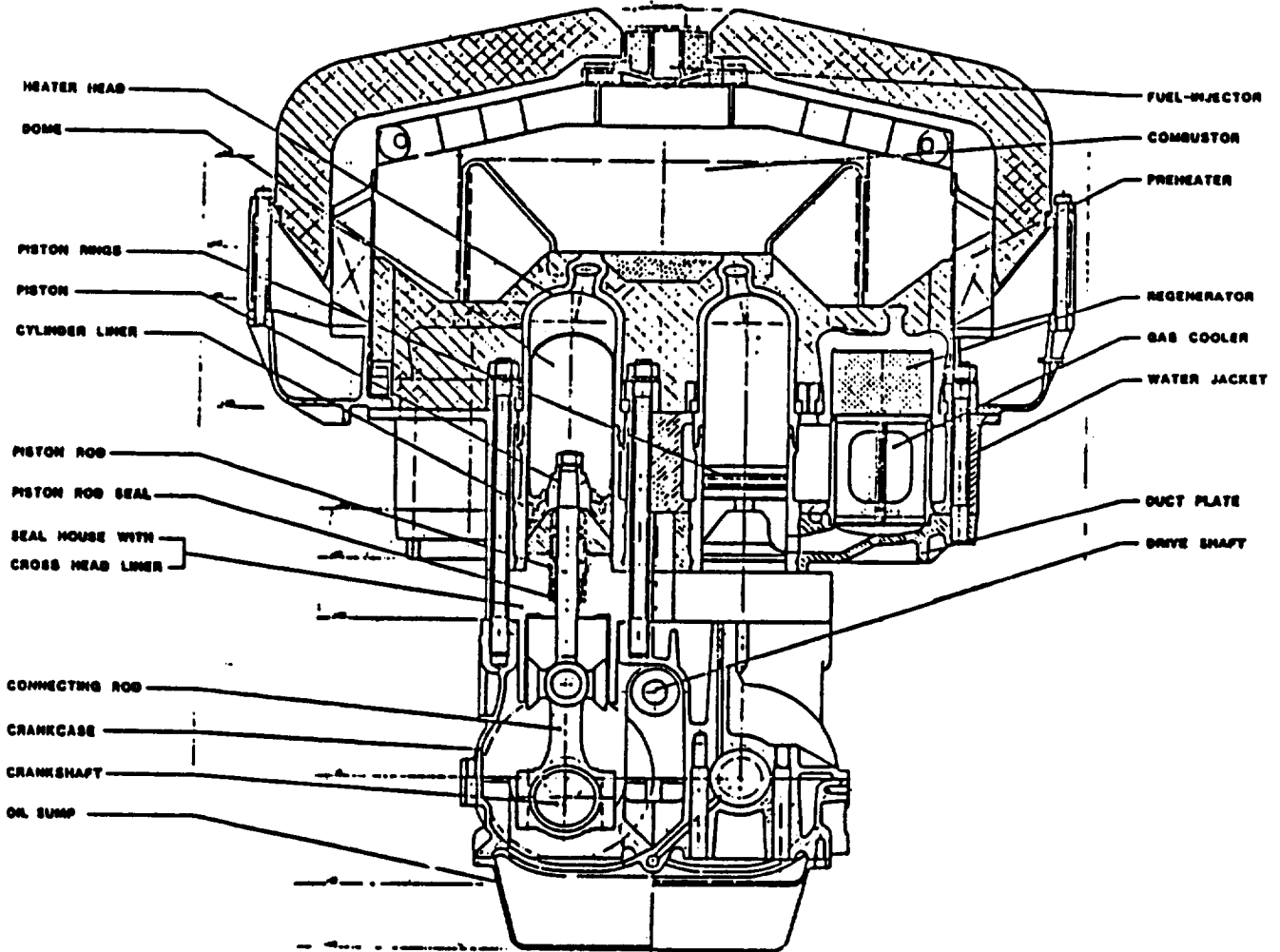


Fig. 5.6—Basic Mod I Stirling engine

Performance calculations were made for this system for the reference conditions for the truck application and for +53°F and -47°F variations of the diesel engine exhaust temperature.

State points conditions for the reference, high temperature, and low temperature cases are listed in Tables 5.14, 5.15 and 5.16 respectively. The calculated performance for these three cases are summarized in Table 5.17 and 5.18. The sensitivity of system specific fuel consumption to diesel engine exhaust temperature is indicated to be about 2.5% per 100°F.

5.3.2 Locomotive and Marine Applications

The state point conditions for the locomotive and marine applications are listed in Tables 5.19 and 5.20, respectively. The values for the locomotive are the same as those for the truck except for flow rate. The flow rate multiplier is 10.0. System performance is unaffected.

For the marine application, heat rejection is to the river water rather than to the air so the cold end temperature of the Stirling engines is reduced from 122°F to 105°F. Temperature and enthalpy values are, therefore, different for the marine application. The system performance is only slightly affected as shown in Table 5.21.

5.4 Performance of Selected Systems

The performances of the three selected systems for each of the three applications are summarized in Table 5.22. This indicates that the organic Rankine cycle has a 2% advantage in the Specific Fuel Consumption (SFC) than the steam injection and 4% better than the Stirling for the truck and locomotives applications. For the marine application, the organic Rankine cycle shows a 4% advantage in SFC than steam injection and 6% better than the Stirling engine.

These results when compared to the NASA reference adiabatic Turbocompound Diesel with aftercooling (Table 2.1) show that the heat recovery subsystem can result in a 5 to 11 percent SFC advantage for the

adiabatic diesel. The cost effectiveness of the SFC advantage will depend on the trade-off between the fuel cost savings and heat recovery system capital investment.

TABLE 5.14—MASS AND ENERGY BALANCE FOR ATC'D WITH DUAL STIRLING ENGINES USING HEAT PIPES (REFERENCE CASE FOR TRUCK APPLICATION)

Station	Pressure (Psia)	Temperature (°F)	Enthalpy (Btu/lb)	Flow Rate (lb/s)	Composition
G1	14.69	59	28.6	0.774	Air
G2	-	-	-	0.774	Air
G3	-	-	-	0.802	(1)
G4	17.54	1247	343.6	0.802	(1)
G5	17.09	900	247.0	0.802	(1)
G6	16.66	553	154.3	0.802	(1)
F1	-	59	-	0.0278	Fuel Oil
W1	-	100	68	3.8	H ₂ O
W2	-	100	68	3.8	H ₂ O
W3	-	115	83	3.8	H ₂ O
W4	-	100	68	4.1	H ₂ O
W5	-	100	68	4.1	H ₂ O
W6	-	115	83	4.1	H ₂ O

(1) Air - 0.4663
 CO₂ - 0.0721
 H₂O - 0.0725
 N₂ - 0.3843
 A - 0.0048

TABLE 5.15—MASS AND ENERGY BALANCE FOR ATCD WITH DUAL STIRLING ENGINES USING HEAT PIPES (HIGH TEMPERATURE CASE FOR TRUCK APPLICATION)

Station	Pressure (Psia)	Temperature (°F)	Enthalpy (Btu/lb)	Flow Rate (lb/s)	Composition
G1	14.69	59	28.6	0.774	Air
G2	-	-	-	0.774	Air
G3	-	-	-	0.802	(1)
G4	17.54	1300	359.2	0.802	(1)
G5	17.09	900	247.0	0.802	(1)
G6	16.66	500	140.5	0.802	(1)
F1	-	59	-	0.0278	Fuel Oil
W1	-	100	68	4.5	H ₂ O
W2	-	100	68	4.5	H ₂ O
W3	-	115	83	4.5	H ₂ O
W4	-	100	68	4.8	H ₂ O
W5	-	100	68	4.8	H ₂ O
W6	-	115	83	4.8	H ₂ O

(1) Air - 0.4663
 CO₂ - 0.0721
 H₂O - 0.0725
 N₂ - 0.3843
 A - 0.0048

TABLE 5.16—MASS AND ENERGY BALANCE FOR ATCD WITH DUAL STIRLING
 ENGINES USING HEAT PIPES (LOW TEMPERATURE CASE FOR TRUCK
 APPLICATION)

Station	Pressure (Psia)	Temperature (°F)	Enthalpy (Btu/lb)	Flow Rate (lb/s)	Composition
G1	14.69	59	28.6	0.774	Air
G2	-	-	-	0.774	Air
G3	-	-	-	0.802	(1)
G4	17.54	1200	330.6	0.802	(1)
G5	17.09	900	247.0	0.802	(1)
G6	16.66	600	166.6	0.802	(1)
F1	-	59	-	0.0278	Fuel Oil
W1	-	100	68	3.3	H ₂ O
W2	-	100	68	3.3	H ₂ O
W3	-	115	83	3.3	H ₂ O
W4	-	100	68	3.5	H ₂ O
W5	-	100	68	3.5	H ₂ O
W6	-	115	83	3.5	H ₂ O

(1) Air - 0.4663
 CO₂ - 0.0721
 H₂O - 0.0725
 N₂ - 0.3843
 A - 0.0048

Table 5.17

STIRLING ENGINE PERFORMANCE SUMMARY
FOR
TRUCK APPLICATION

Case	Base	High Temp	Low Temp
Engine Exhaust Temp - °F	1247	1300	1200
High Temperature Engine			
Bed Temp - °F	900	900	900
Heat Recovered - Btu/hr	271,818	315,714	235,238
Heat Pipe Losses - %	1.0	1.0	1.0
T_h - °F	797	797	797
T_c - °F	122	122	122
η_{carnot} - %	53.1	53.1	53.1
$C \times \eta_m \times f_a$ (1)	0.446 ⁽¹⁾	0.446 ⁽²⁾	0.446 ⁽²⁾
η_{net} - %	23.7	23.7	23.7
Power - hp	25.3	29.5	21.9
Low Temperature Engine			
Bed Temp - °F	553	500	600
Heat Recovered - Btu/hr	260,884	299,675	226,234
Heat Pipe Losses - %	1.0	1.0	1.0
T_h - °F	450	397	497
T_c - °F	122	122	122
η_{carnot} - %	35.7	31.8	38.8
$C \times \eta_m \times f_a$ (1)	0.446 ⁽²⁾	0.446 ⁽²⁾	0.446 ⁽²⁾
η_{net} - %	15.9	14.2	17.3
Power - hp	16.3	16.7	15.4

(1) Where C = Carnot efficiency,
 η_m = mechanical efficiency, and
 f_a = auxiliary

(2) MOD 1 engine

Table 5.18

PERFORMANCE OF SYSTEM WITH SUBPOSED STIRLING
ENGINES FOR TRUCK APPLICATION

Engine Type	ATCD		
Working Fluid	Hydrogen		
Exhaust Temp. - °F	1247, Note 1	1300	1200
Stack Temp. - °F	553	500	600
Cooler Temp. - °F	122		
High Temperature Unit			
Bed Temp. - °F	900	900	900
Heater Temp. - °F	797	797	797
Heat Recovered-Btu/hr	271818	315714	235238
Net Engine Eff. - %	23.7	23.7	23.7
Power - hp	25.3	29.5	21.9
Low Temperature Unit			
Bed Temp. - °F	553	500	600
Heater Temp. - °F	450	397	497
Heat Recovered - Btu/hr	260844	299675	226234
Net Engine Eff. - %	15.9	14.2	17.3
Power - hp	16.3	16.7	15.4
Total Net Power	41.6	46.2	37.3
System Performance			
Power - hp	358.1	362.7	353.8
SFC - lb/hp hr	0.280	0.277	0.284
PIF, Note 2	1.053	1.067	1.041

(1) Reference Case

(2) Relative to ATPDIA Engine Configuration, PIF is Performance Improvement Factor

TABLE 5.19—MASS AND ENERGY BALANCE FOR ATCD WITH DUAL STIRLING ENGINES USING HEAT PIPES (REFERENCE CASE LOCOMOTIVE APPLICATION)

Station	Pressure (Psia)	Temperature (°F)	Enthalpy (Btu/lb)	Flow Rate (lb/s)	Composition
G1	14.69	59	28.6	7.74	Air
G2	-	-	-	7.74	Air
G3	-	-	-	8.02	(1)
G4	17.54	1247	343.6	8.02	(1)
G5	17.09	900	247.0	8.02	(1)
G6	16.66	553	154.3	8.02	(1)
F1	-	59	-	0.278	Fuel Oil
W1	-	100	68	38	H ₂ O
W2	-	100	68	38	H ₂ O
W3	-	115	83	38	H ₂ O
W4	-	100	68	41	H ₂ O
W5	-	100	68	41	H ₂ O
W6	-	115	83	41	H ₂ O

(1) Air - 0.4663
 CO₂ - 0.0721
 H₂O - 0.0725
 N₂ - 0.3843
 A - 0.0048

TABLE 5. 20—MASS AND ENERGY BALANCE FOR ATCD WITH DUAL STIRLING ENGINES USING HEAT PIPES (REFERENCE CASE MARINE APPLICATION)

Station	Pressure (Psia)	Temperature (°F)	Enthalpy (Btu/lb)	Flow Rate (lb/s)	Composition
G1	14. 69	59	28. 6	12. 52	Air
G2	—	—	—	12. 52	Air
G3	—	—	—	12. 97	(1)
G4	17. 54	1247	343. 6	12. 97	(1)
G5	17. 09	900	247. 0	12. 97	(1)
G6	16. 66	553	154. 3	12. 97	(1)
F1	—	59	—	0. 450	Fuel Oil
W1	—	80	48	60. 8	H ₂ O
W2	—	80	48	60. 8	H ₂ O
W3	—	95	63	60. 8	H ₂ O
W4	—	80	48	65. 6	H ₂ O
W5	—	80	48	65. 6	H ₂ O
W6	—	95	63	65. 6	H ₂ O

(1) Air - 0. 4663
CO₂ - 0. 0721
H₂O - 0. 0725
N₂ - 0. 3843
A - 0. 0048

Table 5.21

PERFORMANCE OF SYSTEM WITH SUBPOSED STIRLING
ENGINES FOR MARINE APPLICATION

Engine Type	ATCD
Working Fluid	Hydrogen
Exhaust Temp. - °F	1247, Note 1
Stack Temp. - °F	553
Cooler Temp. - °F	105
High Temperature Unit	
Bed Temp. - °F	900
Heater Temp. - °F	797
Heat Recovered-Btu/hr	4,232,000
Net Engine Eff. - %	24.3
Power - hp	404.8
Low Temperature Unit	
Bed Temp. - °F	553
Heater Temp. - °F	450
Heat Recovered - Btu/hr	4,061,000
Net Engine Eff. - %	16.8
Power - hp	267.8
Total Net Power	672.6
System Performance	
Power - hp	5600
SFC - lb/hp hr	0.279
PIF, Note 2	1.053

(1) Reference Case

(2) Relative to ATCPD/A Engine Configuration, PIF is Performance Improvement Factor

Table 5.22

PERFORMANCE OF SELECTED SYSTEMS
FOR
THREE APPLICATIONS

System	Truck	Application Locomotive	Marine
Organic Rankine			
System Power-hp	373.3	3500	5600
Subsystem Power-hp	56.2	526.9	904.4
System SFC-lb/hphr	0.269 (1.000)	20.269 (1.000)	0.264 (1.000)
Steam Injection			
System Power-hp	362.0	3500	5600
Subsystem Power-hp	62.2	601.4	962.2
System SFC-lb/hphr	0.275 (1.022)	0.275 (1.022)	0.275 (1.042)
Stirling Engine			
System Power-hp	358.1	3500	5600
Subsystem Power-hp	41.6	416.0	672.6
System SFC-lb/hphr	0.280 (1.041)	0.280 (1.041)	0.279 (1.057)

Note - Numbers in parenthesis are SFC Ratios relative to Organic Ranking System.

6. PRELIMINARY DESIGN AND COSTS OF FLUIDIZED BED HEAT EXCHANGERS FOR SELECTED SYSTEMS

6.1 Conceptual Description of the Heat Recovery Unit

Conceptually, the unit consists of one or more stages of fluidized bed heat recovery with the possibility of a final convective heat recovery stage as is shown in Figure 6.1. Horizontal runs of tubes in many possible configurations pass through each stage of bed and the convective section in a direction generally in counter-current flow with the rising diesel exhaust gas. Each stage of bed is made up of a distributor plate for distributing the diesel gas across the bed cross-section, a fluidized bed of the selected particles, a splash zone directly above the bed and the freeboard region where particles ejected from the bed due to bubbles rising through the bed are allowed to disengage from the gas and drop back into the bed. Diesel exhaust gas is introduced through an inlet plenum to the first distributor plate. The distributor plates are orifice-type plates that are insulated from the fluidized bed to keep it at maximum temperature to minimize deposition. The gas passes through each shallow bed in a mode of turbulent fluidization, resulting in high rates of circulation of the particles in the bed, uniform bed temperature on each stage, and high rates of heat transfer from the bed to the tubes.

Deposits formed on the tubes are removed by the circulating bed material in the form of agglomerated flakes of sooty material. Likewise, deposits on the bed particles are removed as agglomerates, much larger than the original submicron soot particles in the diesel exhaust gas. The agglomerates are assumed to pass through the unit without significant accumulation and to be of a size that could be easily collected downstream.

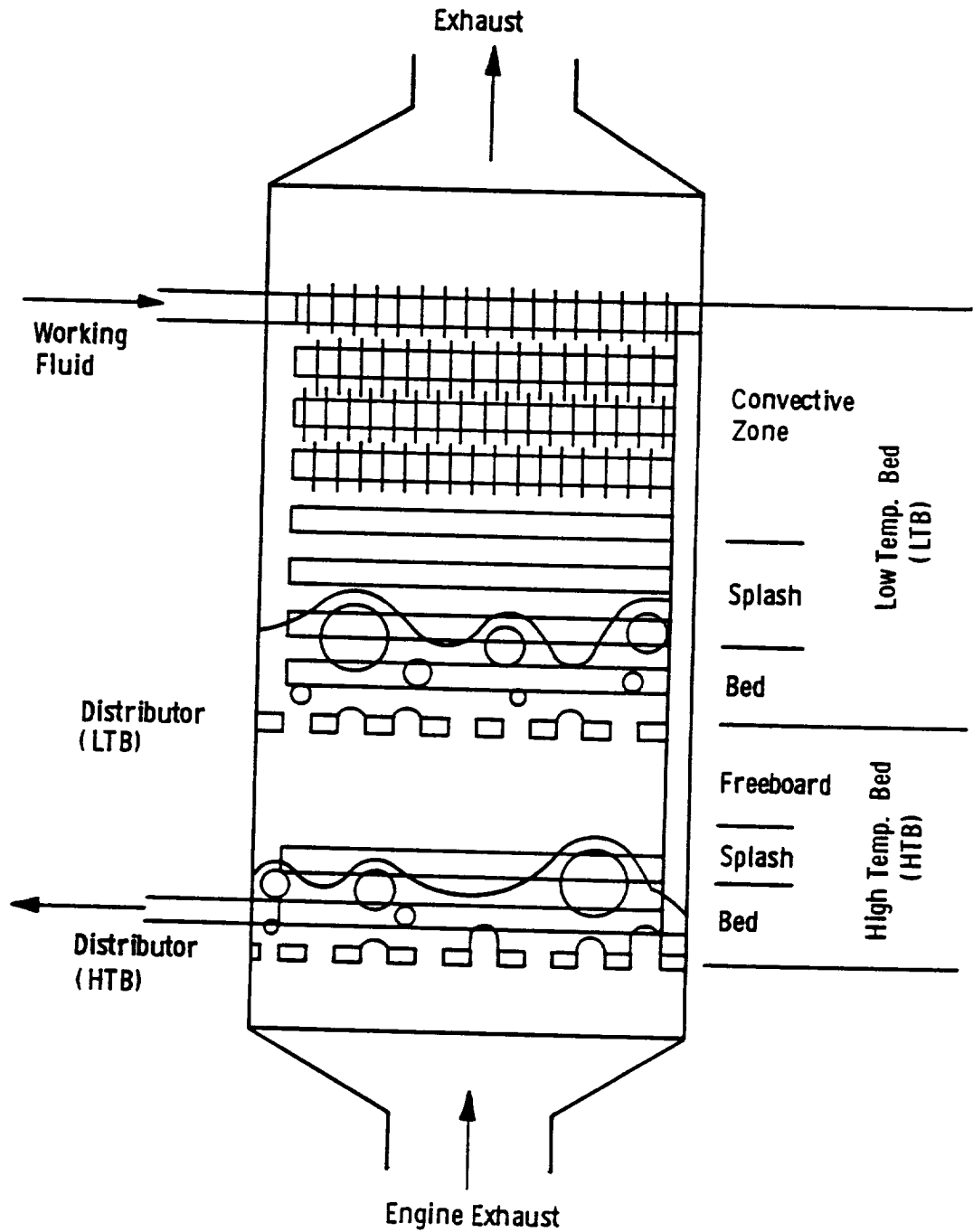


Fig. 6.1—Fluid bed heat recovery unit schematic

The splash region is a dilute zone above each bed where solids are rapidly recirculating and heat transfer rates are nearly as large as they are in the more dense bed. Tubes placed in the splash zone provide effective heat transfer which results in a shallower dense bed while also reducing the height of the freeboard required above each bed. The freeboard, which may contain convective heat transfer surface, simply permits particles ejected from the bed to decay in velocity before they impinge on the underside of the distributor plate above or before they approach the gas exit port.

6.2 Design Procedure

The fluidized bed heat recovery units have been designed using state-of-the-art design techniques for fluidized bed equipment. The following design philosophy and design objectives have been applied:

- 1) The units are designed to meet constraints on exhaust gas pressure drop, set at about 20 inches of water, by proper selection of operating conditions, particle size and density, and tube bundle layout.
- 2) The units are designed to meet constraints on the working fluid pressure drop, set at less than 10% of the supply pressure, by proper sizing of tubes.
- 3) The units are designed to satisfy the thermal effectiveness specified by selection of number of stages, stage temperatures and distribution of heat transfer surface.
- 4) The superficial velocity is selected to give acceptable vessel cross-section dimensions and to be representative of general practice while promoting self-cleaning tube conditions, but limiting tube erosion.
- 5) The units are designed to be operable over the range of capacities desired by proper design of the gas distributors and by bed depth selection. Distributor plates are designed to give stable fluidization, acceptable jet lengths and limited flowback (weeping) of bed particles through the distributor holes.
- 6) The units are designed to be fully functional under expected conditions of translation, acceleration and vibration by proper bed sizing or use of baffles.

- 7) The vessel height is minimized by making maximum use of the splashing zone above the dense bed for heat transfer and by minimizing freeboard height (by using shallow beds, by selecting particle sizes to give limited bubble eruption heights and by using the gas distributor on the above stage and/or the convective surface tubes above the bed for splash baffles).
- 8) The vessel shape and tube layout is selected for economy of space and materials. Hairpin-type tube bends for maximum bundle compactness are used and extended heat transfer surfaces are applied in the convective heat recovery zones. The finned tube fin spacing is selected so that the fins will not plug with the relatively coarse bed particles splashed from the bed and it is assumed that the deposit potential of the exhaust gas is sufficiently depleted by the time it has passed through the bed stages that convective surface deposition will not be significant.
- 9) The heat transfer surface is minimized by proper particle size and density selection and by proper tube pitch determination and tube bundle arrangement in the shallow beds and splash zones.
- 10) The vessel cross-sectional area is minimized by selecting relatively high fluidizing velocities and suitable particle size distributions. The particle size distribution is selected to yield optimum fluidization over the range of operating velocities desired.
- 11) Plugging of gas distributor plates is avoided by maintaining the initial stage at a temperature slightly greater than the temperature at which deposition in the diesel gas begins (assumed to be about 900°F) and by using hot, uncooled distributor plate surfaces in all stages of the unit.
- 12) The bed particle material is selected to be compatible with the temperature and gas environment in the unit, as well as being resistant to attrition -- commercially available alumina beads are tentatively selected.
- 13) The unit weight is minimized by proper selection of low-density materials for convective tube fins and vessel insulation.
- 14) Tube number, tube diameter and tube length is determined to give stable tube-side heat transfer and to meet pressure drop constraints using standard design practice.

- 15) Vessel wall, tube wall, distributor plate thicknesses and insulation thicknesses are determined from standard design practice.

An outline of the iterative design procedure is presented in Appendix A, explaining the details of the design technique, the assumptions and correlations applied and the areas of limited information.

The detailed design procedure was applied for the truck application to develop a highly effective heat recovery unit design for each of three cycles, the organic rankine cycle, the steam injection cycle and the stirling engine cycle. The truck design was then scaled up directly to the locomotive and marine applications of the three cycles using the following procedure:

- the unit operating conditions, general vessel shape, tube bundle layout, distributor plates and material thicknesses were assumed to be the same for the truck, locomotive and marine applications
- the heat recovery unit diameter (or width) was scaled according to the square root of the increase in unit capacity
- the vessel height was assumed to remain at the truck heat recovery unit height
- the heat transfer surface area and its weight were scaled up in direct proportion to the increase in unit capacity
- the vessel weight was scaled up in direct proportion to the increase in the unit diameter

6.3 Heat Recovery Unit Design Summary

Table 6.1 summarizing the major characteristics of the heat recovery units for the truck, locomotive and marine applications with each of the three cycles is shown below. Overall, the designs for the three cycles do not differ greatly, although the design details are significantly different.

Table 6.1

SUMMARY TABLE
DIESEL HEAT RECOVERY UNIT CHARACTERISTICS

<u>APPLICATION</u>	<u>Vessel Shape</u>	<u>Vessel Diameter(m)</u>	<u>Vessel Height(m)</u>	<u>Surface Area(m²) or Width</u>	<u>Number Tubes</u>	<u>Total Weight (kg)</u>
TRUCK						
Organic	cylindrical	0.64	1.3	39 (finned)	3	289
Steam	cylindrical	0.63	1.4	23 (finned)	5	265
Sterling	rectangular (square)	0.56 (width)	1.6	9 (bare)	12	292
LOCOMOTIVE						
Organic	cylindrical	1.99	1.3	378 (finned)	30	2395
Steam	cylindrical	1.96	1.4	223 (finned)	50	2246
Sterling	rectangular (square)	1.82 (width)	1.6	92 (bare)	120	2377
MARINE						
Organic	cylindrical	2.46	1.3	579 (finned)	45	3707
Steam	cylindrical	2.48	1.4	359 (finned)	77	3497
Sterling	rectangular (square)	2.25 (width)	1.6	149 (bare)	194	3747

- Notes: 1) truck heat recovery unit characteristics based on detailed conceptual design
- 2) locomotive and marine heat recovery unit designs based on direct scaleup of truck design

6.4 Organic Rankine Cycle

The organic Rankine cycle fluidized bed heat recovery unit consists of two stages of fluid beds, a high temperature bed and a low temperature bed, followed by a convective section. The vessel is cylindrical in shape. Tubes enter the convective section and are coiled within the freeboard of the low temperature bed. Radially finned tubes are placed in the convective region, while bare tubes are used in the bed sections. The coiled tube bundles in the convective section and the beds are connected with downcomer tubes. Figure 6.2 shows the layout of the truck unit.

The common characteristics of the truck, locomotive and marine organic Rankine cycle heat recovery units are summarized in Tables 6.2 and 6.3.

The particle material selected for the fluidized beds is alumina, available in nearly spherical particle shapes having a density of about 3685 kg/m^3 (230 lb/ft^3). The average particle diameter (surface/volume average) on both bed stages is about $750 \text{ }\mu\text{m}$, with a minimum diameter of about $275 \text{ }\mu\text{m}$ and a maximum particle diameter of about $1200 \text{ }\mu\text{m}$. The minimum fluidization velocity of the bed is about 0.6 m/s (2 ft/s). At their operating velocities the shallow beds have bubble volume fractions of about 43% and the tubes occupy about 18% of the bed volume. The relative heights of the dense beds, splash zones and freeboards are indicated in Figure 6.2.

6.5 Steam Injection Cycle

The steam injection cycle heat recovery unit is very similar in design to the organic Rankine cycle unit. It has two stages of fluid bed heat recovery followed by a convective section and is cylindrical in shape. The tubes are arranged in coils which enter the top of the unit and exit at the bottom. Finned tubes are placed in the convective section and bare tubes in the shallow beds and their splash zones. Significantly less heat transfer surface is required in the convective

10-26-54
 10-26-54
 10-26-54
 10-26-54

ORIGINAL PAGE IS
 OF POOR QUALITY

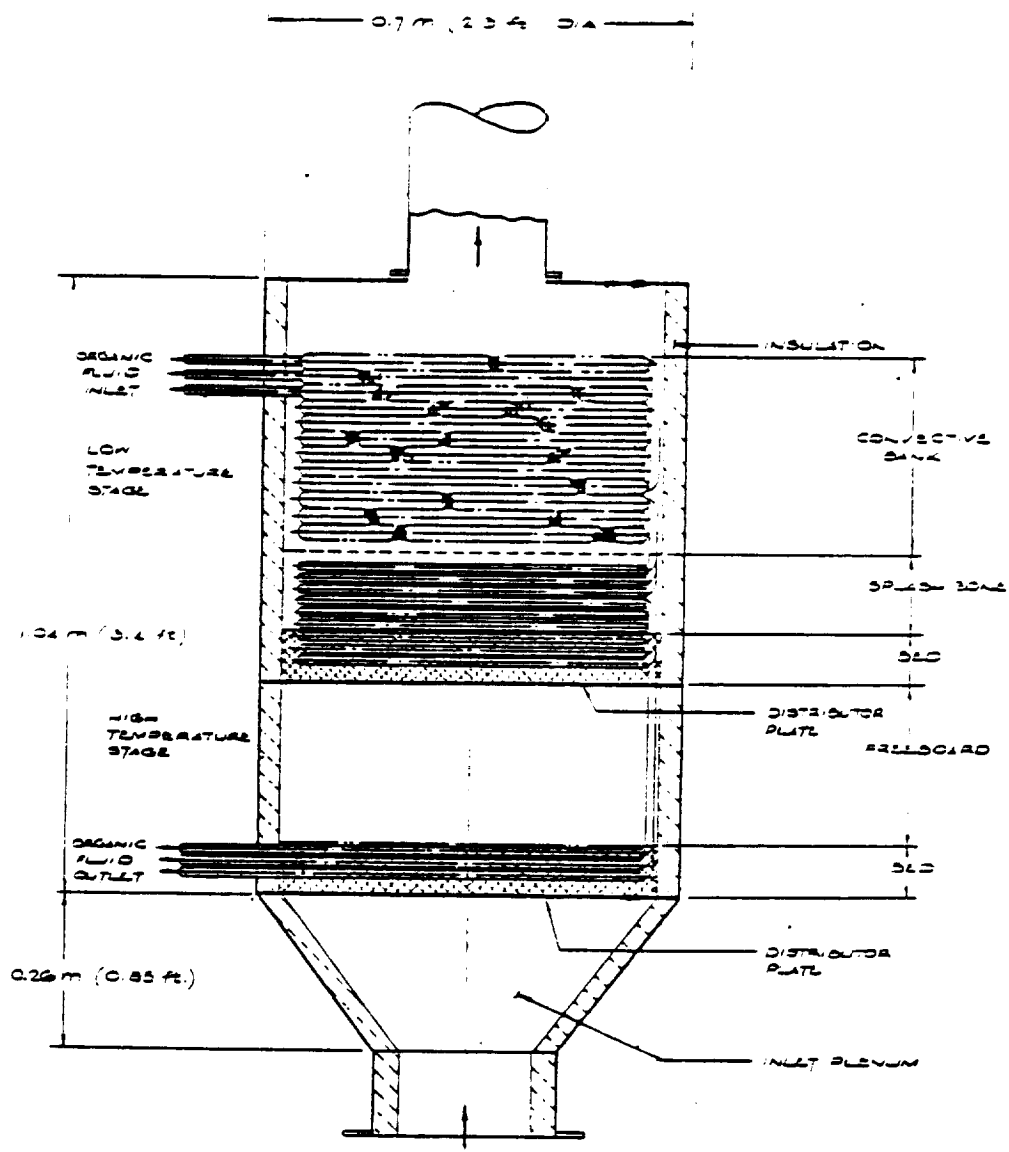


Fig. 6.2 - FLUID BED HEAT EXCHANGER
FOR ORGANIC RANKINE BOTTOMING
CYCLES

DWG NO 2018930

Washington Electric Corporation
 114
 20261300
 (R)

Table 6.2
COMMON ORGANIC RANKINE CYCLE
HEAT RECOVERY UNIT OVERALL CHARACTERISTICS

General Construction: Integral fluid bed stages and convective bank
Vessel Shape: Cylindrical
Number of Beds: 2
Number of Convective Banks: 1
Vessel Shell Material: Carbon steel
Shell Thickness: 0.24 cm (3/32 in)
Insulation Material: Kaolin Firebrick
Insulation Thickness: 3.8 cm (1.5 in)
Tube Type: Bare in beds; radially finned in the convective bank
Tube Material: Steel body with aluminum fins
Tube Diameter: 1.37 cm (0.5 in)
Tube Thickness: 0.09 cm (0.035 in)
Tube Pitch: 2.5 by 1.9 cm in-line pitch (1.0 by 0.75 in)
Tube Configuration: Horizontal Coils
Tube Length: 89.1 m (292 ft)
Fin length: 0.64 cm (0.25 in)
Fin Thickness: 0.16 cm (1/16 in)
Fin Pitch: 0.32 cm (1/8 in)
Particle Diameter: 725 μ m
Working Fluid: RC-1
Engine Exhaust Temperature: 947^oK (1245 F)
Stack Temperature: 448 K (347^oF)
Vessel Height: 1.3 m (4.25 ft)
Working Fluid Pressure Drop: 7.1 %
Exhaust Gas Pressure Drop: 2.1 %

Table 6.3
COMMON ORGANIC RANKINE CYCLE HEAT RECOVERY UNIT
STAGE CHARACTERISTICS

	<u>High-temperature Bed</u>	<u>Low-temperature Bed</u>	<u>Convective Zone</u>
Bed Temperature, K (°F)	755 (900)	581 (587)	--
Pinch, K (°F)	83 (150)	17 (30)	17 (30)
Log-Mean Temperature Diff K (°F)	129 (233)	44 (79)	44 (79)
Overall Heat Transfer Coeff J/m ² s°K (Btu/ft ² hr°F)	388 (68)	348 (61)	272 (48)
Superficial Velocity m/s (ft/s)	2.4 (8.0)	1.9 (6.2)	1.7 (5.5)
Tube Length, m (ft)	13.3 (44)	39.1 (128)	36.7 (120)
Bed Depth, m (ft)	0.09 (0.3)	0.09 (0.3)	--
Freeboard Height, m (ft)	0.3 (1.0)	0.55 (1.8)	--
Working Fluid Pressure Drop, kPa (psi)	121 (17.5)	233 (33.8)	72 (10.4)
Bed Pressure Drop, kPa (psi)	0.7 (0.1)	0.7 (0.1)	--
Distributor Pressure Drop, kPa (psi)	0.4 (0.06)	0.3 (0.04)	--

zone than is in the organic Rankine unit. Figure 6.3 shows the truck heat recovery unit layout for the steam injection cycle. Because the exhaust gas temperature entering the heat recovery unit is much lower than the engine exhaust temperature in this case, the criteria stated that the first stage temperature should be about 900°F to avoid distributor plate deposition can not be satisfied. The impact of the high steam content on the deposit potential of the exhaust gas is not known.

The common characteristics of the truck, locomotive and marine heat recovery units for the steam injection cycle are listed in Tables 6.4 and 6.5.

Essentially, the same particle material and size distribution is selected for the steam injection cycle as was for the organic Rankine cycle. The bed minimum fluidization velocity in the steam injection cycle case is about 0.7 m/s (2.4 ft/s) and the beds operate with bubble volume fractions of about 38 % and a tube volume fraction of about 11 % on the high-temperature stage and 22 % on the low-temperature stage.

6.6 Stirling Engine Cycle

The Stirling engine cycle heat recovery unit differs significantly in design from the previous two units. It is made up of two fluidized bed heat recovery stages, a high temperature bed and a low temperature bed, and is without any convective heat transfer section. The low temperature bed and its splash zone contains toluene heat pipes in a hairpin serpentine configuration. The high temperature stage contains mercury heat pipes in a similar configuration. The heat pipes require only a single point of entry through the vessel wall since they have internal circulation of the heat transfer fluid. The vessel is rectangular in cross-section to accommodate the passage of a large number of tubes through a single flat wall. The Stirling engine heat recovery unit layout is presented in Figure 6.4.

0.68 m (2.23 FT)

ORIGINAL PAGE IS
OF POOR QUALITY

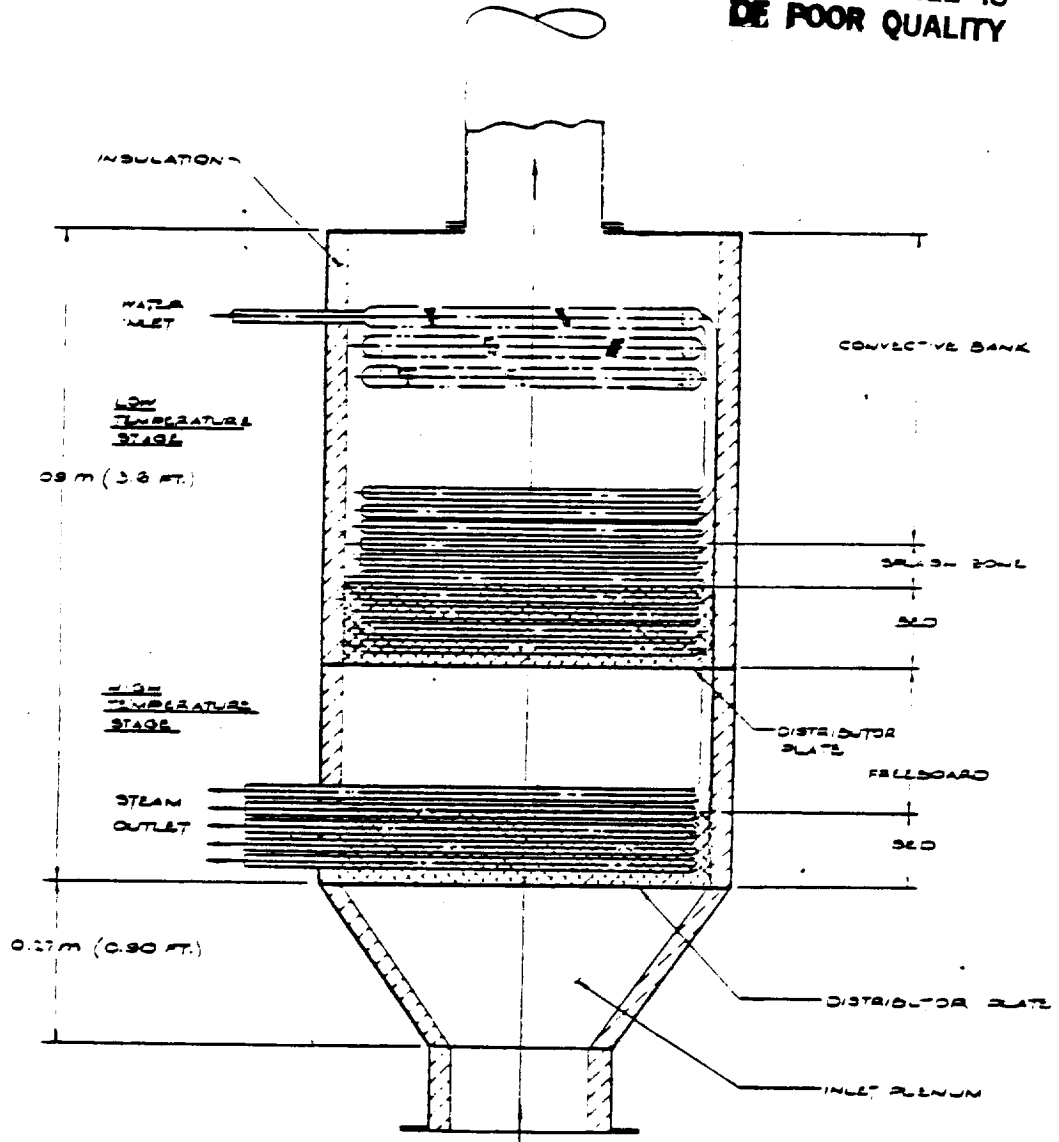


Fig. 6.3 - FLUID BED HEAT EXCHANGER
FOR STEAM INJECTION
(NO WATER PREHEAT)

DWG NO 3016383

Westinghouse Electric Corporation
 THE FLUID BED HEAT EXCHANGER IS
 A TRADE SECRET OF WESTINGHOUSE
 COMPANY
 1954
 20220103

Table 6.4

COMMON STEAM INJECTION CYCLE
HEAT RECOVER UNIT OVERALL CHARACTERISTICS

General Construction: Integral fluid bed stages and convective bank
Vessel Shape: Cylindrical
Number of Beds: 2
Number of Convective Banks: 1
Vessel Shell Material: Carbon steel
Shell Thickness: 0.16 cm (1/16 in)
Insulation Material: Kaolin Firebrick
Insulation Thickness: 2.5 cm (1.0 in)
Tube Type: Bare in beds; radially finned in the convective bank
Tube Material: Steel body with aluminum fins
Tube Diameter: 1.9 cm (0.75 in)
Tube Thickness: 0.09 cm (0.035 in)
Tube Pitch: 3.8 by 2.9 cm in-line pitch (1.5 by 1.125 in)
Tube Configuration: Horizontal Coils
Tube Length: 42.1 m (138 ft)
Fin length: 0.64 cm (0.25 in)
Fin Thickness: 0.16 cm (1/16 in)
Fin Pitch: 0.32 cm (1/8 in)
Particle Diameter: 725 μm
Working Fluid: steam
Engine Exhaust Temperature: 707 $^{\circ}\text{K}$ (813 $^{\circ}\text{F}$)
Stack Temperature: 413 $^{\circ}\text{K}$ (284 $^{\circ}\text{F}$)
Vessel Height: 1.4 m (4.5 ft)
Working Fluid Pressure Drop: 4.9%
Exhaust Gas Pressure Drop: 2.8%

Table 6.5
COMMON STEAM INJECTION CYCLE HEAT RECOVERY UNIT
STAGE CHARACTERISTICS

	<u>High-temperature Bed</u>	<u>Low-temperature Bed</u>	<u>Convective Zone</u>
Bed Temperature, °K (°F)	589 (600)	462 (373)	--
Pinch, °K (°F)	182 (327)	56 (100)	34 (60)
Log-Mean Temperature Diff °K (°F)	182 (327)	56 (100)	44 (79)
Overall Heat Transfer Coeff J/m ² s°K (Btu/ft ² hr°F)	377 (49)	232 (41)	225 (40)
Superficial Velocity m/s (ft/s)	2.4 (8.0)	1.8 (6.0)	1.8 (5.8)
Tube Length, m (ft)	4.2 (14)	17.1 (56)	21.1 (69)
Bed Depth, m (ft)	0.12 (0.4)	0.13 (0.4)	--
Freeboard Height, m (ft)	0.24 (0.8)	0.61 (2.0)	--
Working Fluid Pressure Drop, kPa (psi)	7.0 (1.0)	7.0 (1.0)	1.4 (0.2)
Bed Pressure Drop, kPa (psi)	1.1 (0.2)	1.2 (0.2)	--
Distributor Pressure Drop, kPa (psi)	0.3 (0.06)	0.3 (0.04)	--

The common characteristics of the truck, locomotive and marine heat recovery units for the sterling engine cycle are listed in Tables 6.6 and 6.7.

An alumina bed material is used in the Stirling engine cycle heat recovery unit having an average particle diameter of about 700 μm . The high-temperature bed has a minimum fluidization velocity of about 0.8 m/s (2.6 ft/s) and the low-temperature bed 0.6 m/s (1.8 ft/s). The bubble volume fraction in both beds is about 40% and the tubes occupy about 16%.

6.7 Fluid Bed Heat Exchanger Cost Estimate

Costs for the fluid bed heat exchangers were based on the designs described above. The fluid bed shells are assumed to be constructed of carbon steel and costed based on cost quotes from fabricators for other small carbon steel welded assemblies designed for atmospheric pressure, non-coded service on fuel conversion systems. Bed tubing is taken as carbon steel in the low temperature zone and as 1-1/2 Cr-1/2 MO in the high temperature zone. Aluminum fins are assumed in the convective tube sections. Preliminary cost estimates for the convective heat exchange tubing assemblies were derived based on Westinghouse ThermoKing truck mounted units, plus stationary heat exchange units for 40 kw fuel cell systems as quoted by Harrison Radiator Division of General Motors from their stock designs for automotive and diesel locomotive units. For the distributor grid plates, alumina bed material, and vessel refractory a dollar per pound cost was used derived from Westinghouse R&D pilot plant construction cost data. Tables 6.8, 6.9 and 6.10 show the weight and cost breakdown for the respective fluid bed designs for each application and heat recovery cycle.

As evident from the tables, the major cost component on the fluid bed unit is the finned-tubed convective section that is present in the organic Rankine and steam injection cycles. The convective section accounts for over 50% of the costs in the organic Rankine cycle and

Table 6.6
COMMON STIRLING ENGINE CYCLE
HEAT RECOVERY UNIT OVERALL CHARACTERISTICS

General Construction: Integral fluid bed stages
Vessel Shape: Rectangular
Number of Beds: 2
Number of Convective Banks: 0
Vessel Shell Material: Carbon steel
Shell Thickness: 0.56 cm (7/32 in)
Insulation Material: Kaolin Firebrick
Insulation Thickness: 3.8 cm (1.5 in)
Tube Type: Bare
Tube Material: Steel
Tube Diameter: 1.9 cm (0.75 in)
Tube Thickness: 0.09 cm (0.035 in)
Tube Pitch: 3.8 by 2.9 cm in-line pitch (1.5 by 1.125 in)
Tube Configuration: Horizontal serpentine
Tube Length: 6.1 m (20 ft) in each bed
Particle Diameter: 700 μm
Working Fluid: mercury and toluene heat pipes
Engine Exhaust Temperature: 948 $^{\circ}\text{K}$ (1247 $^{\circ}\text{F}$)
Stack Temperature: 562 $^{\circ}\text{K}$ (553 $^{\circ}\text{F}$)
Vessel Height: 1.6 m (5.2 ft)
Exhaust Gas Pressure Drop: 3.3 %

Table 6.7
COMMON STIRLING ENGINE CYCLE HEAT RECOVERY UNIT
STAGE CHARACTERISTICS

	<u>High-temperature Bed</u>	<u>Low-temperature Bed</u>
Bed Temperature, °K (°F)	755 (900)	562 (553)
Pinch, °K (°F)	56 (100)	56 (100)
Log-Mean Temperature Diff °K (°F)	56 (100)	56 (100)
Overall Heat Transfer Coeff J/m ² s°K (Btu/ft ² hr°F)	327 (58)	274 (51)
Superficial Velocity m/s (ft/s)	2.4 (8.0)	1.8 (5.8)
Tube Length, m (ft)	6.1 (20)	6.6 (22)
Bed Depth, m (ft)	0.12 (0.4)	0.18 (0.6)
Freeboard Height, m (ft)	0.24 (0.8)	0.73 (2.4)
Bed Pressure Drop, kPa (psi)	1.0 (0.15)	1.5 (0.2)
Distributor Pressure Drop, kPa (psi)	0.45 (0.06)	0.3 (0.04)

Table 6.8

ESTIMATED PRICE FOR HEAT RECOVERY FLUID BED
ORGANIC RANKINE

ITEM	APPLICATION					
	TRUCK		LOCOMOTIVE		MARINE	
	Wt(lb)	Cost (\$)	Wt(lb)	Cost (\$)	Wt(lb)	Cost (\$)
Grids, rings, shell, liner, etc.; mild steel components estimated from truck mounted fule cellmethanol tank price for Thermo King study	186	265	1316	1,875	266	3,086
Low temperature bed tubing coils; mild steel 0.5 inch od x 0.035 inch wall tubing priced from an Amer-Std quote on fuel cell cooler	71	530	680	5,080	1041	7,776
High Temperature bed tubing; 1-1/4 tube priced from mild steel cooler price/lb x 1.25 to allow for more expensive material	24	224	233	2,176	357	3,334
Convection section tubing; mild steel tubing with aluminum fins priced from an Amer-Std quote on a fuel cell air cooled condenser	193	1,621	1860	15,624	2848	23,923
Refractory, Norton Kaolin; 19 lb/ft ³ insulating, estimated from Sasol cyclone lining data	61	122	207	414	256	530
Alumina bed material; priced from data on cost of alumina in Oil/Paint/Drug reporter	102	35	983	344	1505	526
TOTAL(S)	637	\$2,797	5279	\$25,513	8173	\$39,175

Table 6.9

ESTIMATED PRICE FOR HEAT RECOVERY FLUID BED
STEAM INJECTION

ITEM	APPLICATION					
	TRUCK		LOCOMOTIVE		MARINE	
	Wt(lb)	Cost (\$)	Wt(lb)	Cost (\$)	Wt(lb)	Cost (\$)
Grids, rings, shell, liner, etc.; mild steel components estimated from truck mounted fule cellmethanol tank price for Thermo King study	181	228	1321	1,882	1931	2,751
Low temperature bed tubing coils; mild steel 0.5 inch od x 0.035 inch wall tubing priced from an Amer-Std quote on fuel cell cooler	77	575	742	5,543	1191	8,897
High Temperature bed tubing; 1-1/4 tube priced from mild steel cooler price/lb x 1.25 to allow for more expensive material	19	178	181	1,690	290	2,709
Convection section tubing; mild steel tubing with aluminum fins priced from an Amer-Std quote on a fuel cell air cooled condenser	103	865	994	8,350	1594	13,390
Refractory, Norton Kaolin; 19 lb/ft ³ insulating, estimated from Sasol cyclone lining data	43	86	134	268	169	338
Alumina bed material; priced from data on cost of alumina in Oil/Paint/Drug reporter	164	57	1579	553	2534	887
TOTAL(S)	587	\$1,989	4951	\$18,286	7709	\$28,972

Table 6.10

ESTIMATED PRICE FOR HEAT RECOVERY FLUID BED STIRLING ENGINE

ITEM	APPLICATION					
	TRUCK	LOCOMOTIVE		MARINE		
	Wt(lb)	Cost (\$)	Wt(lb)	Cost (\$)	Wt(lb)	Cost (\$)
Grids, rings, shell, liner, etc.; mild steel components estimated from truck mounted fule cellmethanol tank price for Thermo King study	234	332	1714	2,434	2661	3,779
Low temperature bed tubing coils; mild steel 0.5 inch od x 0.035 inch wall tubing priced from an Amer-Std quote on fuel cell cooler	72	538	720	5,378	1163	8,688
High Temperature bed tubing; 1-1/4 tube priced from mild steel cooler price/lb x 1.25 to allow for more expensive material	66	616	661	6,174	1068	9,975
Convection section tubing; mild steel tubing with aluminum fins priced from an Amer-Std quote on a fuel cell air cooled condenser	NA		NA		NA	
Refractory, Norton Kaolin; 19 lb/ft ³ insulating, estimated from Sasol cyclone lining data	82	164	266	532	329	658
Alumina bed material; priced from data on cost of alumina in Oil/Paint/Drug reporter	189	66	1880	658	3040	1,064
TOTAL(S)	643	\$1,716	5241	\$15,176	8261	\$24,164

ORIGINAL PAGE IS OF POOR QUALITY

about 40% in the steam injection cycles. Considering the relatively minimal performance improvement to the cycle that the convection section provides in the fluid bed system, it may be more cost effective to eliminate or minimize this duty.

7. SYSTEM DESCRIPTION AND ARRANGEMENT

For each of the three system applications, hardware components were identified to match the performance models and component conceptual arrangement drawings were prepared to illustrate the installation of the heat recovery systems.

7.1 Truck Application

The heavy duty truck configuration selected for the truck application of these supposed systems is a high profile, tilt-cab cab-over-engine tractor with two drive axles and a power range of 240-475 hp. Figure 7.1 shows a typical example of such a truck giving pertinent physical dimensions.

7.1.1 Organic Rankine Cycle

The components for the organic Rankine cycle system in the truck application are as follows:

- Fluidized bed vapor generator
- Convective feed heater
- Regenerator
- Air cooled condenser
- Feed pump
- Air blower
- Controls
- Turbine/Gearbox

All of these components are identical to those used in the TECO design described in Reference 1 except for the fluidized bed vapor generator and the convective feed heater. These components which are described in Section 6 were substituted for the convective vapor generator used by

ORIGINAL PAGE IS
OF POOR QUALITY

Dwg. 9370A35

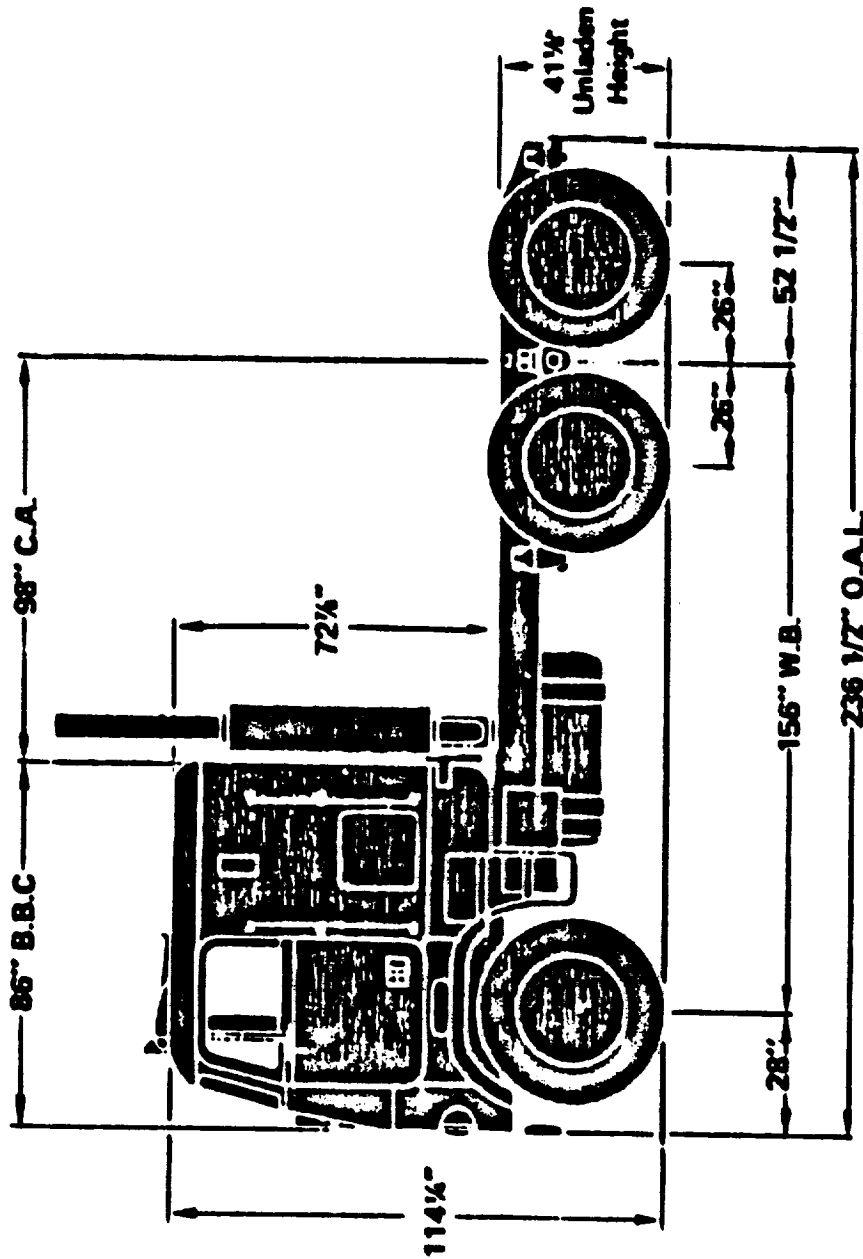


Fig. 7.1—Heavy duty long haul truck tractor

Dwg. 9370A29

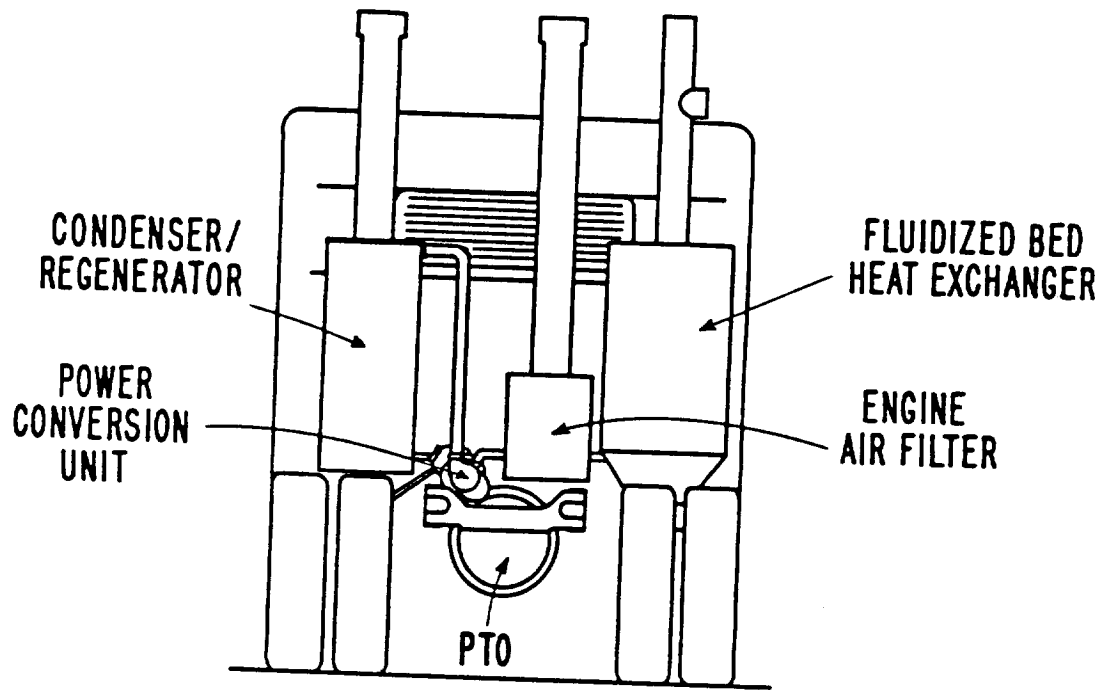


Fig. 7.2—Typical truck installation of organic Rankine cycle system

TECO. The fluidized bed vapor generator and the convective feedheater are integrated into a single vessel and arranged as shown in Figure 7.2.

7.1.2 Steam Injection Cycle

The steam injection cycle system for the truck application consists of the following components

- Feedwater storage tank
- Steam-heated feedwater heater
- Feed pump
- Convection feedwater heater
- Fluidized bed steam generator
- Modified compressor-drive expander
- Modified power expander
- Gearbox

The convection feedwater heater and the fluidized bed steam generator are described in Section 6. The compressor drive expander and the power expander which are based on the Cummins T-46B turbocharger are described in Appendix B. The gearbox and feedwater pump which are also shown in Figure 7.3 are derived from the TECO design in Reference 1, and also described in Appendix B.

The arrangement for all of the components except the feedwater storage tank are shown on Figure 7.3. The feedwater storage tank which is shown on Figure 7.4 is located back of the other components. The installation of the feedwater tank as shown requires that the truck frame be lengthened by two feet.

7.1.3 Stirling Engine

The Stirling engine for the truck application consists of the following components:

- High temperature fluidized bed heat exchanger
- High temperature heat pipe using mercury

Dwg. 9370A28

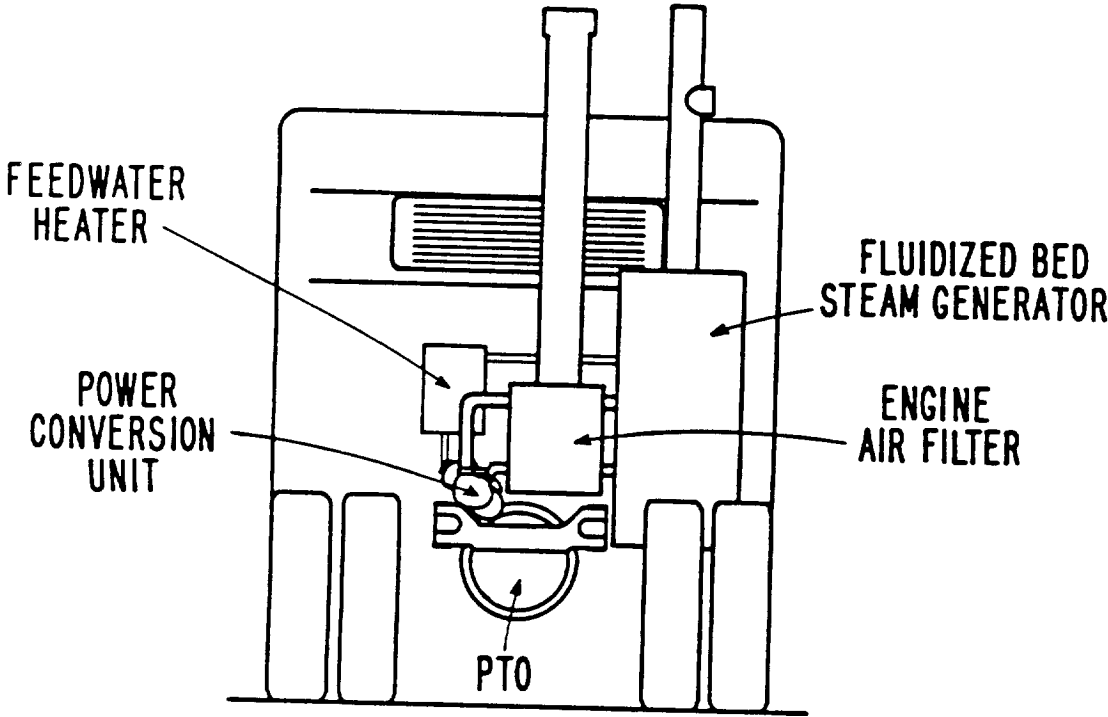


Fig. 7.3—Typical truck installation of steam injection cycle

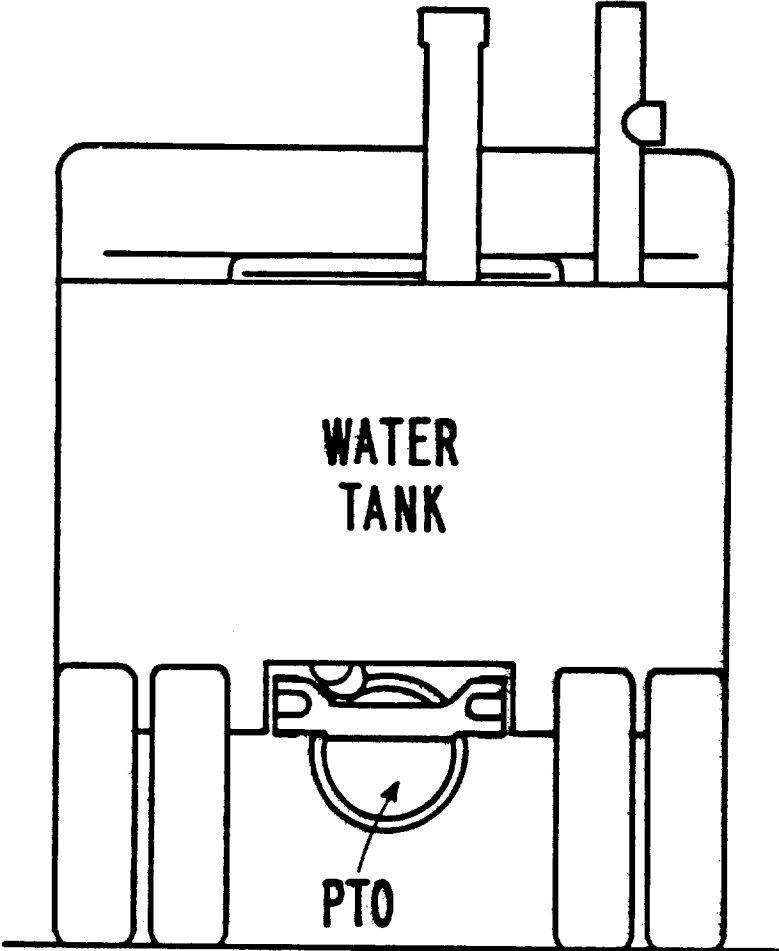


Fig. 7.4—Water tank for steam injection cycle on truck

- High temperature Stirling engine using hydrogen
- Low temperature fluidized bed heat exchanger
- Low temperature heat pipe using toluene
- Low temperature Stirling engine using hydrogen
- Air-cooled heat exchanger for rejecting heat from Stirling engine
- Gearbox.

The high and low temperature fluidized bed heat exchanger designs are described in Section 6. The heat pipe system design is shown in Figure 7.5. The selection of heat pipe working fluids was based on operating temperature considerations.

The Stirling engine modules were scaled from the MODI engine design described in Reference 20. The procedure used for scaling the Stirling engines is described in Appendix C.

The arrangement for the Stirling engines in the truck is shown in Figure 7.6. All of the components except the gearbox and the radiator are shown in this figure. The gearbox is based on the design used by TECO in Reference 1 and scaled according to a procedure given by Dudley(21) that is summarized in Appendix D. The radiator would be located where the normal truck engine radiator is now located.

7.2 Locomotive Application

The railroad locomotive configuration selected for the locomotive application of the three subposed systems is the General Electric 3600 horsepower C 36-7 diesel-electric locomotive described in Reference 3 and illustrated in Figure 7.7.

7.2.1 Organic Rankine Cycle

The components of the organic Rankine cycle system for the locomotive application are similar to those for the truck application since the output from the subposed system goes to the main engine crankshaft through a gearbox. The installation of the system is shown

Dwg. 9370A30

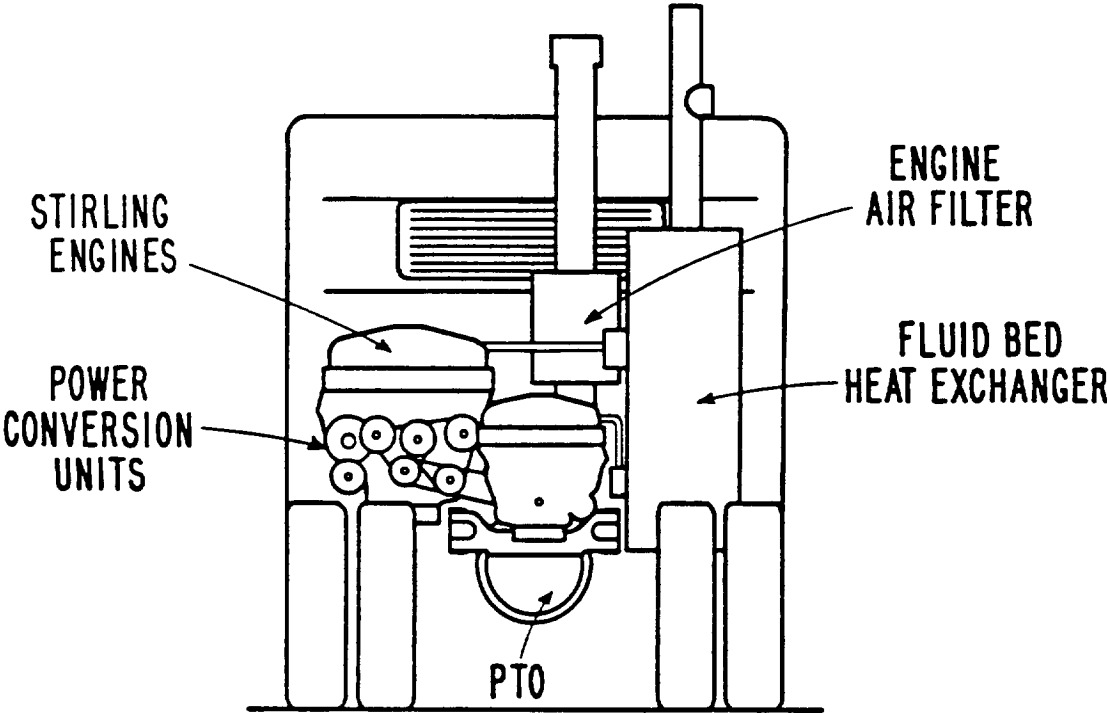


Fig. 7. 6—Typical truck installation of stirling engine units

ORIGINAL PAGE IS
OF POOR QUALITY

Dwg. 4274845

**location of
major systems**

- 1 Engine - GE Model 7FDL 18
- 2 Auxiliary Generator
- 3 Rectifier
- 4 Equipment Storage
- 5 Radiator Fan Drive Unit
- 6 Radiator Exhaust Branch
- 7 Engine Air Filter
- 8 Engine Air Filter
- 9 Radiator Fan Drive Unit
- 10 Lub Oil Cooler
- 11 Lub Oil Filter
- 12 Radiator
- 13 Radiator
- 14 Radiator
- 15 Radiator
- 16 Radiator
- 17 Hand Fire
- 18 Hand Fire
- 19 Battery Box
- 20 Upper Control Compartment
- 21 Lower Control Compartment
- 22 Fuel Filter
- 23 Fuel Filter
- 24 Toilet
- 25 Engine Control Panel
- 26 Air Brake Valve
- 27 Control Console
- 28 Air Brake Valve
- 29 Electric Cab Heater
- 30 Electric Cab Heater
- 31 Heating Sash
- 32 Hand Brake
- 33 Equipment Air Filter
- 34 Air Filter
- 35 Emergency Chute

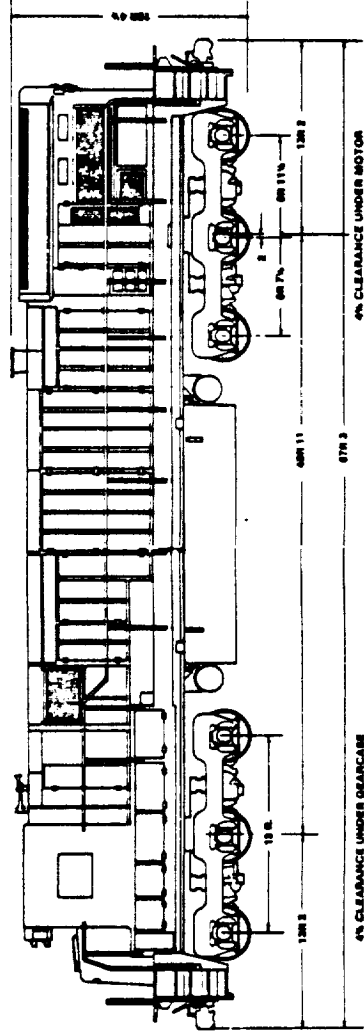
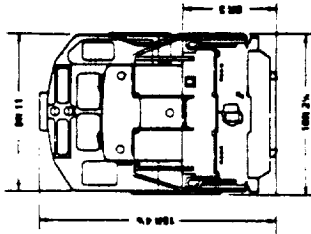
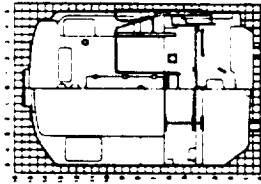
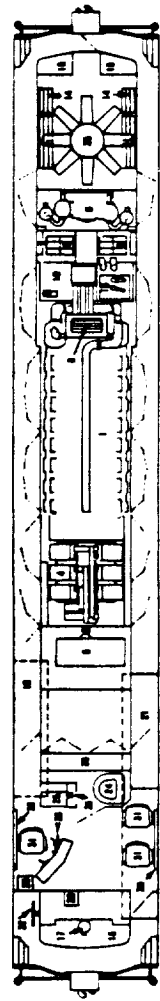


Fig. 7.7 - General electric 3600 hp C 36-7 diesel-electric locomotive - source reference 3

Dwg. 4274845

in Figure 7.8. It was possible to eliminate a significant number of the engine auxiliary associated with a non-adiabatic engine and to conserve space by rearranging the residual auxiliaries and by shortening the length of the diesel engine.* It was necessary, however, to lengthen the locomotive chassis by about 18 in. to fit in the components required for the fluidized bed system. This is, of course, such a small percentage increase that it can probably be reduced to zero by judicious detailed design which is outside the scope of this study.

7.2.2 Steam Injection Cycle

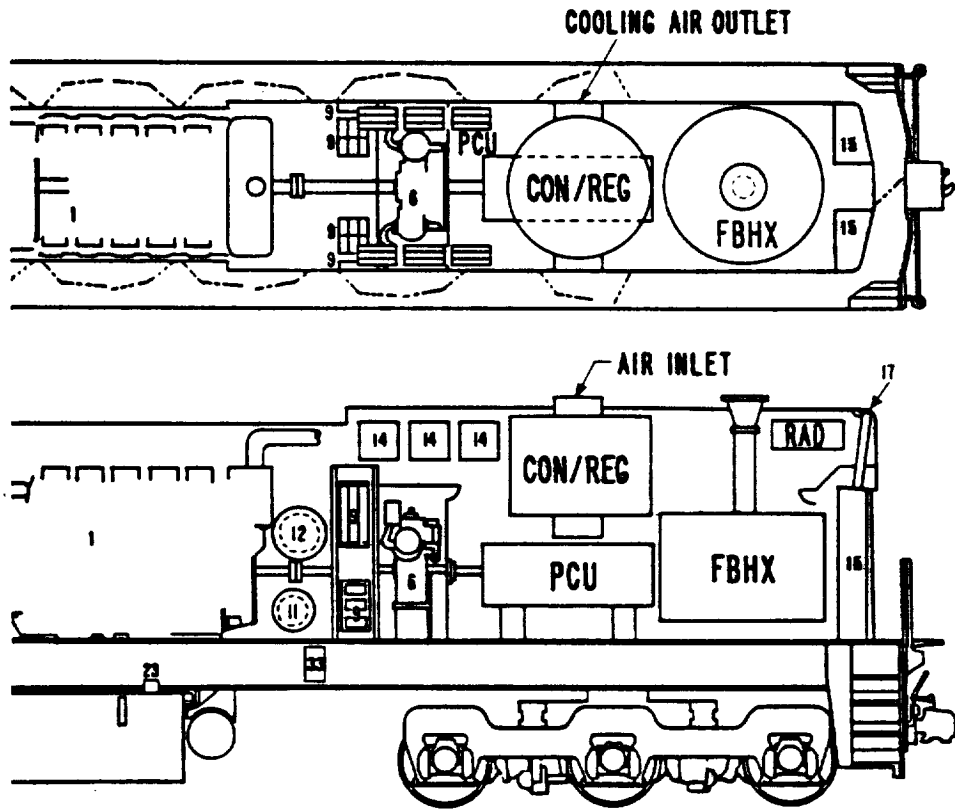
The components of the steam injection cycle system for the locomotive application are similar to those for the truck since the supposed power conversion unit connects to the diesel engine crankshaft through a gearbox. Information on the turbomachinery is given in Appendix C. All of the system components except the feedwater storage tank are shown in the arrangement drawing given in Figure 7.9. The incremental length required by the supposed system was almost equal to the reduction in diesel engine length as the overall locomotive chassis length is unchanged.

A separate tender with cylindrical tank 6 ft in diameter and 24 ft long will be required for feedwater to match the fuel storage capacity of the unit.

7.2.3 Stirling Engine

The components of the Stirling engine system for the locomotive application are significantly different from that for the truck. The system is made up of multiple MODI Stirling engine modules described in Reference 20. Seven (7) high temperature modules and seventeen (17) low temperature modules are required. These 24 modules are arranged in six batteries as shown in Figure 7.10.

*Total power was maintained at 3600 hp so length of engine could be reduced.

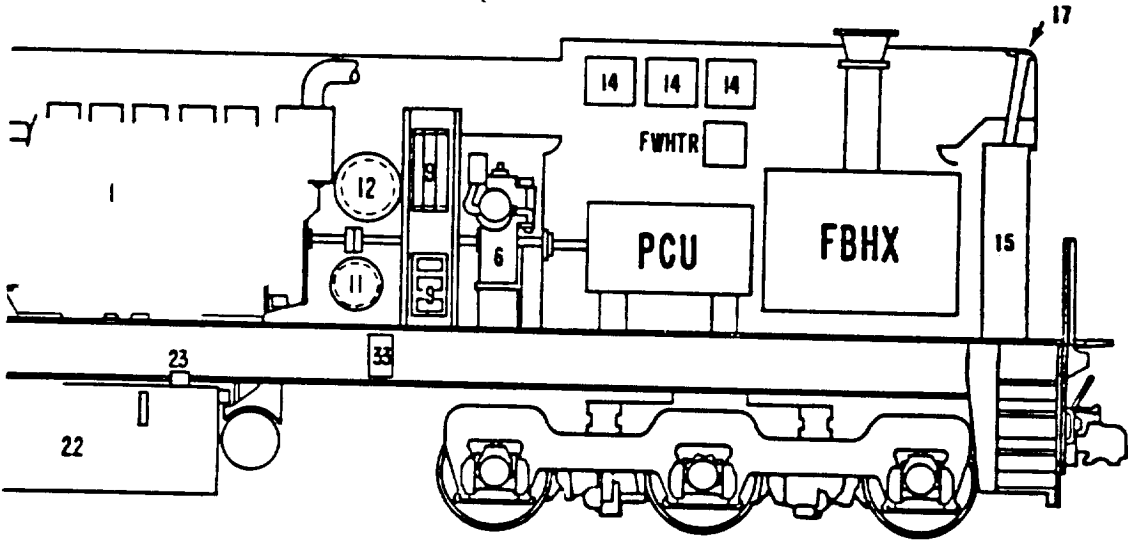
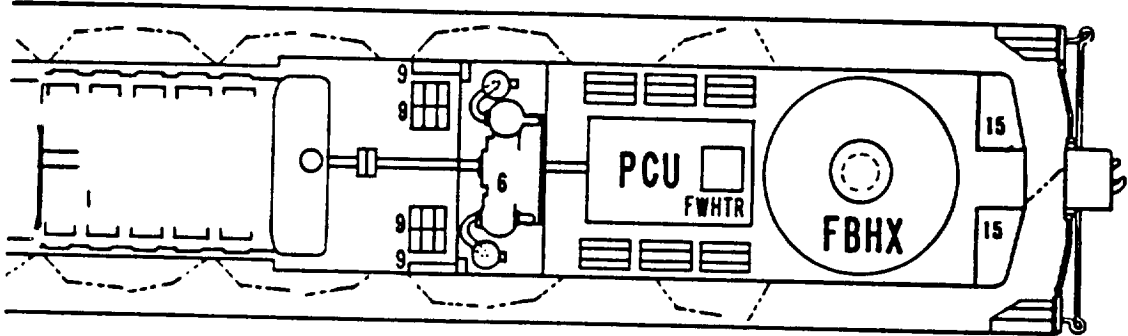


LENGTH INCREMENT = 18"

Numbers Refer to Equipment Identified in Fig. 7.7

Fig. 7.8—Arrangement for organic Rankine cycle system in locomotive

Dwg. 4274847

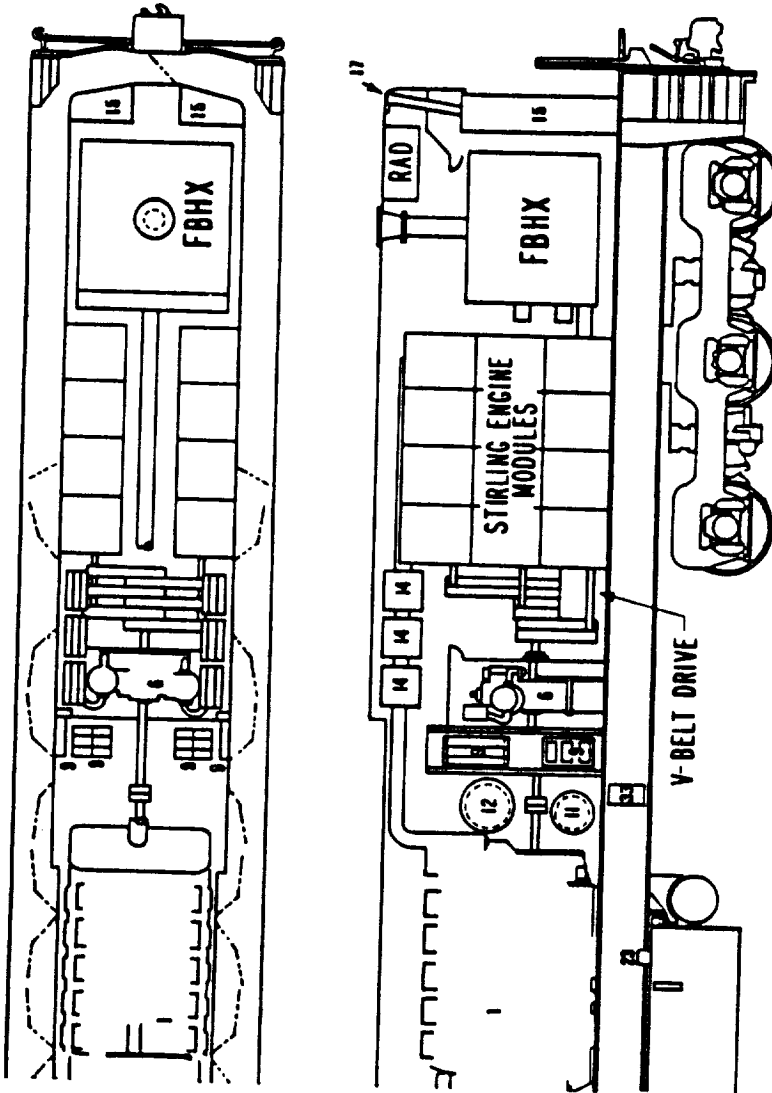


LENGTH INCREMENT = 0"

Numbers Refer to Equipment Identified in Fig. 7.7

Fig. 7.9—Arrangement for steam injection system in locomotive

Desg. 4274848



LENGTH INCREMENT = 84"

Numbers Refer to Equipment Identified in Fig. 7.7

Fig. 7.10—Arrangement of Stirling engine system in locomotive

The V-belt drive described in Appendix E is used to transmit the power from the six Stirling engine batteries in the main diesel engine crankshaft.

The Stirling engine system installation shown in Figure 7.10 has a net length increment of 84 inches which is a result of the larger volume of the Stirling engine modules.

7.3 Marine Application

The marine application of the adiabatic diesel engine with subposed cycles was made to the 5600 hp push-pull boat for inland river service described in Reference 4. Figure 7.11 shows the installation of the two main engines with a deck mounted subposed F-85 organic Rankine cycle which is electrically connected to the main engine drives. Modifications of this basic configuration were used for the three subposed cycles evaluated in this study.

7.3.1 Organic Rankine Cycle

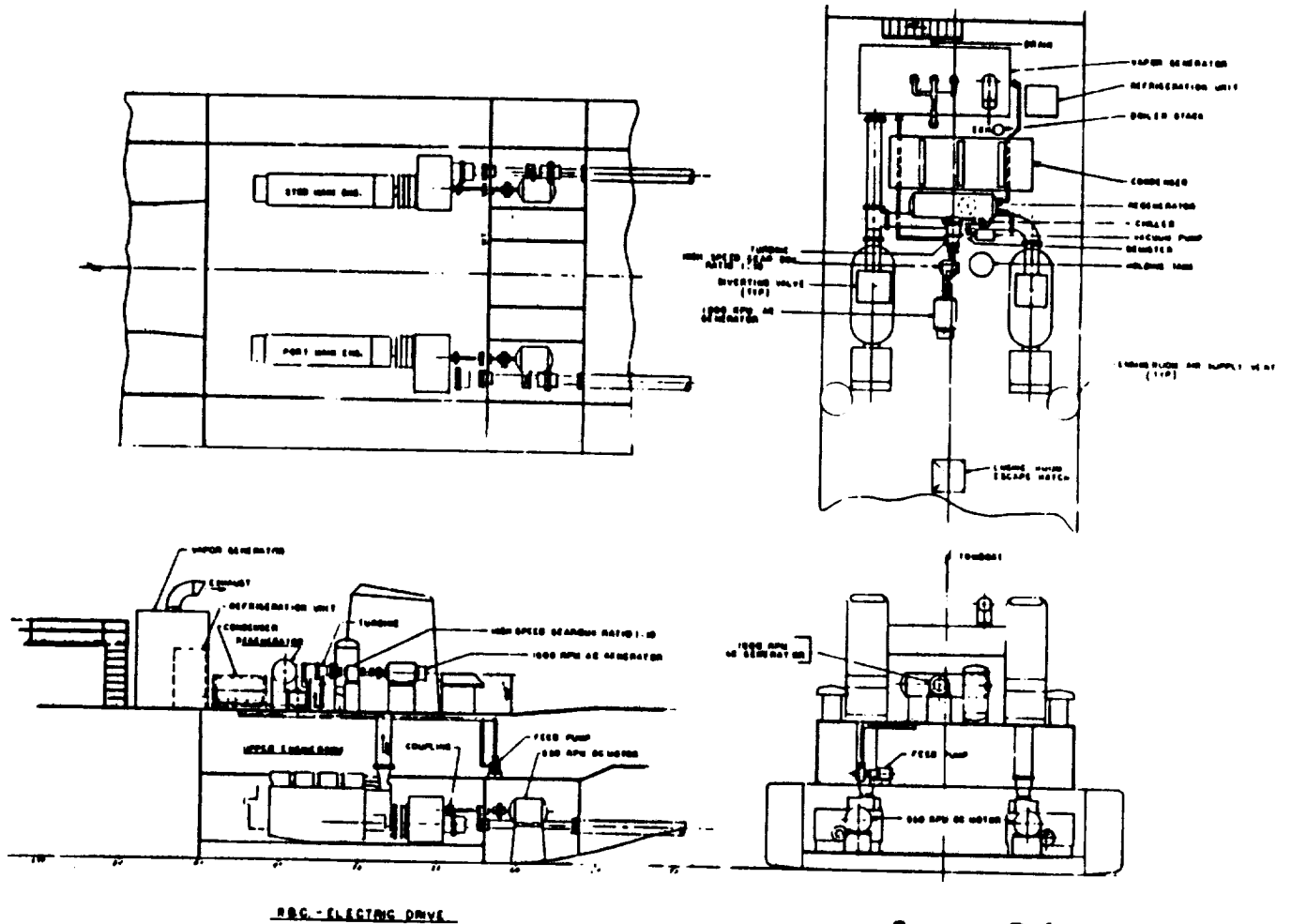
The components of the organic Rankine cycle for the marine application are similar to those for the truck and locomotive applications except for the condenser and the drive. The condenser is water-cooled rather than air-cooled and the drive is electrical rather than directly connected. The installation of the organic Rankine cycle system with the fluidized bed heat exchanger in the vessel deck is shown in Figure 7.12. The space required for the RC-1 organic Rankine cycle is less than that used by the F-85 cycle from Reference 4.

7.3.2 Steam Injection Cycle

The components of the steam injection cycle system for the marine application are similar to those in the truck and locomotive applications except for the drive and the feedwater system. Information on the turbomachinery is given in Appendix B. The drive is electrical rather than directly connected. The feedwater system consists of a

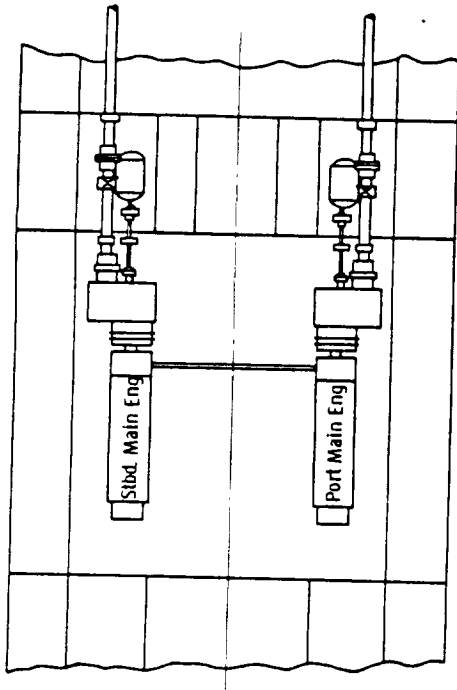
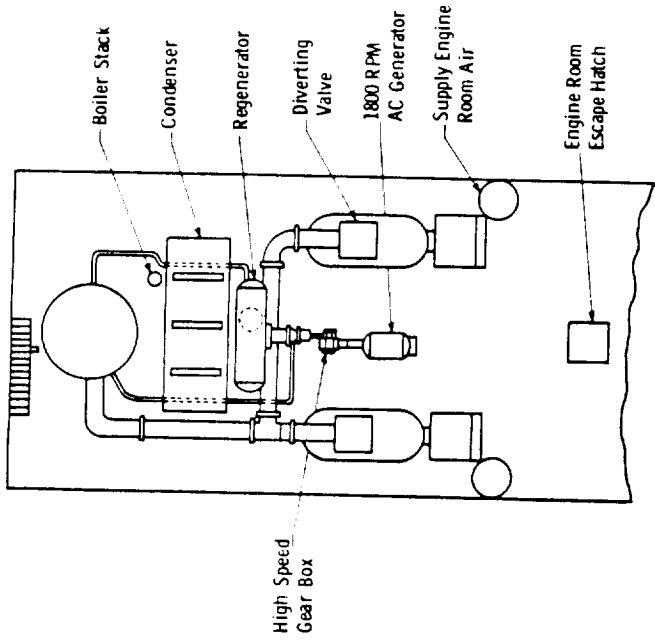
ORIGINAL PAGE IS
OF POOR QUALITY

Dwg. 9370A33



Source: Reference 4

Fig. 7.11—RBC/vessel installation



ORIGINAL PAGE IS
OF POOR QUALITY

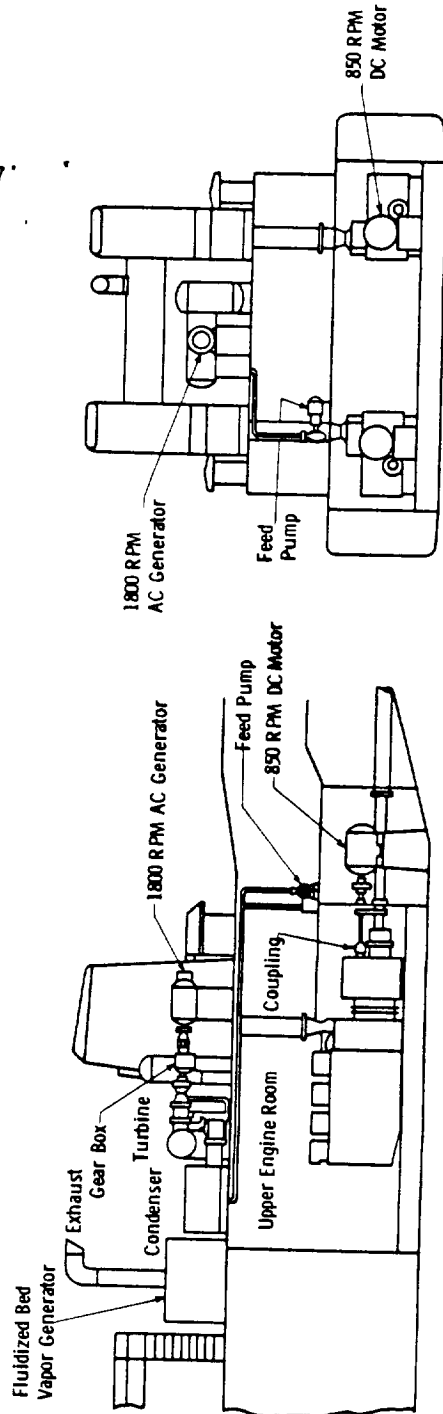


Fig. 7.12—Installation of RC-1 organic Rankine cycle system on deck of push-pull boat for inland river service

river-water treatment subsystem plus a relatively small storage tank rather than a storage tank which matches the fuel tank capacity. The river water treatment subsystem consists of a filter, a reverse osmosis process, and a mixed-resin bed demineralization process. The treated water holding tank has a capacity of about 31,000 gallons which is sufficient for about 37 hours of operation at design capacity.

The installation of the steam injection cycle system with the fluidized bed heat exchanger on the vessel deck is shown in Figure 7.13. The volume required for the steam injection system including the water treatment subsystem but not the holding tank is about the same as that for the F-85 organic Rankine system from Reference 4. The treated water holding tank is that portion of the hull's fuel tank which is made available by the improved performance of the compound cycles over the conventional diesel engine.

7.3.3 Stirling Engine System

The components of the Stirling engine system for the marine application are similar to those for the locomotive application except for the heat rejection equipment and the drive. Heat rejection from the engine is to the river water rather than to the air which results in a reduced cold end temperature for the engine. The drive is electrical rather than V-belts.

Here again the system is made up of MODI engine modules arranged in batteries. As shown in Figure 7.14 there are 11 high temperature modules in three batteries which drive a generator through a common gearbox. On each side there are two stacked batteries of seven low temperature modules which drive a generator through a common gearbox. The fluidized bed heat exchanger with high and low temperature beds coupled to the engine modules with heat pipes is centrally located. The volume required for this system is approximately equal to that used by the F-85 organic Rankine cycle system described in Reference 4.

ORIGINAL PAGE IS
OF POOR QUALITY

Dwg. 7202C-07

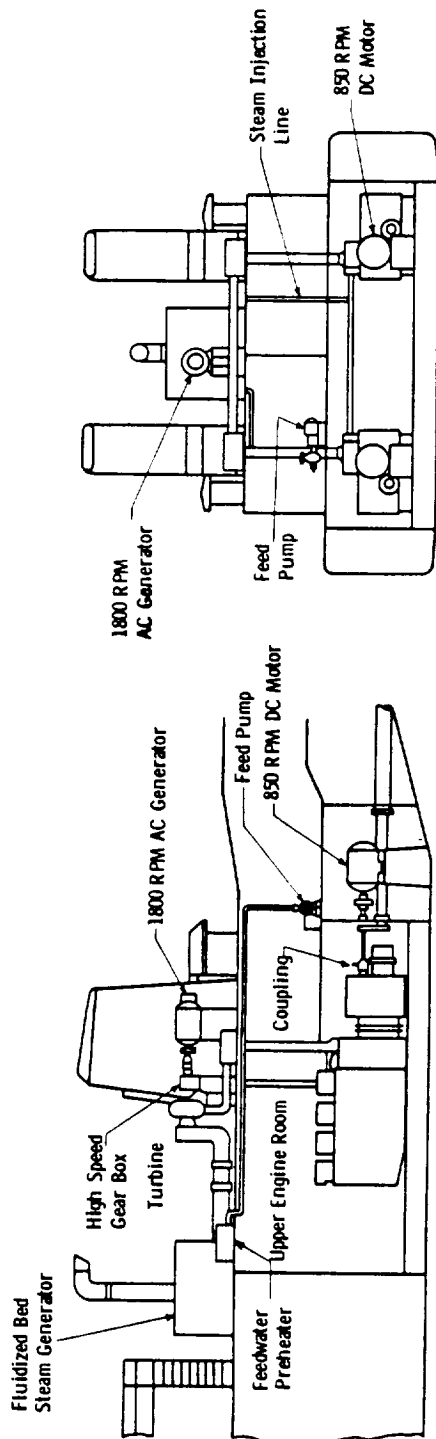
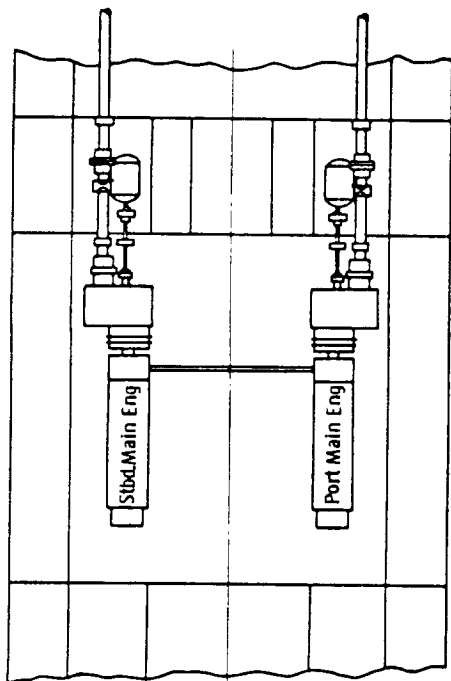
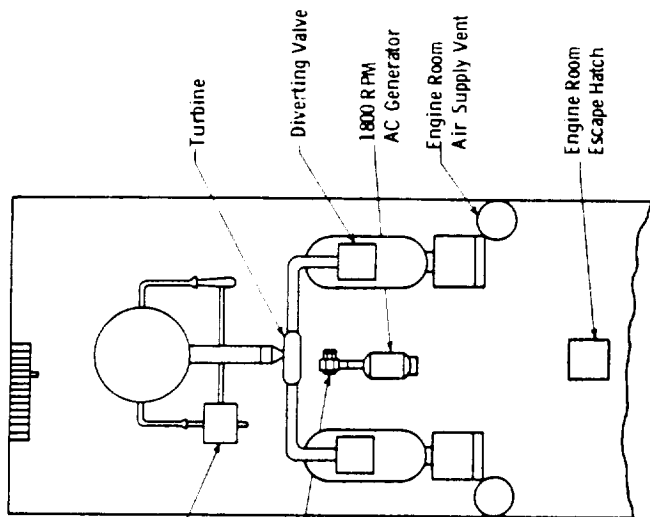


Fig. 7.13—Installation of steam injection cycle system on deck of push-pull boat for inland river service

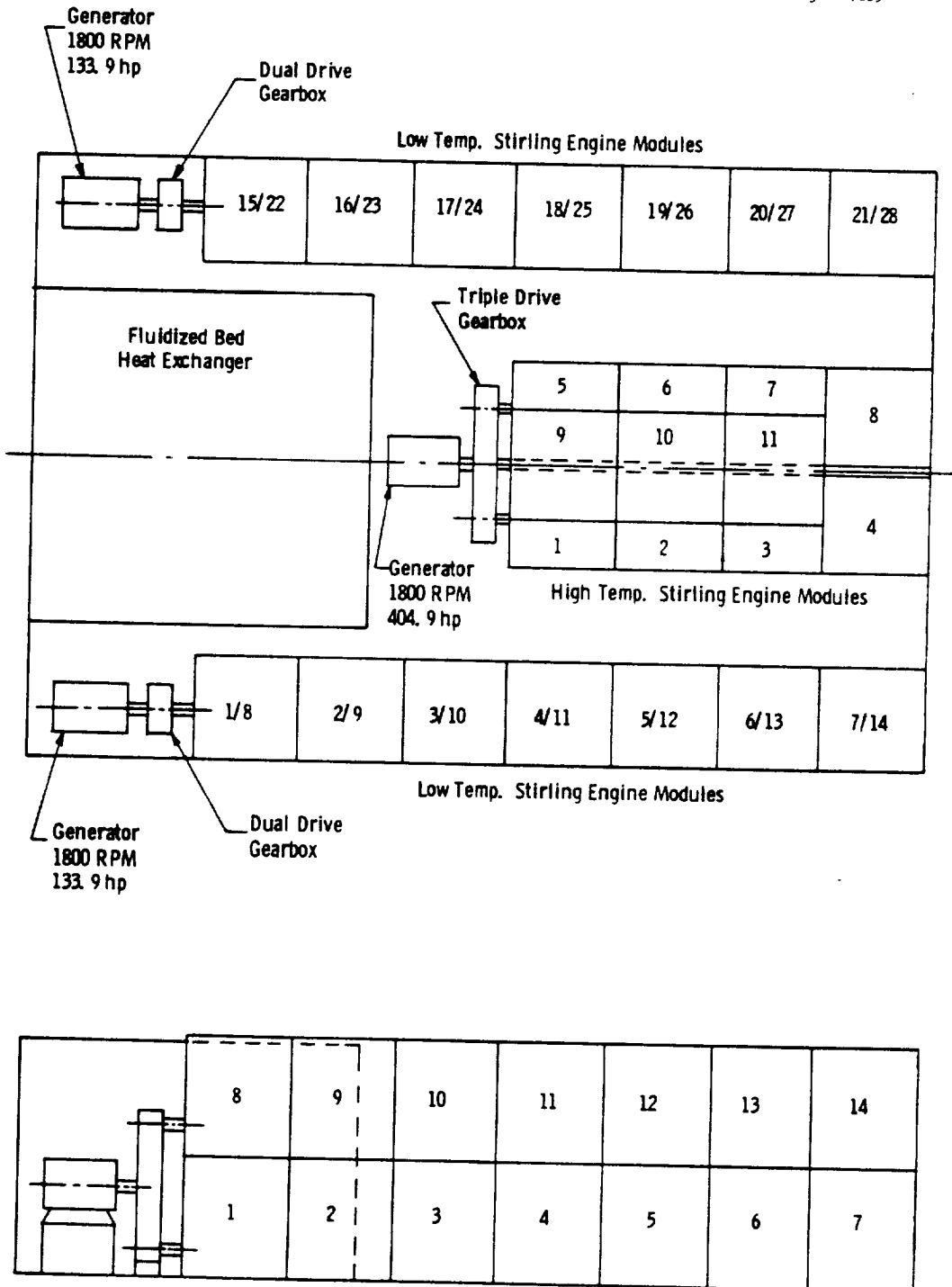


Fig. 7. 14—Stirling engine system arrangement for marine application

8. SYSTEM COSTS AND ECONOMIC ASSESSMENT

8.1 System Component Weights and Costs

This section summarizes the heat recovery subsystem component weights and costs derived from the conceptual design studies described. The design and cost basis for the different fluid bed heat exchangers was described in Section 6 above. Tables 8.1 through 8.9 summarize the estimated weights and costs for the major components comprising the heat recovery system for three different subposed cycles for the three applications. Where applicable, costs were scaled and indexed from available studies, References 1 through 4, and by weight and cost factors derived for similar mechanical equipment, piping, controls and other hardware. All prices have been indexed to mid-1984 dollars.

8.1.1 Rankine Cycle System

The weights for all of the system components except the fluidized bed vapor generator were based on the TECO design in Reference 1. The procedures used for scaling the turboexpander and the planetary gearbox for the locomotive and marine applications are described in Appendix F.

8.1.2 Steam Injection Cycle System

The procedures for estimating the weights of compressor drive expander, the power expander, and the planetary gearbox for all applications of the steam injection cycle system are described in Appendix B. The weights of the feed pump and the feed pump drive were derived from Reference 1. The weights of the other components were calculated or derived from generic data.

Table 8.1
 SUMMARY OF RANKINE BOTTOMING CYCLE COMPONENT COSTS
 FOR ADIABATIC DIESEL-HEAVY DUTY TRUCK APPLICATION

<u>ITEM DESCRIPTION</u>	<u>ESTIMATED WEIGHT, LBS.</u>	<u>ESTIMATED COST, \$</u>
Fluid Bed Vapor Generator	637	2797
Turbine/Gearbox	69.5	827
Feedpump/Drive	53.3	504
Plumbing/Hardware	12.2	118
Condenser/Regenerator Module	119	759
Control System	7	305
RC-1 Inventory	54	176
	<hr style="width: 20%; margin: auto;"/> 952.0	<hr style="width: 20%; margin: auto;"/> 5486

Cost Data Updated from TECO Report No. NASA CR-168256, Dec., 1983. (Ref. 1)

Table 8.2

SUMMARY OF RANKINE BOTTOMING CYCLE COMPONENT COSTS
FOR ADIABATIC DIESEL - LOCOMOTIVE APPLICATION

ITEM DESCRIPTION	ESTIMATED WEIGHT, LBS.	ESTIMATED COST, \$
Fluid Bed Vapor Generator	5279	25,513
Turbine/Gearbox Feedpump/Drive	3673	39,809
Plumbing/Hardware	87	840
Condenser/Regenerator Module	1860	8,150
Control System	7	305
RC-1 Inventory	287	932
	<hr/>	<hr/>
Subtotal	11193	75,549
Locomotive Chassis 66 Inch "Stretch" (Note 1)	15335	10,395
	<hr/>	<hr/>
TOTAL	26528	85,944

NOTE 1 - The GE-C36-7, 6 axle locomotive with standard turbocharged diesel engine is estimated to be priced at \$1,045,000 in mid-1984. The same locomotive with an adiabatic diesel 10 cylinder engine replacing the 16 cylinder standard diesel is estimated to cost \$967,510 and is 48.5 inches shorter. Thus, the incremental 66 inch addition for the RC-1 system brings the total length to 17.5 inches greater than the standard locomotive, or a total of 68 ft. 8.5 inches long. The incremental weight of the RC-1 system of 25,968 lbs., when added to the estimated net weight of the adiabatic engine equipped locomotive of 312,150 lbs., provides a total weight of 338,118 lbs. which is 1018 lbs. more than the standard diesel equipped C36-7.

Basis for data applicable to locomotive systems derived from JPL Publication 81-101 with appropriate cost indexing. (Ref. 2)

Table 8.3
 SUMMARY OF RANKINE BOTTOMING CYCLE COMPONENT COSTS
 FOR ADIABATIC DIESEL - MARINE APPLICATION

ITEM DESCRIPTION	ESTIMATED WEIGHT, LBS.	ESTIMATED COST, \$
Fluid Bed Vapor Generator	8173	39,175
Turbine/Gearbox Feedpump/Drive	5786	62,720
Plumbing/Hardware	145	1,400
Condenser/Regenerator Module	2232	13,650
Control System	20	1,000
RC-1 Inventory	480	1,560
Water Pumps (2)	1120	2,800
AC-Generator	5020	37,300
SCR AC/DC Units (2)	2400	83,600
DC Drive Motors (2)	12400	103,700
TOTAL	37776	346,905

Data on power transmission train (AC-Gen., SCR Units, and DC-Motors) to inject power into the twin diesel propulsion system were extracted from the JPL-81-101 Report on diesel propulsion systems for locomotives (Ref. 2)

Table 8.4
 SUMMARY OF STEAM INJECTION CYCLE COMPONENT COSTS
 FOR ADIABATIC DIESEL - HEAVY DUTY TRUCK APPLICATION

ITEM DESCRIPTION	ESTIMATED WEIGHT, LBS.	ESTIMATED COST, \$
Fluid Bed Boiler	587	1,989
Turbine/Gearbox Feedpump/Drive	136	1,475
Oil Cooler	3	15
Plumbing/Hardware	24	235
Control System	10	390
Water Tank, Empty	750	1,875
(Full)	(5750)	
TOTAL	<hr/> 1510 (6510)	<hr/> 5,979

Table 8.5
 SUMMARY OF STEAM INJECTION CYCLE COMPONENT COSTS
 FOR ADIABATIC DIESEL - LOCOMOTIVE APPLICATION

ITEM DESCRIPTION	ESTIMATED WEIGHT, LBS.	ESTIMATED COST, \$
Fluid Bed Boiler	1316	18,286
Turbine/Gearbox Feedpump/Drive	4160	40,750
Oil Cooler	29	150
Plumbing/Hardware	175	1,690
Control System	10	390
Water Tender, dry (full)	65000 (135,800)	46,580
Subtotal	70290 (141,090)	107,846
Locomotive Chassis 46 inch Stretch (Note 1)	10690	7,245
TOTAL	80980 (151,780)	115,091

Note 1 - The GE-C36-7, 6 axle locomotive with standard turbocharged diesel engine is estimated to be priced at \$1,045,000 in mid-1984. The same locomotive with an adiabatic diesel 10 cylinder engine replacing the 16 cylinder standard diesel is estimated to cost \$967,510 and is 48.5 inches shorter. Thus, the incremental 46 inch addition for the steam injection system brings the total length to 2.5 inches shorter than the standard locomotive, or a total of 67 ft. 0.5 inches long. The incremental weight of the steam injection system of 15,980 lbs. brings the locomotive weight to 328,130 lbs., and the tender net weight is 65,000 lbs, in addition to that.

Basis for data applicable to locomotive systems derived from JPL Publication 81-101 with appropriate cost indexing. (Ref. 2)

Table 8.6
 SUMMARY OF STEAM INJECTION CYCLE COMPONENT COSTS
 FOR ADIABATIC DIESEL - MARINE APPLICATION

ITEM DESCRIPTION	ESTIMATED WEIGHT, LBS.	ESTIMATED COST, \$
Fluid Bed Boiler	1930	28,972
Turbine/Gearbox Feedpump/Drive	5407	73,765
Oil Cooler	45	222
Plumbing/Hardware	255	2,460
Control System	30	1,500
Water Treatment System	5650	17,000
AC-Generator	5020	37,300
SCR AC/DC Units (2)	2400	83,600
DC Drive Motors (2)	12400	103,700
TOTAL	34535	348,519

Data on power transmission train (AC-Gen., SCR Units, and DC-Motors) to inject power into the twin diesel propulsion system were extracted from the JPL-81-101 Report on diesel propulsion systems for locomotives (Ref. 2).

Table 8.7
 SUMMARY OF STIRLING ENGINE CYCLE COMPONENT COSTS
 FOR ADIABATIC DIESEL - HEAVY DUTY TRUCK APPLICATION

ITEM DESCRIPTION	ESTIMATED WEIGHT, LBS.	ESTIMATED COST, \$
Fluid Bed Vapor Generator	645	1,716
S. Engine/Drives/Accessories (Note 1)	385	4,080
Piping/Hardware	60	600
Reservoirs/Sump/Pump for Heat Transfer Fluid	42	455
Control System	10	300
Heat Transfer Fluid Inventory	350	1,750
TOTAL	1492	8,901

Note 1 - Data on Stirling engine, drive and accessories were extracted from Ref. 20.

Table 8.8
SUMMARY OF STIRLING ENGINE CYCLE COMPONENT COSTS
FOR ADIABATIC DIESEL - LOCOMOTIVE APPLICATION

ITEM DESCRIPTION	ESTIMATED WEIGHT, LBS.	ESTIMATED COST, \$
Fluid Bed Vapor Generator	5240	15,176
S. Engine/Drives/Accessories	3875	40,970
Piping/Hardware	400	4,000
Reservoirs/Sump/Pump for Heat Transfer Fluid	420	4,550
Control System	10	300
Heat Transfer Fluid Inventory	3500	17,500
Subtotal	13445	82,496
Locomotive Chassis 60 inches Longer	13940	9,450
TOTAL	27385	91,946

Table 8.9
SUMMARY OF STIRLING ENGINE CYCLE COMPONENT COSTS
FOR ADIABATIC DIESEL - MARINE APPLICATION

<u>ITEM DESCRIPTION</u>	<u>ESTIMATED WEIGHT, LBS.</u>	<u>ESTIMATED COST, \$</u>
Fluid Bed Vapor Generator	8260	24,164
S. Engine/Drives/Accessories	6215	65,830
Piping/Hardware	600	6,000
Reservoirs/Sump/Pump for Heat Transfer Fluid	675	7,310
Control System	20	1,000
Heat Transfer Fluid Inventory	5650	28,270
AC Generators (3)	5720	42,500
SCR AC/DC Units (2)	2400	83,600
DC Drive Motors (2)	8650	72,325
TOTAL	38190	330,999

8.1.3 Stirling Engine System

The procedure for estimating the weights of the Stirling engine for all applications is described in Appendix G. The procedure for estimating the gearbox weight for the truck application is also described in Appendix G. The weights of the other components were calculated, obtained from vendors, or derived from generic data.

8.2 Comparison of System Weights

8.2.1 Truck Application

The system weights for the organic Rankine cycle, steam injection cycle, and Stirling engine systems for the truck application are summarized in Tables 8.1, 8.4, and 8.7, respectively. Comparison of the totals shows that the Rankine cycle system weight is significantly less than that of the Stirling engine systems. The dry weight of the steam injection cycle system is approximately the same as that of the Stirling engine. The weight of the water required to match the fuel tank capacity for the steam injection cycle, however, is significant.

8.2.2 Locomotive Applications

The system weights for the organic Rankine cycle, the steam injection cycle, and the Stirling engine systems are summarized in Tables 8.2, 8.5 and 8.8, respectively. The total weights shown are the sum of the energy conversion system weights and the net incremental weight of the locomotive. The net incremental weight of the locomotive is the increase in weight of the stretched chassis, minus the decrease in weight of the main engine.

Comparing the weights of the energy conversion systems show that the Rankine cycle is the least with the Stirling about 20% greater. The dry weight of the steam injection cycle including the dry tender is substantially greater than those of the other two systems. Comparing the total weights shows that the organic Rankine cycle and the Stirling

engine systems are nearly equal. The total dry weight of the steam injection system is about 3 times that of the other two systems. Adding the weight of the water to match the fuel storage tanks makes the difference even greater.

8.2.3 Marine Application

The system weights for the organic Rankine cycle, steam injection cycle, and Stirling engine systems for the marine application are summarized in Tables 8.3, 8.6, and 8.9, respectively. Comparing the total weights shows that the steam injection cycle system weighs the least. The weights of the two other systems are nearly equal and are about 15% greater than that of the steam injection cycle system.

The steam injection cycle system is superior in the marine application because provision is made for processing the feedwater during the duty cycle and no additional below deck tankage is required.

8.3 Economic Assessment of Turbocompound Diesel Engine Systems

The derived component cost and system performance data are used to calculate simple payback periods for the various heat utilization cycles and applications. In this analyses, the simple payback period (in years) is obtained by dividing the incremental capital investment for a given system by the annual value of fuel savings for that system. Table 8.10 shows the assumed economic and operational data used in calculating annual fuel consumption. Annual duty cycles were obtained from the previously cited reference studies.(1,2,4) Maintenance costs have not been included in this analysis. The incremental capital and fuel basis assumes comparison with the NASA Reference Adiabatic Turbocompounded Diesel with aftercooling. The pertinent engine parameters, costs and payback calculations are given in Tables 8.11 through 8.19 for each study case. Selling price for the reference diesel truck engine is taken from Reference 1 and adjusted to an equivalent Brake Horsepower Rating (BHP) using the recommended 30 \$/hp factor. For the locomotive

Table 8.10
 NASA REFERENCE
 ECONOMIC/OPERATIONAL DATA
 DIESEL ENGINES

Diesel Fuel Price	\$1.20/Gallon
Selling Price/Mfg. Cost Ratio	2.0

TRUCKS

Annual Mileage Per Truck	100,000
Annual Truck Engine Production Rate (Note 1)	10,000
Engines Produced by Year 2000	150,000

LOCOMOTIVES

Annual Horsepower-Hours Used	20 million
Annual Locomotive Engine Production Rate (Note 1)	10
Engines Produced by Year 2000	150

MARINE ENGINES

Annual Horsepower-Hours Used	35 million
Annual Marine Engine Production Rate (Note 2)	2
Engines Produced by Year 2000	30

Note 1 - Production rate assumes approximately a 10% market penetration

Table 8.11
NASA REFERENCE SIMPLE PAYBACK PERIOD
TURBOCHARGED + RC-1 BOTTOMING
VS
TURBOCOMPOUND-AFTERCOOLED
TRUCK APPLICATION

Bottoming Cycle Parameters

- Output as Applied to Turbocharged Engine = 56 HP
- Bottoming Cycle Selling Price = \$10972

Turbocharged + RC-1 Bottoming Engine Parameters

- Rated BHP = 317 + 56 = 373
- Specific Fuel Consumption/MPG = 0.268/6.65
- Annual Fuel Consumption = 15,038 Gal. @ \$18,046
- Engine System Selling Price = \$14,000 + \$10972 = \$24972

Comparable Turbocompound-Aftercooled Engine Parameters

- Rated BHP = 373
- Specific Fuel Consumption/MPG = 0.293/6.08
- Annual Fuel Consumption = 16,447 Gal. @ \$19,736
- Engine System Selling Price = \$16,500 + (373-340)(\$30/HP) = \$17,490

Simple Payback

- Annual Fuel Savings = 1409 Gal. @ \$1690
- Engine System Price Difference = \$7484
- Payback Period = 4.43 Years

Table 8.12
NASA REFERENCE SIMPLE PAYBACK PERIOD
TURBOCHARGED + STEAM INJECTION
VS
TURBOCOMPOUND-AFTERCOOLED
TRUCK APPLICATION

Bottoming Cycle Parameters

- Output as Applied to Turbocharged Engine = 62 HP
- Bottoming Cycle Selling Price = \$11,958

Turbocharged + Steam Injection Engine Parameters

- Rated BHP = $300 + 62 = 362$
- Specific Fuel Consumption/MPG = 0.276/6.46
- Annual Fuel Consumption = 15,480 Gal. @ \$18,576
- Engine System Selling Price = $\$14,000 + \$11,958 = \$25,958$

Comparable Turbocompound-Aftercooled Engine Parameters

- Rated BHP = 362
- Specific Fuel Consumption/MPG = 0.293/6.08
- Annual Fuel Consumption = 16,447 Gal. @ \$19,736
- Engine System Selling Price = $\$16,500 + (362-340)(\$30/HP) = \$17,160$

Simple Payback

- Annual Fuel Savings = 967 Gal. @ \$1160
- Engine System Price Difference = \$8798
- Payback Period = 7.58 Years

Table 8.13
NASA REFERENCE SIMPLE PAYBACK PERIOD
TURBOCHARGED + STIRLING ENGINE
VS
TURBOCOMPOUND-AFTERCOOLED
TRUCK APPLICATION

Bottoming Cycle Parameters

- Output as Applied to Turbocharged Engine = 42 HP
- Bottoming Cycle Selling Price = \$17,802

Turbocharged + Stirling Engine Parameters

- Rated BHP = 316 + 42 = 358
- Specific Fuel Consumption/MPG = 0.279/6.39
- Annual Fuel Consumption = 15,649 Gal. @ \$18,779
- Engine System Selling Price = \$14,000 + \$17,802 = \$31,802

Comparable Turbocompound-Aftercooled Engine Parameters

- Rated BHP = 358
- Specific Fuel Consumption/MPG = 0.293/6.08
- Annual Fuel Consumption = 16,447 Gal. @ \$19,736
- Engine System Selling Price = \$16,500 + (358-340)(\$30/HP) = \$17,040

Simple Payback

- Annual Fuel Savings = 798 Gal. @ \$958
- Engine System Price Difference = \$14,762
- Payback Period = 15.4 Years

Table 8.14
NASA REFERENCE SIMPLE PAYBACK PERIOD
TURBOCHARGED + RC-1 BOTTOMING
VS
TURBOCOMPOUND-AFTERCOOLED
LOCOMOTIVE APPLICATION

Bottoming Cycle Parameters

- Output as Applied to Turbocharged Engine = 542 HP
- Bottoming Cycle Selling Price = \$171,888

Turbocharged + RC-1 Bottoming Engine Parameters

- Rated BHP = 3058 + 542 = 3600
- Specific Fuel Consumption = 0.267
- Annual Fuel Consumption = 746,900 Gal. @ \$896,280
- Engine System Selling Price = \$675,000 - (3600-3058) x 120 + \$171,888 = \$781,848

Comparable Turbocompound-Aftercooled Engine Parameters

- Rated BHP = 3600
- Specific Fuel Consumption = 0.293
- Annual Fuel Consumption = 819,600 Gal. @ \$983,520
- Engine System Selling Price = \$675,000

Simple Payback

- Annual Fuel Savings = 72,700 Gal. @ \$87,240
- Engine System Price Difference = \$106,848
- Payback Period = 106,848/87,240 = 1.22 Years

Table 8.15
NASA REFERENCE SIMPLE PAYBACK PERIOD
TURBOCHARGED + STEAM INJECTION
VS
TURBOCOMPOUND-AFTERCOOLED
LOCOMOTIVE APPLICATION

Bottoming Cycle Parameters

- Output as Applied to Turbocharged Engine = 617 HP
- Bottoming Cycle Selling Price = \$230,182

Turbocharged + Steam Injection Engine Parameters

- Rated BHP = 2983 + 617 = 3600
- Specific Fuel Consumption = 0.261
- Annual Fuel Consumption = 730,100 Gal. @ \$876,120
- Engine System Selling Price = \$675,000 - (3600-2983) x 120 + \$230,182 = \$831,142

Comparable Turbocompound-Aftercooled Engine Parameters

- Rated BHP = 3600
- Specific Fuel Consumption = 0.293
- Annual Fuel Consumption = 819,600 Gal. @ \$983,520
- Engine System Selling Price = \$675,000

Simple Payback

- Annual Fuel Savings = 89,500 Gal. @ \$107,400
- Engine System Price Difference = \$156,142
- Payback Period = 156,142/107,400 = 1.45 Years

Table 8.16
NASA REFERENCE SIMPLE PAYBACK PERIOD
TURBOCHARGED + STIRLING ENGINE
VS
TURBOCOMPOUND-AFTERCOOLED
LOCOMOTIVE APPLICATION

Bottoming Cycle Parameters

- Output as Applied to Turbocharged Engine = 418 HP
- Bottoming Cycle Selling Price = \$183,892

Turbocharged + Stirling Engine Parameters

- Rated BHP = $3182 + 418 = 3600$
- Specific Fuel Consumption = 0.278
- Annual Fuel Consumption = 777,600 Gal. @ \$933,120
- Engine System Selling Price = $\$675,000 - (3600-3182) \times 120 + \$183,892 = \$808,732$

Comparable Turbocompound-Aftercooled Engine Parameters

- Rated BHP = 3600
- Specific Fuel Consumption = 0.293
- Annual Fuel Consumption = 819,600 Gal. @ \$983,520
- Engine System Selling Price = \$675,000

Simple Payback

- Annual Fuel Savings = 42,000 Gal. @ \$50,400
- Engine System Price Difference = \$133,732
- Payback Period = $133,732/50,400 = 2.65$ Years

Table 8.17
NASA REFERENCE SIMPLE PAYBACK PERIOD
TURBOCHARGED + RC-1 BOTTOMING
VS
TURBOCOMPOUND-AFTERCOOLED
MARINE APPLICATION

Bottoming Cycle Parameters

- Output as Applied to Turbocharged Engine = 904 HP
- Bottoming Cycle Selling Price = \$693,810

Turbocharged + RC-1 Bottoming Engine Parameters

- Rated BHP = 4696 + 904 = 5600
- Specific Fuel Consumption = 0.264
- Annual Fuel Consumption = 1,293,000 Gal. @ \$1,551,600
- Engine System Selling Price = \$1,050,000 - (5600-4696) x 120 + \$693,810 = \$1,635,330

Comparable Turbocompound-Aftercooled Engine Parameters

- Rated BHP = 5600
- Specific Fuel Consumption = 0.293
- Annual Fuel Consumption = 1,435,000 Gal. @ \$1,722,000
- Engine System Selling Price = \$1,050,000

Simple Payback

- Annual Fuel Savings = 142,000 Gal. @ \$170,400
- Engine System Price Difference = \$585,330
- Payback Period = 585,330/170,400 = 3.43 Years

Table 8.18
NASA REFERENCE SIMPLE PAYBACK PERIOD
TURBOCHARGED + STEAM INJECTION
VS
TURBOCOMPOUND-AFTERCOOLED
MARINE APPLICATION

Bottoming Cycle Parameters

- Output as Applied to Turbocharged Engine = 962 HP
- Bottoming Cycle Selling Price = \$697,038

Turbocharged + Steam Injection Engine Parameters

- Rated BHP = 4638 + 962 = 5600
- Specific Fuel Consumption = 0.261
- Annual Fuel Consumption = 1,279,000 Gal. @ \$1,534,800
- Engine System Selling Price = \$1,050,000 - (5600-4638) x 120 + \$697,038 = \$1,631,598

Comparable Turbocompound-Aftercooled Engine Parameters

- Rated BHP = 5600
- Specific Fuel Consumption = 0.293
- Annual Fuel Consumption = 1,435,000 Gal. @ \$1,722,000
- Engine System Selling Price = \$1,050,000

Simple Payback

- Annual Fuel Savings = 156,000 Gal. @ \$187,200
- Engine System Price Difference = \$581,598
- Payback Period = 581,598/187,200 = 3.11 Years

Table 8.19
NASA REFERENCE SIMPLE PAYBACK PERIOD
TURBOCHARGED + STIRLING ENGINE
VS
TURBOCOMPOUND-AFTERCOOLED
MARINE APPLICATION

Bottoming Cycle Parameters

- Output as Applied to Turbocharged Engine = 673 HP
- Bottoming Cycle Selling Price = \$661,998

Turbocharged + Stirling Engine Parameters

- Rated BHP = 4927 + 673 = 5600
- Specific Fuel Consumption = 0.277
- Annual Fuel Consumption = 1,357,000 Gal. @ \$1,628,400
- Engine System Selling Price = \$1,050,000 - (5600-4927) x 120 + \$661,988 = \$1,631,228

Comparable Turbocompound-Aftercooled Engine Parameters

- Rated BHP - 5600
- Specific Fuel Consumption = 0.293
- Annual Fuel Consumption = 1,435,000 Gal. @ \$1,722,000
- Engine System Selling Price = \$1,050,000

Simple Payback

- Annual Fuel Savings = 78,000 Gal. @ \$93,600
- Engine System Price Difference = \$581,228
- Payback Period = 581,228/93,600 = 6.21 Years

Table 8.20
 SUMMARY OF SIMPLE PAYBACK PERIOD (YRS)

Bottoming Cycle

<u>Application</u>	<u>RC-1</u>	<u>Steam Injection</u>	<u>Stirling Engine</u>
Truck	4.43	7.58	15.4
Locomotive	1.22	1.45	2.65
Marine	3.48	3.11	6.21

and marine applications, the reference adiabatic turbocompound-aftercooled diesel engine performance is assumed. For both the locomotive and marine application, the payback period calculations are based on reference engines of comparable size (3600 hp - locomotive and 5600 hp - marine) to the study case. The price for both the locomotive and marine diesel turbocompound-aftercooled reference engine was estimated by using a 120 \$/hp factor to adjust the price data given in References 2 and 4 respectively. The 120 \$/hp factor was derived by assuming that the incremental hp-factor for the larger engines would be proportional to that given for the heavy duty truck (Reference 1). In all cases, the price and size of the comparison "Turbocompound-Aftercooled" engine was adjusted to that of the turbocharged engine with its bottoming cycle. Note that for the locomotive engines, the cost of \$675,000 for the base case 3600 hp engine was derived from the cost breakdown given in Reference 2 and adjusted for mid 1984 dollars. The cost of the 5600 hp marine engine was based on the same \$/hp as for the locomotive.

Table 8.20 shows a separate summary of the calculated payback periods for the nine different cases based on the annual duty and fuel cost assumptions listed previously in Table 8.10.

Based on the simple payback period calculations, the RC-1 subposed heat recovery cycle appears as the most attractive of the three options for both the truck and locomotive applications while the steam injection cycle shows the lowest payback for the marine application. In this study, the Stirling engine system showed poorest economics. For this case, the engine and system drive appeared to be a major cost consideration. The fluid bed costs were relatively low because this cycle does not utilize any finned tubed, inbed convective section.

Although the RC-1 system in the truck application shows a lower payback period than the other two cycle options, the 4.43 years calculated does not represent a particularly attractive time period. This calculated simple payback period exceeds the payback target identified

in Reference 3 and would be even further extended if maintenance costs and costs of money were included.

Adiabatic diesel heat recovery appears most attractive for the locomotive application. For this case, payback periods ranging from 1.22 to 2.65 years were calculated for the three different cycle options. Again for the simple payback period calculation, the RC-1 cycle showed lowest time period. Based on these results continued consideration of efficient and cost effective heat recovery for the diesel locomotive appears warranted.

For the marine application, the subposed cycle heat recovery systems showed payback periods ranging from 3.48 to 6.21 years. In this application, the steam injection cycle showed the lowest payback periods, a result of the slightly better system performance (than the RC-1) and application with high annual fuel costs. The calculated payback periods may be marginal as an incentive for investment particularly considering the maintenance costs and cost of money have not been included.

9. REFERENCES

1. DiNanno, L., F. DiBella and M. Koplow, "An RC-1 Organic Rankine Bottoming Cycle for an Adiabatic Diesel Engine," DOE/NASA/0302-1, NASA CR-168256, TE4322-251-83, December 1983.
2. Bailey, M. M., "Overview of Waste Heat Utilization Systems," DOE/NASA/50194-41 NASA TM 86901, paper presented 22nd Automotive Technology Development Contractors' Coordination Meeting, Dearborn, Michigan, October 29-November 1, 1984.
3. Liddle, S. G., et al., "Future Fuels and Engines for Railroad Locomotives," JPL Publication 81-101, November, 1981.
4. "For the Study of the Validation of the Application of Rankine Bottoming Cycle Technology to Marine Diesel Engines," Final Report, DOE Contract No. DE-AC01-78C554224, AED-EO-17, July 1980.
5. Klaren, D. G., Fluid Bed Heat Exchanger: A Major Improvement In Severe Fouling Heat Transfer, Proceedings of a Seminar, "Heat Exchangers", 885, 1983.
6. U.S. Department of Energy, Idaho Operations Office, Energy Conservation Branch, Background Information for Advanced Heat Exchanger Notice of Program Interest, NOPI No. DE-NP07-83ID 12482, Aug. 1983.
7. Parkinson, G., Ceramics Make a Try for Tough Heat-recovery Jobs, Chemical Engineering, 61, April, 1982.
8. Cole, W. E., Investigation of Waste Heat Recovery Utilizing Fluidized Bed Heat Exchangers, United Technologies Research Center Final Report, Report R78-912942, Nov. 1978.
9. Stoeffler, R. C., Enhancement of Heat Transfer in Waste-heat Heat Exchangers, United Technologies Research Center Final Report, July 1980, DOE/ET/11348-T1.
10. Rudnicki, M. I., C. S. Mah, and H. W. Williams, Status of Fluidized-Bed Waste Heat Recovery, Proceedings of a Seminar, "Heat Exchangers", 549, 1983
11. Cox, D., M. Lytton, and C. Rao, Potential Industrial Applications for Fluidized-Bed Waste Heat Recovery Systems.

12. The Econo-Therm Hot-Blast System, The Econo-Therm Corporation, Englewood, N.J.
13. Ikeda, S., S. Ito and T. Someya, An Experimental Marine Fluidized Bed Boiler Plant, Power, 15, Oct., 1983.
14. Virr, M. J., Fluidized Bed Heat Recovery Systems, Chapter 11 in Fluidized Beds, Combustion and Applications, J. R. Howard, editor, Applied Science Pub., New York, 1983.
15. Carlomagno, G. M., et al, Heat Recovery From Diesel Exhausts By Means Of A Fluidized Bed Heat Exchanger, paper presented at the 75th Annual AIChE Meeting, Los Angeles, California, November, 1982.
16. Campanile, A., et al, United States Patent Number 4,340,400, July, 1982.
17. H. E. Khalifa, "Waste Heat Recovery from Adiabatic Diesel Engines by Exhaust-Driven Brayton Cycles," United Technologies Research Center, East Hartford, CT, NASA CR-168257 Dec. 1983, (DOE/NASA/0304-1, 1983).
18. "Cogeneration Technology Alternatives Study (CTAS)" DOE/NASA/0031-80/1, NASA CR-159765, Prepared by General Electric Co. for NASA/DOE, Jan. 1980.
19. Martini, W. R., "Stirling Engine Design Manual," 2nd ed. DOE/NASA/3194-1, NASA CR-168088, January 1983.
20. "Automotive Stirling Engine MOD 1 Design Review Report," Vol. I, II and III, DOE/NASA/0032-16, NASA CR-167935, prepared by MTI for DOE/NASA, August 1982.
21. "Stirling Engine Design Manual," Second Edition DOE/NASA/3194-1, NASA CR-168088, January 1983.

APPENDIX A
FLUID BED HEAT RECOVERY UNIT DESIGN PROCEDURE

NOMENCLATURE APPENDIX A

Design Characteristics

- A: area;
subscripts: none = outer tube surface; b = vessel cross-section; surface; f = ratio of fin area per unit bare tube area
- d: diameter;
subscripts: none = particle; b = bubble; mx = maximum; m = minimum; t = outer tube; ti = inner tube; or = orifice; v = vessel; bo = initial bubble at base of bed
- L: length:
subscripts: a = above the tube bundle to the top of the bed surface; u = under tube bundle to the distributor; b = bed height; f = fin height; fb = freeboard height; j = jet length; tdh = transport disengaging height; v = vessel height; p = inlet plenum height; l = vessel length; w = vessel width, in the direction of the horizontal tubes; z = plenum outlet to top of freeboard bundle; sp = splash zone height; tube length
- N: number:
subscripts: t = tubes; r = tube runs per tube; l = tube layers or columns; or = orifices per unit area; s = number of tubes per column with tubes on vertical plane
- n: number:
subscripts: none = ratio of numbers N_t to N_l ; r = number of coil rotations on a plane
- Q: the heat load on each stage
- S: pitch:
subscripts: h = horizontal tube; v = vertical tube; or = orifice; w = tube to vessel wall; f = fins
- t: thickness:
subscripts: f = fin; t = tube wall; w = vessel wall; d = deposit; dis = distributor; in = insulation; c = corrosion allowance
- ϵ_d : free area fraction on the distributor
- γ : ratio of vessel length to width

Operating Conditions

Cd: drag coefficient for an orifice

F: mass flow rate:

subscripts: none = exhaust gas to tube convectively of in bed;
f = working fluid to inner tube surface; o = overall; a = ambient to vessel surface; ft = finned tube

P: pressure:

subscripts: none = exhaust gas; b = bed; f = working fluid

rt: velocity turndown ratio

T: temperature:

subscripts: none = exhaust gas; f = working fluid; mn = minimum operating; a = ambient; s = outside surface of vessel; o = inlet exhaust gas; l = outlet exhaust gas

U: velocity:

subscripts: none = exhaust gas superficial through the beds; m = minimum; mx = maximum; mf = minimum fluidization; t = terminal; or = orifice

δ : volume fraction:

subscripts: none = bubbles in bed; t = tubes in bed

Properties

Cp: heat capacity:

subscripts: none = exhaust gas; s = particles

g: gravitational constant

k: thermal conductivity:

subscripts: none = exhaust gas; f = working fluid; t = tube material; d = deposit material; in = insulation

Pr: Prandtl Number:

subscripts: none = exhaust gas; f = working fluid

St: maximum allowable stress:

subscripts: dis = distributor plate; w = vessel wall; t = tube wall

ϵ : voidage:

subscripts: non = in the bed emulsion phase; mf = at minimum fluidization velocity; o = total for whole bed

ρ : density:
subscripts: none = exhaust gas; f = working fluid; p = particle;
m = at minimum operation temperature

μ : viscosity:
subscripts: none = exhaust gas; f = working fluid

ϕ : particle sphericity

APPENDIX A
FLUID BED HEAT RECOVERY UNIT DESIGN PROCEDURE

The fluid bed heat recovery unit is designed following the procedure outlined below. The description of the design procedure given represents the major design equations and design philosophy applied. Pertinent references from the general literature are also listed. The calculational steps are presented in the order in which they are performed and points of iteration are noted.

The input conditions to the design are the diesel exhaust conditions (flow rate, temperature, pressure, composition, physical and thermodynamic properties) and the working fluid conditions (flow rate, inlet and outlet temperatures, pressure, physical and thermodynamic properties). The heat recovery unit stage conditions (bed temperatures and convective section temperatures) are selected to provide the desired heat recovery unit effectiveness using an overall energy balance. The log-mean temperature difference and heat transfer duty on each stage of the unit are determined.

A) VELOCITY SELECTION

The fluidization velocity on the first stage of the unit, $U(1)$, (the high-temperature stage, having the highest velocity of all the unit stages) is selected to yield a reasonable unit cross-sectional area. This velocity may be modified if the resulting overall design is unacceptable. The fluidization velocity on each of the other fluid bed stages is determined from this by

$$U(i) = U(1) \rho(1) / \rho(i) \quad (1)$$

The minimum operating velocity on each fluid bed stage is determined using the unit turndown ratio

$$r_t = F_m / F \quad (\rho(1) / \rho_m(1)) \quad (2)$$

to yield

$$U_m(i) = U(i) r_t \quad (3)$$

B) PARTICLE SIZE DETERMINATION

The initial selection in this step is for the particle material. The material must be physically and chemically stable in the exhaust gas environment and should be commercially available in suitable particle sizes having sufficient fluid bed attrition resistance. The particle density, r_p , and the particle average sphericity, ϕ , should be estimated for input into the design procedure. Iteration of the design procedure with respect to the particle material may be required in order to achieve an acceptable design. In general, the same particle material would be specified on all of the stages.

The maximum-average particle diameter (using the surface-to-volume average) on each fluid bed stage is determined, using the Ergun equation (1)* to maintain the minimum fluidization velocity 0.5 ft/s below the minimum operating velocity, U_m :

$$d_{mx}(i) = \frac{[B + (B + 600 (\rho_p g (1 - \epsilon) \mu(i) (U_m(i) - 0.5))^2 / (r(i) \phi \epsilon)^2)]^{1/2}}{(2 \rho_p g / \rho(i))} \quad (4)$$

where $B = 1.75 (U_m(i) - 0.5)^2 / (\phi \epsilon^3)$

*Numbers in parenthesis refer to References listed at the end of Appendix A.

An additional constraint is placed on the maximum-average particle diameter that

$$d_{mx}(i) < (S_h - d_t) / 10 \quad (5)$$

in order not to hinder particle circulation within the bed and not to promote poor bed-to-tube heat transfer.

The minimum-average particle diameter is determined to result in a bed terminal velocity that is 1 ft/s above the operating velocity on each stage, $U(i)$: defining

$$GA(i) = 4 g \rho_p \rho(i) / (3\mu^2(i)) \quad (6)$$

and

$$RE(i) = (U(i) + 1) \rho(i) / \mu(i) \quad (7)$$

then

$$d_m(i) = [24 RE(i) / GA(i)]^{3/2} \quad \text{if } GA(i) d_m^3(i) < 2.44 \quad (8)$$

$$d_m(i) = [22.31 RE(i) / GA(i)^{0.9375}]^{0.5517} \quad \text{if } GA(i) d_m^3(i) < 76.9 \quad (9)$$

$$d_m(i) = [11.12 RE(i) / GA(i)^{0.7738}]^{0.7568} \quad \text{if } GA(i) d_m^3(i) < 1496 \quad (10)$$

$$d_m(i) = [6.324 RE(i) / GA(i)^{0.6943}]^{0.9234} \quad \text{if } GA(i) d_m^3(i) < 10940 \quad (11)$$

$$d_m(i) = [2.752 RE(i) / GA(i)^{0.6076}]^{1.215} \quad \text{if } GA(i) d_m^3(i) < 707946 \quad (12)$$

$$d_m(i) = [0.552 RE(i) / GA(i)^{0.4898}]^{2.130} \quad \text{if } GA(i) d_m^3(i) > 707946 \quad (13)$$

The same procedures may be used to find the maximum particle diameter in the desired size distribution (the maximum diameter that can be maintained in the fluidized state at the minimum operating velocity) and the minimum particle diameter in the desired size distribution (the minimum diameter that can be maintained in the bed without elutriation at the operating velocity).

The average particle diameter on each stage is then determined from the relationship

$$d(i) = 1/2 [d_{mx}(i) + d_m(i)] \quad (14)$$

and, unless the average particle diameters on the fluid bed stages differ significantly, a single commercially available average particle diameter, d , is selected for all of the stages that is close to the determined averages and satisfies all of the constraints set in the procedure.

With this single average particle diameter the average terminal velocity for each bed is determined by defining

$$NGA(i) = 4 g \rho_p \rho(i) d^3 / (3\mu^2(i)) \quad (15)$$

and

$$NRE(i) = \rho(i) d / \mu(i) \quad (16)$$

for use in

$$U_t(i) = NRE(i)^{-1} NGA(i) / 24 \quad \text{if } NGA(i) < 2.44 \quad (17)$$

$$U_t(i) = 0.04483 NRE(i)^{-1} NGA(i)^{0.9375} \quad \text{if } NGA(i) < 76.9 \quad (18)$$

$$U_t(i) = 0.08991 \text{ NRE}(i)^{-1} \text{ NGA}(i)^{0.7738} \quad \text{if NGA}(i) < 1496 \quad (19)$$

$$U_t(i) = 0.15812 \text{ NRE}(i)^{-1} \text{ NGA}(i)^{0.6943} \quad \text{if NGA}(i) < 10940 \quad (20)$$

$$U_t(i) = 0.3634 \text{ NRE}(i)^{-1} \text{ NGA}(i)^{0.6076} \quad \text{if NGA}(i) < 707946 \quad (21)$$

$$U_t(i) = 1.811 \text{ NRE}(i)^{-1} \text{ NGA}(i)^{0.4898} \quad \text{if NGA}(i) > 707946 \quad (22)$$

Likewise, the minimum fluidization velocity, U_{mf} , on each stage is determined from

$$U_{mf}(i) = [B' + \{ B' + 7 d^3 \rho_p g / (\phi \epsilon^3 \rho(i)) \}^{1/2}] / (3.5 d / (\phi \epsilon^3)) \quad (23)$$

$$\text{where } B' = -150 (1-\epsilon) \mu(i) / (\phi^2 \epsilon^3 \rho(i))$$

C) FLUID BED HEAT TRANSFER COEFFICIENTS

A variety of correlations for heat transfer coefficients between fluidized beds and horizontal, bare tubes immersed in the bed have been developed for various ranges of operating conditions(3-5). Some have been developed specifically for shallow fluidized beds, but in general they apply more directly to relatively deep beds and small-scale laboratory equipment(6-8). It has been observed that the heat transfer coefficients measured in shallow fluidized beds can be significantly larger than those in deeper beds(9,10). For the purposes of the heat recovery unit design the following correlations are applied:

For particles greater in diameter than 2.953×10^{-3} ft (900 μm) the correlation of Glicksman and Decker is used(11):

$$h(i) = k(i) (1-\delta(i)) / d \{ 9.42 + 0.042 U(i) d \rho(i) C_p / k(i) \} \quad (24)$$

This correlation for large particles reflects the fact that radiation has a negligible contribution to the heat transfer coefficient at the temperatures of interest. The impact of the tube spacing on the heat transfer coefficient is approximated by applying a factor

$$\left[1 - d_t/S_h \left(1 + 1 / \left(1 + S_v/d_t \right) \right) \right]^{1/4}$$

to the heat transfer coefficient, as given by Gelperin, et al (12). The bubble volume fraction in the bed must also be estimated to use this correlation and this is done using the relationship proposed by Bar-Cohen for slow bubbles(13):

$$\alpha(i) = (U(i) - U_{mf}(i)) / [U(i) + U_{mf}(i) + 0.71 (g d_b(i))^{1/2}] \quad (25)$$

To use this relationship the average bubble diameter in the bed, $d_b(i)$, must first be guessed and an iterative procedure performed to converge to the proper value of the bubble volume fraction once the bed depth has been determined. For particles having diameter less than 2.953×10^{-3} ft but larger than 1.312×10^{-3} ft (400 μ m) the correlation of Andeen and Glicksman is used(14):

$$h(i) = 900 k(i) (1 - \epsilon_o(i)) Pr(i)^{0.3} / dt^{0.674} [U(i) \mu(i) / (d^3 \rho_p g)]^{0.326} \quad (26)$$

This correlation is based on shallow bed data and uses the correlation of Leva(15) for the total bed voidage $\epsilon_o(i)$:

$$\epsilon_o(i) = 0.48 [200 U(i) \mu(i) / (d^2 (\rho_p - \rho(i)) g)]^{1/3} - 0.19 \quad (27)$$

The impact of the tube bundle spacing is expressed by a factor

$$\left[1 - d_t/S_h \left(1 + 1 / \left(1 + S_v / d_t \right) \right) \right]^{1/4}$$

if the tube are in a staggered arrangement, and a factor

$$[1 - d_t / S_h]^{1/4}$$

if the tube are in a square arrangement.

For particles having diameters less than 1.312×10^{-3} ft the correlation of Grewal and Saxena is used(16):

$$h(i) = 0.46 k(i) / (d_t^{0.21} d^{0.37}) (C_p/C_{ps})^{0.2} [\rho(i) \rho_p g/\mu(i)^2] \quad (28)$$

This correlation for small particles is actually for the maximum heat transfer coefficient achieved as a function of velocity and will tend to over estimate the coefficient. The impact of tube spacing in the bundle is given by the factor

$$[1 - 0.21 (S_h / d_t)]^{-1.75}$$

If the tubes have extended surfaces on them the heat transfer coefficient is known to be significantly modified depending on the fin characteristics. The study of finned tube heat transfer in fluidized beds has been studies extensive(17-19) and the following procedure for estimating the finned tube heat transfer coefficient has been proposed.

Specifically we restrict attention to tubes with radial fins having rectangular profile and we define the fin efficiency factor as

$$E_f = 1/3 [1 + L_f / d_t]^{1/2} \quad (29)$$

and the total finned tube area over the bare tube area as

$$A_f = 1 + d_t/(4 S_f) [(1 + L_f/d_t^2) - 1] + t_f L_f / (S_f d_t) \quad (30)$$

Based on Zabrodsky's work on finned tube heat transfer in fluid beds(20)

$$h_f(i) = [4 E_f L_f^2 / (A_f k_t t_f)]^{-1} [(1+8 A_f^{-.1} h(i) E_f L_f^2 / (k_t t_f))^{1/2} - 1] \quad (31)$$

expresses the relationship between the finned tube heat transfer coefficient, h_f , per unit of "bare" tube heat transfer surface, and the bare tube heat transfer coefficient, h . Note that in some cases the fin material and its thermal conductivity, k_t , may differ from the tube body material to provide both weight and heat transfer advantages.

Some constraints are also imposed on the finned tube dimensions:

- 1) the gap between the fins should not be less than five particle diameters in order to avoid a loss in tube heat transfer coefficient or,

$$S_f - t_f > 5 d$$

- 2) the fin height, L_f , should not exceed 0.5 inches in order to avoid a reduction in the heat transfer coefficient below the correlation values
- 3) the tube pitch should not be less than the tube diameter plus twice the fin length to avoid finned tube interaction

While it is certainly not expected that these correlations will provide extremely accurate estimates of the bed-to-tube heat transfer coefficient, it is expected that they will provide correct trends in the heat transfer behavior and order-of-magnitude estimates of the coefficients that are sufficient for the purpose of conceptual design.

D) HEAT TRANSFER IN THE SPLASH ZONE

It has been reported that, especially in shallow fluidized beds, the zone directly above the densely fluidized bed where high concentrations of particles are ejected upward and drop back into the bed contributes significantly to heat transfer if tubes are immersed in this

"splash" zone(6-10). Here, the splash zone is defined as being the zone directly above the bed where the heat transfer coefficient to the immersed tubes is identical to those in the dense bed and the effective temperature driving force is equal to the bed temperature. The splash zone behaves simply as an extension of the dense bed. The height of the splash zone is estimated in a following section.

E) CONVECTIVE HEAT TRANSFER COEFFICIENTS ABOVE THE SPLASH ZONE

For the design procedure the simplifying assumption is made that there is a step jump in heat transfer behavior from the splash zone, where ejected particles contribute to the rate of heat transfer, to the convective zone above, where heat transfer is that of a particle free gas. In reality, it is to be expected that some increase in the heat transfer coefficient above the splash zone might exist, but some reduction in the effectiveness of heat transfer would also exist due to the recirculating particles in the convective zone. Overall, this is a reasonable assumption for conceptual design evaluation, with the two effects counteracting each other to some extent.

Based on standard references, Afgan and Schlunder(21), for example, the convective heat transfer coefficients for bare tubes are given by:

$$h = 0.021 [G d_t / \mu]^{0.84} Pr^{0.36} k / d_t \quad (32)$$

$$\text{if } G d_t / \mu \geq 2 \times 10^5$$

If $G d_t / \mu < 2 \times 10^5$ then

$$h = 0.27 k / d_t [G d_t / \mu]^{0.63} Pr^{0.36} \quad (33)$$

if the tubes are in-line and, if the tubes have a staggered arrangement, then

$$h = 0.35 k / d_t [4 S_v / S_h]^{0.2} [G d_t / \mu]^{0.6} Pr^{0.36} \quad (34)$$

if $S_h / S_v > 2$

$$h = 0.40 k / d_t [G d_t / \mu]^{0.2} Pr^{0.36} \quad (35)$$

if $S_h / S_v < 2$.

If finned tubes are used in the convective zone then the two factors in equations 29 and 30 may be used to compute the finned tube heat transfer coefficient relative to the bare tube value, based on the bare tube surface area:

$$h_f = [4 E_f L_f^2 / (A_f k_t t_f)]^{-1} [(1 + 8 h E_f L_f^2 / (k_t t_f))^{1/2} - 1] \quad (36)$$

This equation is restricted to radial fins of rectangular cross-section, but other forms of fins can easily be considered by modifying the factors E_f and A_f .

F) TUBE INNER DIAMETER

The tube wall thickness is determined by standard methods(22):

$$t_t = d_t / [2 (0.8 ST_t / P_f + 0.4)] + t_c \quad (37)$$

where the tube thickness is rounded up to the next larger standard thickness and all tubes in the unit are assigned the same dimensions unless they differ significantly enough to justify differing tube dimensions in each stage. The tube inner diameter is then

$$d_{ti} = d_t - 2 t_t \quad (38)$$

G) TUBE NUMBER

The heat recovery unit internal cross-sectional area is

$$A_b = F / (\rho(1) U(1)) \quad (39)$$

For a heat recovery unit that is rectangular in cross-section the width and length are given by

$$L_w = (A_b / \gamma)^{1/2} \quad \text{and} \quad L_1 = \gamma L_w \quad (40)$$

where L_w is the length in the direction in which the tubes run. With the tubes oriented on horizontal planes the number of tube runs, N_r , on any stage of the heat recovery unit is

$$N_r = 1 + (L_1 - 2 S_w - d_t) / S_h \quad] / n \quad (41)$$

where the distance between the inner vessel wall and the outer row of tubes is generally set to be greater than one tube diameter to maintain good bed circulation(23). The number of tubes per layer of tubes, n , is a parameter which may be adjusted during the design to yield better design features. The number of tube runs obtained from equation 41 is rounded off to the nearest whole number. The number of tubes, N_t , on any stage of the heat recovery unit is

$$N_t = A / (\pi d_t) [L_w N_r - 2(N_r - 1)(S_w + d_t/2) + (N_r - 1) S_h]^{-1} \quad (42)$$

where A is now the total heat transfer surface area on the specific stage estimated using the bed-to-tube heat transfer coefficient by $A = Q / h$, Q being the heat load on the stage. N_t is again rounded up to the next highest whole number. It is also convenient to obtain the tube numbers on all stages to be identical so that single tube lengths can be used throughout the unit, or that the tube numbers are even multiples of each other. With the tubes arranged in vertical planes, the tube number is

$$N_t = N_s [(L_1 - 2 S_w - d_t) / S_h + 1] \quad (43)$$

rounded to the nearest whole number, where N_s is the number of tubes per column of vertical tubes.

The geometry of a cylindrical vessel dictates some kind of coiled tube configuration. The coil configuration with compactly arranged coils can make n_r rotations on a single level:

$$n_r = [(d_v - d_t) / 2 - S_w] / S_h \quad (44)$$

where d_v is the vessel inner diameter (= ($4 / \pi A_b^{1/2}$)).
The number of tubes is given by

$$N_t = n A / \{ 2 \pi^2 d_t [n_r d_t + .5 (n_r + 1) n_r S_h] \} \quad (45)$$

rounded to the next closest whole number. Again, it is convenient if the number of tubes on each stage are identical or are even multiples of each other.

H) INSIDE TUBE HEAT TRANSFER COEFFICIENTS

We are now in a position to estimate the heat transfer coefficients on the inside of the tubes. For sections of heat transfer surface that function to preheat or superheat a gas or vapor or to cool a gas or liquid, the heat transfer coefficient is(21)

$$h_f = k_f 0.027 / d_{ti} \{ 4 F_f / (\mu_f \pi d_{ti} N_t) \}^{0.8} Pr_f^{1/3} \quad (46)$$

where $4 F_f / (\mu_f \pi d_{ti} N_t)$ must be larger than 10.4 . This same correlation may be used in a steam system in the zone of "departure from nucleate boiling" if $F_f / (\rho_f \pi d_{ti} N_t)$ is greater than 1.5. DNB is assumed to occur when 80% of the water evaporation has been completed. On evaporation stages the inside tube heat transfer coefficient is assumed to be very large relative to the other heat transfer resistances and a fixed value of $3000 \text{ btu/hr-ft}^2 \text{ } ^\circ\text{F}$ is used for approximation purposes.

I) OVERALL HEAT TRANSFER COEFFICIENT

The overall heat transfer coefficient is given by

$$h_o = [1/h + 1/h_f (d_t/d_{ti}) + t_d/k_d + t_t/k_t + 2 \ln(d_t/d_{ti})/(1-d_{ti}/d_t)]^{-1} \quad (47)$$

based on the outside tube area.

J) TUBE SURFACE AREAS AND CHECK ON TUBE NUMBER AND PITCH

The actual tube surface area may now be calculated from

$$A = Q / h_o$$

The tube numbers are then recalculated and compared to the original estimates. If the corrected tube numbers change significantly then a reiteration of the heat transfer coefficients in the tube is needed until a fixed tube number is obtained. Because of the rounding off procedure, the equations converge very quickly. Finally, the tube vertical and horizontal pitches and the tube spacing with the wall is recalculated. All constraints on the tube pitches must still be satisfied.

K) TUBE-SIDE PRESSURE DROP

The tube length is given by

$$L_t = A / (\pi d_t N_t) \quad (49)$$

in any section of the heat recovery unit. For a gas or vapor preheat or superheat section, or for a liquid or gas cooler(24)

$$\Delta(P_f) = 0.0075 \mu_f^{1/4} / \rho_f \quad 1 / d_{ti}^{19/4} \quad (F_f / N_t^{7/4}) L_t \quad (50)$$

expresses the pressure drop. Over the evaporation and DBN section the pressure drop is estimated by(25)

$$\Delta(P_f) = 0.0038 \mu_{f1}^{1/4} / \rho_{fv}^{1/4} / d_{ti}^{19/4} (F_f / N_t^{7/4}) L_t / (1+f_1/f_v)^{1/4} + (4 F_f / (\pi d_{ti}^2 N_t))^2 (1/r_{fv} + 1/r_{f1}) / g \quad (51)$$

where the subscripts 1 and v stand for liquid and vapor properties.

The total pressure drop should be less than 10% of the working fluid supply pressure or the tube diameter must be modified and the design reiterated.

L) GAS DISTRIBUTOR DESIGN

It can be shown that the distributor pressure drop required for stable operation of the bed is roughly given by(26)

$$\Delta(P_d) \{ \text{lb/ft}^2 \} = U \{ \text{ft/s} \} \quad (52)$$

as compared to other criteria that call for a minimum distributor pressure drop of from 10 to 35% of the bed pressure drop. The distributor design is selected to be an orifice plate having uniformly distributed holes of diameter, d_{or} , no more than four times the average particle diameter in diameter(rounded up to the closest standard size) to limit particle weeping. The orifice velocity is

$$U_{or} = C_d (2 g \Delta(P_d) / \rho^{1/2}) \quad (53)$$

with C_d being the orifice coefficient, equal to about 0.7.

The jet length issued at the orifices is estimated by(27)

$$L_j = 15 d_{or} [\rho / \rho_p U_{or}^2 / (g d_{or})]^{0.187} \quad (54)$$

and the number of orifices per unit area is

$$N_{or} = U / U_{or} \rho / \rho_p \quad 4 / (\pi d_{or}^2) \quad (55)$$

The initial bubble diameter produced by each jet is(28)

$$d_{bo} = 1.3 [F / (\rho A_b N_{or} g^{1/2})]^{0.4} \quad (56)$$

Other characteristics of interest in the design of a gas distributor plate are the orifice pitch,

$$S_{or} = 1 / (N_{or}^{1/2}) \quad (57)$$

and the orifice free area fraction,

$$\epsilon_d = (U / U_{or}) (\rho / \rho_{in}) \quad (58)$$

where ρ_{in} is the gas density of the gas entering the distributor. The plate thickness is determined from standard thickness relationships for the selected plate material at the temperature of the inlet gas to the plate, and is based on the plate supporting its own weight and the weight of the bed. Supports to prevent warping of the flat plates may be required for plates of very large cross-section and an insulating layer on top of the plate will be applied in general to keep the plate at the highest temperature to minimize deposition of diesel soot.

M) BED DEPTH

The tube surface areas determined previously must be immersed in the bed or the splash zone above the bed. If all of the tubes are to be immersed completely in the dense bed region, the required bed depth (expanded) for tubes on horizontal planes (rectangular or cylindrical vessels) are

$$L_b = d_t + L_u + L_a + [N_1 - 1] S_v \quad (59)$$

where the number of tube layers, N_1 , is equal to N_t / n . The distance from the distributor plate to the first row of the tubes, L_u , is selected to be about 1 inch to minimize the bed height. The distance from the top tube row to the top of the expanded bed, L_a , is selected to be 1 inch to maintain the tubes within the bed during velocity turndown. The specific turndown requirements must be evaluated to select L_u . With tubes arranged in vertical planes and completely immersed in the dense bed

$$L_b = d_t + L_u + L_a + [N_r - 1] \beta_v S_v$$

where β_v is equal to 1 if the tubes are arranged "in line" and is equal to 2 if the tubes are staggered.

The bed depth must exceed the jet length by about 50% in order to maintain a fluid bed and if this condition is not satisfied the bed depth is set at 1.5 times the jet length or the distributor orifices are redesigned to give shorter jets.

If the splash zone above the dense bed is to be used to contain heat transfer surface then, for tubes on horizontal planes

$$L_b + L_{sp} = d_t + L_u + [N_1 - 1] S_v \quad (61)$$

where L_{sp} is the splash height. For tubes on vertical planes

$$L_b + L_{sp} = d_t + L_u + [N_r - 1] \beta_v S_v \quad (62)$$

In this case the bed depth is specified as being greater than or equal to 1.2 times the jet length. The work of George and Grace, on splash height is used as the basis for determining the splash height(29). From this work, the total height of the splash zone above a fluidized bed containing horizontal tubes is about 29% of the transport disengaging

height, based on the deterioration of the heat transfer coefficient. For the definition of the splash height used here, being the height over which the heat transfer coefficient and particle-gas temperature does not differ significantly from the bed heat transfer coefficient and the bed temperature, the splash height is about 1/4 of the total splash height determined by George and Grace, or about 7.1% of the transport disengaging height. Above this point it is assumed that the heat transfer coefficient is equal to the particle-free convective heat transfer coefficient. The transport disengaging height is estimated from the work of Zenz(30) as

$$L_{tdh} = 1.67 \quad 4 d_{bmx})^{0.75} (U - U_{mf})^{(1/(4 dbmz))0.25} \quad (63)$$

where d_{bmx} is the maximum bubble diameter at the surface of the bed. The correlation of Rowe(31) for the bubble size distribution in a fluid bed is used to estimate the maximum bubble diameter:

$$d_{bmx} = 1.75 d_{b0} + 0.42 (U - U_{mf})^{1/2} (L_b - L_j^{3/4}) \quad (64)$$

The splash height criteria above and equations 63 and 64 are solved iteratively for the terms L_b , L_{sp} , L_{tdh} and d_{bmx} .

N) THE FREEBOARD HEIGHT

The height of the freeboard region above the dense fluid bed is selected to minimize particle splashing on the above-stage distributor plate, with the possibility of particle attrition, plate erosion and orifice plugging, and to minimize particle elutriation from the unit while maintaining the vessel total height at a reasonable level. For stages that are below the top stage of the heat recovery unit the particle elutriation is not a concern and the freeboard height is selected to be

$$L_{fb} = L_{sp} \quad (65)$$

if there are tubes located in the splash zone, and

$$L_{fb} = 0.1 L_{tdh} \quad (66)$$

if all of the tubes are immersed in the dense bed.

For the top stage of the unit where particle elutriation is a concern a greater freeboard height is specified and

$$L_{fb} = 0.25 L_{tdh} \quad (67)$$

if tubes are located in the splash zone, while

$$L_{fb} = 0.35 L_{tdh} \quad (68)$$

if all tubes are immersed in the dense bed. If a convective zone of heat recovery is located in the top stage freeboard then the freeboard must be large enough to accomodate this surface of height

$$d_t + L_{sp} + L_z + [N_r - 1/2] B_v S_v$$

for vertical tubes, and

$$d_t + L_{sp} + L_z + [N_1 - 1/2] S_v$$

for horizontal tubes. L_z is the height from the top of the convective tube bundle to the gas outlet.

O) THE BED PRESSURE DROP

The bed pressure drop is given by

$$\Delta(P_b) = L_b \rho_p [1 - \delta_t] [1 - \delta] [1 - \epsilon_{mf}] \quad (69)$$

The fraction of the bed volume occupied by bubbles, δ , is taken to be(13)

$$\delta = [U - U_{mf}] / [U + U_{mf} + 0.71 (g \bar{d}_b)^{1/2}]$$

where the average bubble diameter in the bed, \bar{d}_b , is $d_{bmx}/1.75$. The volume fraction of tubes in the bed is

$$\delta_t = [d_t A (L_b - L_u) / ((L_b + L_{sp} - L_u) (4 A_b L_b))] \quad (71)$$

P) INSULATION THICKNESS

The average thickness of insulation around the heat recovery vessel is estimated to be

$$t_{in} = k_{in} / h_a [((t_0 + t_1) / 2 - t_a) / (t_s - t_a) - 1] \quad (72)$$

where this layer of insulation may be distributed nonuniformly with the thickest portions at the base and the thinner ones at the top. The specified outer surface temperature of the insulation is t_s , while t_0 and t_1 are the inlet and outlet gas temperatures, and t_a is the ambient temperature. The ambient to surface heat transfer coefficient, h_a is treated as a free parameter because it is highly dependent on the speed of the vehicle and its geometry.

REFERENCES - Appendix A

1. Ergun, S., Chem. Eng. Progr., 48, 89 (1952)
2. Fuchs, N. A., Mechanics of Aerosols, Trans., editor C. N. Davies, Pergamon Press, 1956.
3. Kunii, D., and O. Levenspiel, Fluidization Engineering, John Wiley & Sons, Inc., New York, 1969.
4. Botterill, J. S. M., Fluid-Bed Heat Transfer, Academic Press, London, 1975.

5. Saxena, S. C., et al, Heat Transfer Between A Gas Fluidized Bed and Immersed Tubes, in Advances in Heat Transfer, Editor T. F. Irvine and J. P. Hartnett, Academic Press, New York, 1978.
6. Williams, H. W., R. Hernandez and C. S. Mah, Choosing the Optimum Bed Material for a Fluidized Bed Heat Exchanger, Proceedings of the 16th Intersociety Energy Conversion Eng. Conf., 1981.
7. Al Ali, B. M. A., and J. Boughton, Shallow Fluidized-Bed Heat Transfer, Applied Energy, 3, 101 (1977).
8. Baker, A., Heat Transfer Studies Between A Horizontal Tube and a Shallow Fluidized Bed, Ph. D. Thesis, Univ. Western Ontario, 1981.
9. Virr, M. J., and H. W. Williams, Heat Transfer in Shallow Fluidized Bed Waste Heat Systems, presented at the 1984 Annual AIChE Meeting, San Francisco, CA.
10. Atkinson, G. A., Extended Surface Fluidized Bed Heat Transfer, Ph. D. Thesis, Univ. Aston in Birmingham, 1974.
11. Glicksman, L. R., and N. Decker, Heat Transfer in Fluidized Beds with Large Particles, MIT Industrial Liaison Program, Symposium, January 18, 1979.
12. Gelperin, N. I., V. G. Einshtein, and L. A. Korotynskaya, Int. Chem. Eng., 9, 137 (1969).
13. Bar-Cohen, A., Fluid Mechanic Characteristics of Bubbling Fluidized Beds, Adv. Mech. Flow Granular Mater., 2, 529 (1983).
14. Andeen, B. R., and L. R. Glicksman, Heat Transfer to Horizontal Tubes in Shallow Fluidized Beds, ASME paper 76-HT-67.
15. Leva, M., Can. J. Chem. Eng., 35, 71 (1957).
16. Grewal, N. S., S. C. Saxena, Experimental Studies of Heat Transfer Between a Bundle of Horizontal Tubes and a Gas-Solid Fluidized Bed of Small Particles, Ind. Eng. Chem. Process Des. Dev., 22, 367 (1983).
17. Goel, I., S. C. Saxena, and A. F. Dolidovich, Heat Transfer From Rough and Finned Horizontal Tubes in a Gas Fluidized Bed, J. Heat Transfer, 106, 91 (1984).
18. Krause, W. E., and A. R. Peters, Heat Transfer from Horizontal Serrated Finned Tubes in an Air-Fluidized Bed of Uniformly-Sized Particles, ASME paper 80-HT-48.

19. Chen, J. C., Heat Transfer to Tubes in Fluidized Beds, ASME paper 76-HT-75.
20. Zabrodsky, S. S., et al, Heat Transfer of Single Horizontal Finned Tubes and Their Bundles in a Fluidized Bed of Large Particles, in Fluidization, editors J. R. Grace and J. M. Matsen, Plenum Press, New York, 1980.
21. Afgan, N., and E. U. Schlunder, Heat Exchangers: Design and Theory Sourcebook, Scripta Book Co., Wash. D.C., 1974.
22. Chemical Engineer's Handbook, editor, J. H. Perry, Fourth Edition, McGraw-Hill Book Co., New York, 1963.
23. Exxon Research and Engineering Co., Industrial Application Fluidized Bed Combustion, Indirect Fired Process Heaters, Final Program Report for July 1, 1976 - September 30, 1980, DOE/ET/10379-T3.
24. Bird, R. B., W. E. Stewart, and E. N. Lightfoot, Transport Phenomena, John Wiley & Sons, Inc., New York, 1960.
25. Collier, J. G., The Design of Boilers, in Heat Exchangers, editors S. Kakac, A. E. Bergles, and F. Mayinger, Hemisphere Pub. Corp., New York, 1981.
26. Wen, C. Y., J. Shang, and D. F. King, Distributor Design, presented at MIT Special Summer Program on Fluidized Bed Combustion, Program 2.60S, July, 1981.
27. Yang, W. C., Jet Penetration in a Pressurized Fluidized Bed, I&EC Fund., 20, 297 (1981).
28. Davidson, J. F., and B. O. G. Schuler, Trans. Inst. Chem. Engrs., 38, 335 (1960).
29. George, S. E., and J. R. Grace, AIChE J., 28(5), 759, (1982).
30. Zenz, F. A., and N. A. Weil, AIChE J., 4(4), 472(1968).
31. Rowe, P. N., Prediction of Bubble Size in a gas Fluidized Bed, Chem. Eng. Sci., 31, 285 (1976).

APPENDIX B
COMPONENT DATA FOR STEAM INJECTION CYCLE SYSTEMS

B.1 Compressor Drive Expander

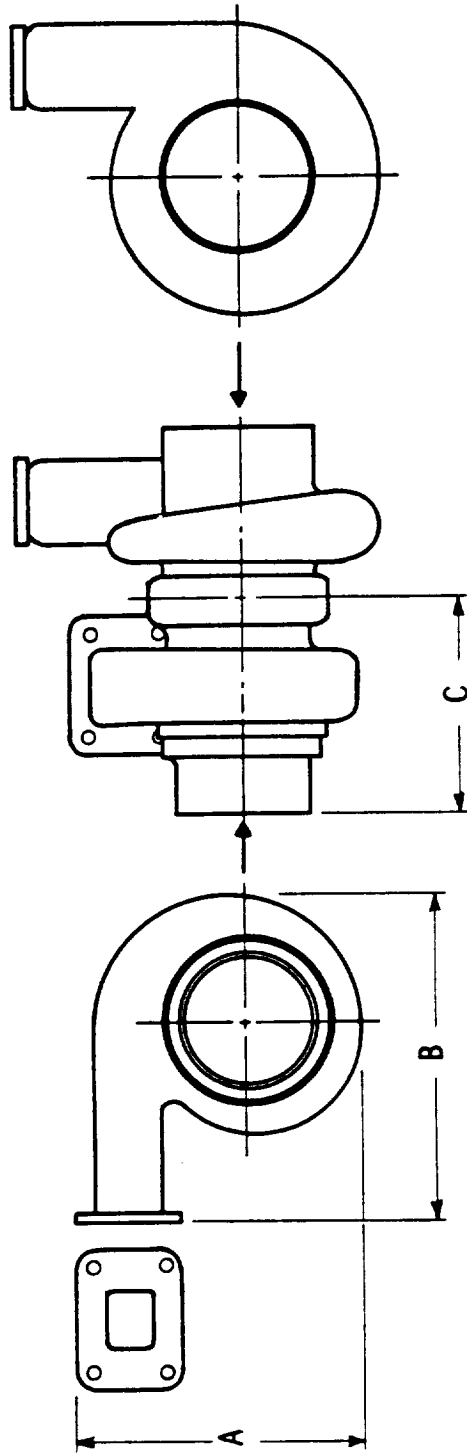
The designs for the compressor drive expander for the steam injection cycle were based on data from the Cummins T-46B turbocharger. The Dimensions for the compressor drive expander for the three applications are tabulated in Figure B1.

The design for the power expander was also based on the Cummins T-46B turbocharger. The designs for the gearbox, the feed pump, and the feed pump drive that are integral with the power expander were also based on the TECO system described in Reference 1. The dimensions for the power expander and the gearbox for the three applications are tabulated in Figure B2.

Conventional procedures for scaling turbomachinery were used for both of these components. The gearboxes were scaled using the procedure described in Appendix D.

For the steam injection systems the compressor drive expander, the power expander, and the gearbox are modifications of standard turbocompound engine components so the weights chargeable to the supposed cycle are the incremental weights of these components. Table B1 lists the incremental weights of the compressor drive expander and the power expander for the three applications. Table B2 lists the incremental weights of the planetary gearboxes for the three applications.

Dwg. 9363A66



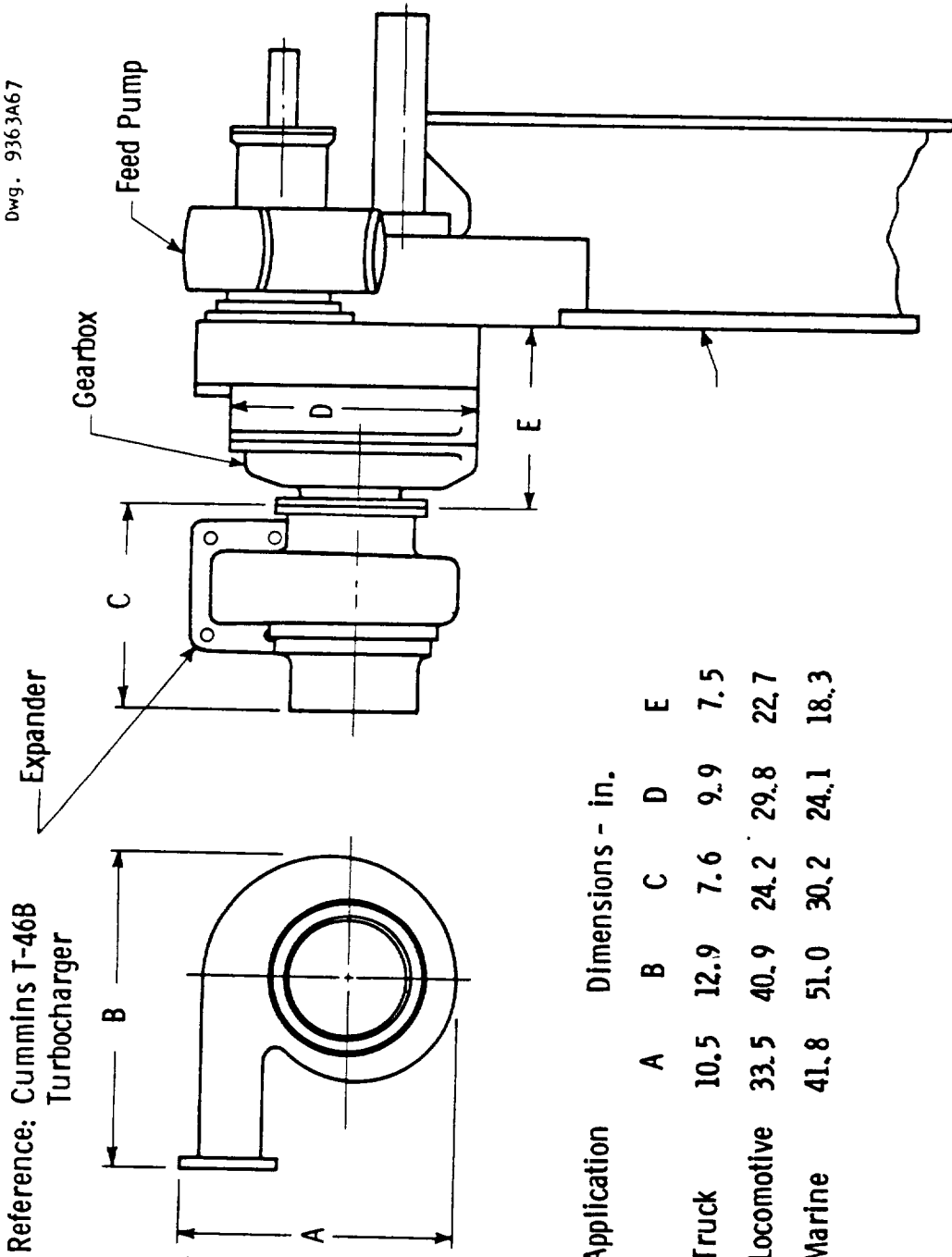
Reference: Cummins T-46B
Turbocharger

Application Dimensions - in.

	A	B	C
Truck	8.6	10.5	6.2
Locomotive	27.1	33.1	19.6
Marine	33.8	41.4	24.4

Fig. B1 — Compressor drive expander dimensions for steam Injection cycle

Dwg. 9363A67



Reference: Cummins T-46B
Turbocharger

Application Dimensions - in.

	A	B	C	D	E
Truck	10.5	12.9	7.6	9.9	7.5
Locomotive	33.5	40.9	24.2	29.8	22.7
Marine	41.8	51.0	30.2	24.1	18.3

Fig. B2 -- Power expander and gearbox dimensions for steam injection cycle

Table B1 - TURBOEXPANDER DATA FOR STEAM INJECTION CYCLE

<u>Application</u>	<u>Truck</u>	<u>Locomotive</u>	<u>Marine</u>
Total Power - hp	362.0	3600	5600
Subsystem Power - hp	62.2	618.6	962.2
Compressor Drive Expander			
Speed - RPM	61,500	19,400	15,700
Rotor Diameter - in	4.8	15.1	18.8
Weight - lb	20.2	641	1249
Incremental Weight ⁽¹⁾ - lb	.4	122	242
Power Expander			
Speed - RPM	46,100	14,500	11,700
Rotor Diameter - in	5.9	18.6	23.2
Housing Length - in	7.6	24.7	30.2
Involute Dimensions - in	10.5x12.9	33.5x40.9	41.8x51.0
Weight - lbs	37.9	1207	2341
Incremental Weight ⁽¹⁾ - lb	(2.2)	(74)	(145)
Total Incremental Weight ⁽¹⁾ - lb	(1.8)	(48)	(97)
Specific Incremental Weight ⁽¹⁾ - lb	(.029)	.079	.101

(1) Relative to turbocompound engine without steam injection

Table B2 - PLANETARY GEARBOXES FOR STEAM INJECTION CYCLE SYSTEM

Application	Truck	Locomotive	Marine
Total Power - hp	362.0	3600	5600
Subsystem Power - hp	62.2	618.6	962.2
Turbine Speed - RPM	46,100	14,500	11,700
Diesel Engine Speed - RPM	1900	1050	1050
Gear Speed - RPM	3000	1050	1800 ⁽¹⁾
Speed Ratio	15.37	13.81	6.5
Gear Q-Factor	.385	10.04	5.34
Weight Factor	.959	26.5	14.0
Weight - lbs	34.5	945	504
Scale Factor	.986	2.98	2.41
Incremental Weight ⁽²⁾ -lb	16.3	439	224

(1) Generator Speed

(2) Relative to turbocompound engine without steam engine

APPENDIX C
SCALING OF STIRLING ENGINES

C.1 Procedure

The Beale number (N_{Be}) is a dimensionless group of quantities which empirically relate the power output of a Stirling engine (watts) to

R_m mean cycle pressure - bar
 f frequency of operation - HZ
 V_o swept volume of power piston - cm

as follows:

$$N_{Be} = W / (P_m \times f \times V_o). \text{ See References C1 and C2.}$$

When the heater temperature is 650°C and the cooler temperature is 65°C, the value of N_{Be} is about 0.015.

The temperature dependence of the Beale number as developed by Walter^(C1) is shown in Figure C1.

C.2 Reference Engine

The MOD 1 automotive Stirling engine being developed by TECO under NASA LeRC Contract DEN 3-32 was used as the reference engine in scaling the Stirling engine for the heavy duty transfer applications. The characteristics of this engine are as follows: (C3, C4, C5)

Engine type - double acting
Drive type - U
Number of Cylinders - 4
Engine speed - 4000 rpm
Working fluid - hydrogen
Bore - 68 cm

ORIGINAL PAGE IS
OF POOR QUALITY

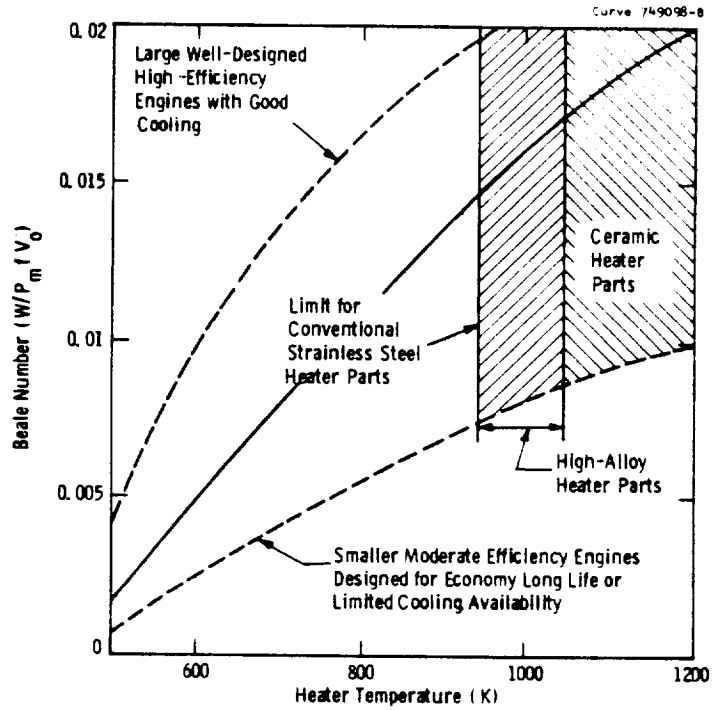


Fig. C1—Beale number as a function of heater temperature (after Walker, 1979)

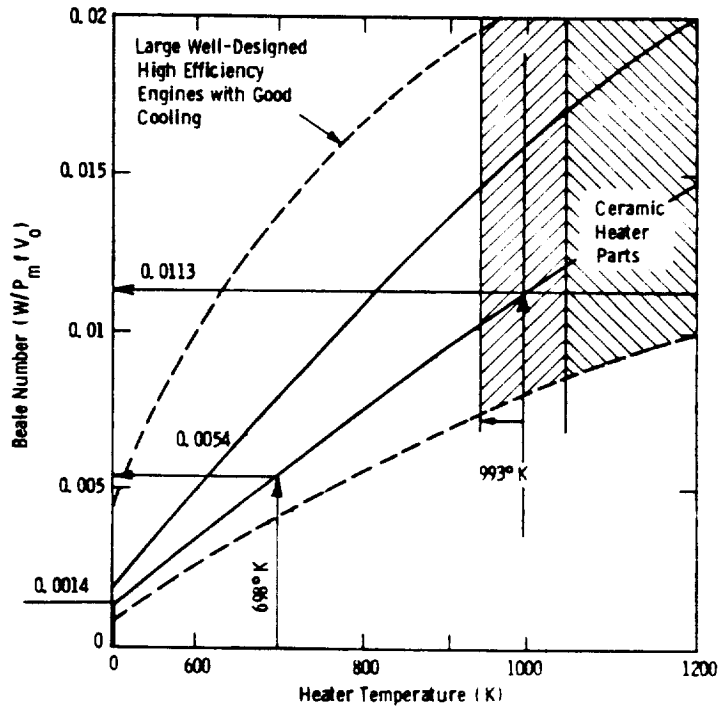


Fig. C3—Beale number as a function of heater temperature showing Stirling engine design parameters

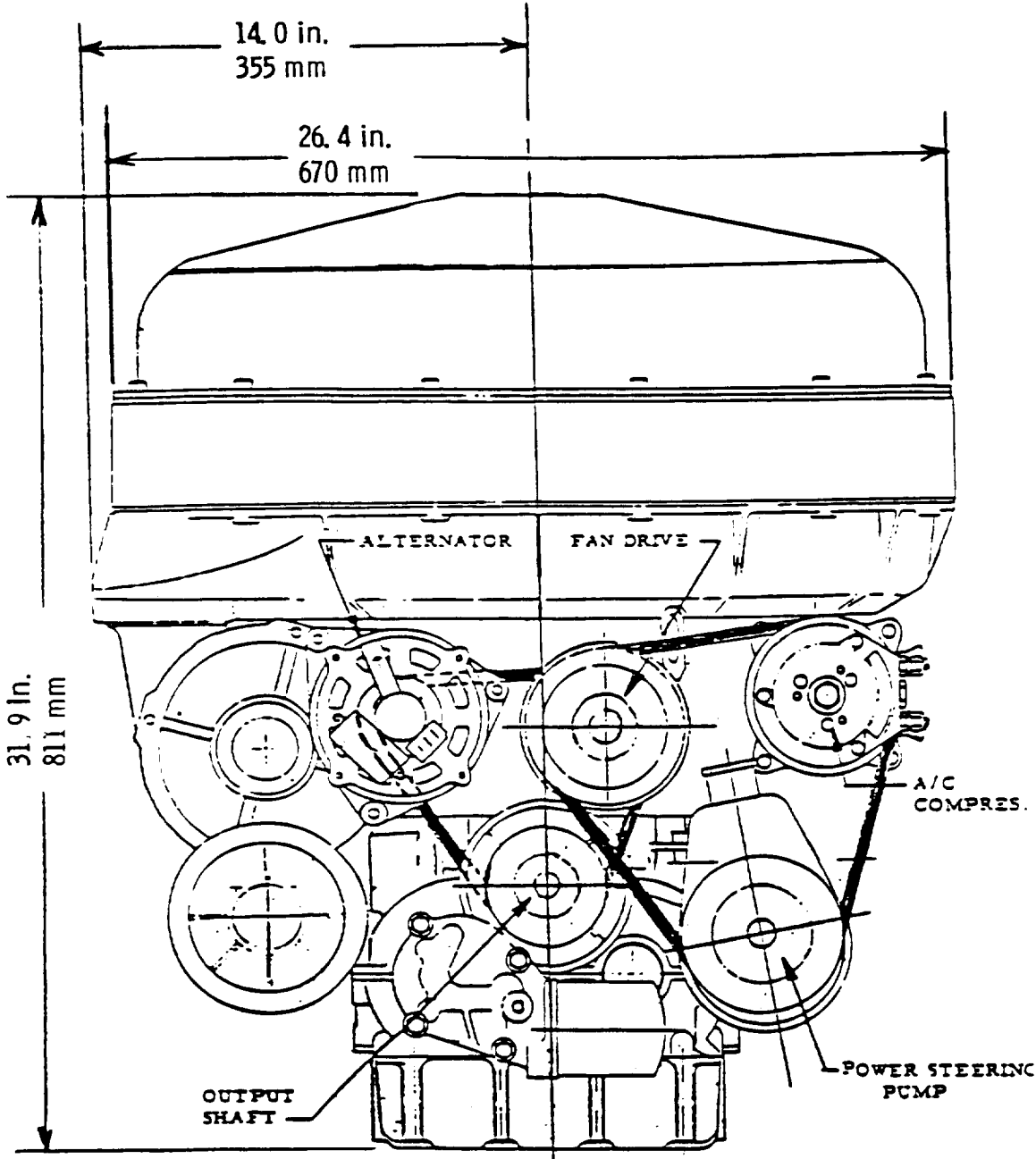


Fig. C2—Conventional V-belt accessory drive

Stroke - 34 cm
 Displacement - 123.5 cm/cylinder
 Heater temperature - 720°C
 Cooler temperature - 50°C
 Mean cycle pressure - 15 MPa
 Net engine power - 56 kW (75 hp)
 Net engine efficiency - 0.277
 Specific weight - 9.3 lb/hr
 Specific cost - 57.5 \$/hp
 Envelope dimensions - see Figure C2

Beale number for MOD 1

$$\begin{aligned}
 N_{Be} &= W / (f \times V_o \times P_m) \\
 &= 56,000 / (66.7 \times 494 \times 150) = 0.0113
 \end{aligned}$$

Temperature correction for MOD 1 power

V_o = constant

Assume

P_m = constant

f = constant

$N_{B3} = \phi(\text{heater temperature})$

Solve for power

High Temperature case

Heater Temp. = 797°F (698 K)

$N_{Be} = 0.0054$ (from Fig. C3)

$W = N_{Be} \times P_m \times f \times V_o = 0.0054 \times 150 \times 66.7 \times 494 = 26,689$

$W = 35.8$ hp

Low Temperature Case

Heater temp = 450°F (506° K)

$N_{Be} = 0.0014$ (from Fig. C3)

$W = .0014 \times 150 \times 66.7 \times 494 = 6920, W = 9.28$ hp

Lumped losses for MOD 1 engine

$$\eta_{net} = (1 - T_C/T_H) \times C \times \eta_H \times \eta_M \times f_a, \text{ Ref. C6}$$

C = Carnot efficiency ratio

η_H = heater efficiency - 0.92

η_M = mechanical efficiency

f_a = auxiliary power ratio

T_C = cooler temperature - 50°C

T_H = heater temperature - 720°C

η_{net} = net engine efficiency - 0.277

$$\begin{aligned} C \times \eta_M \times f_a &= \eta_{net} / ((1 - T_C/T_H) \times \eta_H) \\ &= 0.277 / ((1 - 323/933) \times 0.92) = 0.446 \end{aligned}$$

Modified net engine efficiency for MOD 1 engine

For heat recovery with heat pipe assume η_H - 0.99

$$\eta_{net} = 0.99/0.92 \times 0.277 = 0.298$$

Scaling for long haul truck application

High temperature unit

$$T_{EXH} = 1247^\circ\text{F}$$

$$H_{EXH} = 343.6 \text{ Btu/lb}$$

$$T_{BED} = 900^\circ\text{F}$$

$$H_{BED} = 247.0 \text{ Btu/lb}$$

$$W_p = 2886 \text{ lb/hr}$$

$$\eta_{HX} = 0.975$$

$$Q_{REC} = 2886 \times (343.6 - 247.0) \times 0.975 = 271,818 \text{ Btu/hr}$$

$$T_H = 797^\circ\text{F}$$

$$T_C = 122^\circ\text{F}$$

$$\eta_{net} = (1 - 583/1257) \times 0.446 \times 0.99 = 0.237$$

$$\text{Power} = 0.237 \times 271818/2545 = 25.3 \text{ hp}$$

Reference power - 35.8 hp

$$\text{Scaling factor} = 25.3/35.8 = 0.707$$

Mean cycle pressure - 150 bars

Frequency - 66.7 HZ 4000 RPM

Piston stroke

$$S = S_o \times 0.707^{0.333} = 0.891 S_o$$

Cylinder diameter

$$D = D_o \times 0.707^{0.333} = 0.891 D_o$$

$$\text{Engine volume/weight factor} = 0.891^3 = 0.707$$

Low temperature unit

$$T_{IN} = 900^\circ\text{F}$$

$$H_{IN} = 247.0 \text{ Btu/lb}$$

$$T_{ST} = 553^\circ\text{F}$$

$$H_{ST} = 154.3 \text{ Btu/lb}$$

$$W_p = 2886 \text{ lb/hr}$$

$$\eta_{HX} = 0.975$$

$$Q_{REC} = 2886 \times (247.0 - 154.3) \times 0.975 = 260,844 \text{ Btu/hr}$$

$$T_H = 450^\circ\text{F}$$

$$T_C = 122^\circ\text{F}$$

$$\eta_{NET} = (1 - 583/910) \times 0.466 \times 0.99 = 0.157$$

$$\text{Power} = 0.159 \times 260,844/2545 = 16.3 \text{ hp}$$

$$\text{Reference power} = 9128 \text{ hp}$$

$$\text{Scaling factor} = 16.3/9.28 = 1.76$$

$$\text{Mean cycle pressure} = 150 \text{ bar}$$

$$\text{Frequency} = 66.7 \text{ HZ } 4000 \text{ RPM}$$

Piston stroke

$$S = S_o \times 1.76^{0.333} = 1.21 \times S_o$$

Cylinder diameter

$$D = D_o \times 1.76^{0.333} = 1.21 \times D_o$$

$$\text{Engine volume/weight factor} = 1.21^3 = 1.76$$

C.3 REFERENCES - Appendix C

- C1. Walker, G. "Elementary Design Guidelines for Stirling Engines," Proc. 14th Intersociety Energy Conversion Engineering Conference, ACS, Boston, August 1979.

- C2. West, C. D., "Theoretical Basis for the Beale Number," Proceedings of the 16th IECEC, August, 1981, p. 1986-7.
- C3. Nightingale, N. P., "Automotive Stirling Engine Development Program," Proc. 21st Auto. Tech. Dev. Contractor's Coordination Meeting, Dearborn, Michigan, Nov. 14-17, 1983.
- C4. Richey, A. E., "MOD 1 Stirling Engine Performance Data and Analysis," Proceedings 21st Auto. Tech. Dev. Contractor's Coordination Meeting, Dearborn, Michigan, Nov. 14-17, 1983.
- C5. Personal communication with A. E. Richey, MTI
- C6. Martin, W. R., "Stirling Engine Design Manual - Second Edition," DOE/NASA/3194-1, Jan. 1983, p. 77.
- C7. Gedeon, David, "Scaling Rules for Stirling Engines," Proceedings of the 16th IECEC, August, 1981, p. 1929-35.

APPENDIX D
PLANETARY GEARBOX SCALING

The procedure for estimating weights of planetary gears is given by Dudley(D1) as

$$W = 20 \times Q^{1.0184}$$

where W is weight in pounds and

$$Q = \frac{\text{horsepower}}{\text{pinion RPM}} \times \frac{(\text{Mg} + 1)^3}{\text{Mg}}$$

Mg = speed, ratio of gears

The gearbox design from Reference 1 which is shown on the attached Figure D1 was used as the basis for scaling as follows:

$$W = W_{\text{ref}} \times (Q/Q_{\text{REF}})^{1.0184}$$

$$W_{\text{ref}} = 36 \text{ lbs}$$

$$Q_{\text{ref}} = 0.401$$

$$W = 36 \times (Q/0.401)^{1.0184}$$

Since the weight is proportional the cube of the unit dimensions

$$L = L_{\text{ref}} \times (W/36)^{0.333}$$

(D1) Dudley, Darle W., "Practical Gear Design, McGraw-Hill, New York, 1954.

Dwg. 9370A32

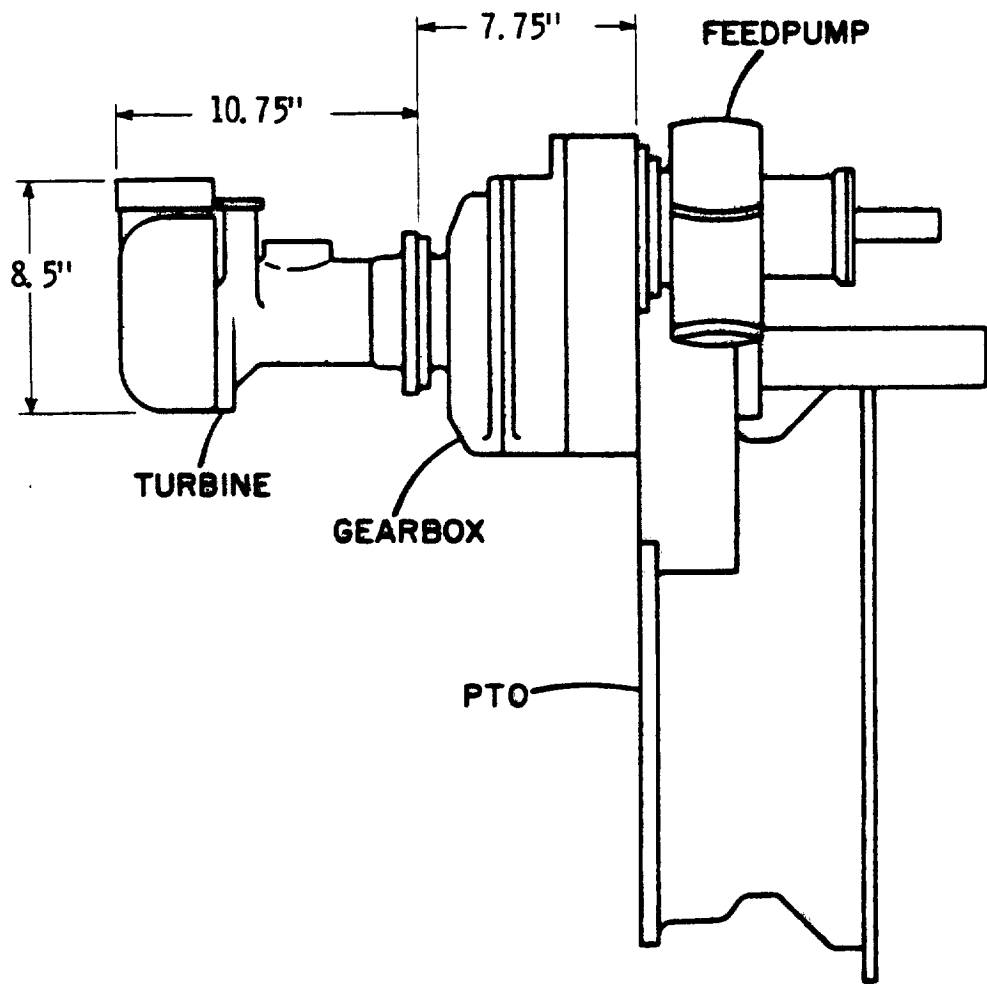


Fig. D1-TECO reference system, power conversion unit (PCU)

APPENDIX E

V-BELT DRIVE DESIGN INFORMATION



The Gates Rubber Company
 999 South Broadway
 P O. Box 5887
 Denver, Colorado 80217
 (303) 744-1911

ORIGINAL EQUIPMENT
 OF POOR QUALITY

Robert Hamm
 Westinghouse R & D Center
 1310 Beulah Road
 Pittsburgh, Pennsylvania 15235

September 12, 1984

Dear Mr. Hamm:

During our phone conversation of September 6, you asked me to design drives for a six unit, Sterling battery locomotive drive. The drive parameters were:

Battery:	One 91.8 h.p., five 65.1 h.p.
DriveR:	4000 rpm
DriveN:	1050 rpm
Center Distance:	30" for bottom four batteries 56" for top two batteries

The belts were picked to obtain the center distances nearest your specifications. Less expensive drives are available, but have larger center distances than you specified.

The proposed drive is shown in the accompanying drawings. The drives I am recommending are as follows:

Drive:	Four bottom batteries, 65.1 h.p. each
DriveR:	5/5VX4.9
DriveN:	5/5VX18.7
Belt:	5/5VX1000
Center Distance:	30.7"
Tensioning:	Apply force of 8 to 11 pounds, for deflection of 15/32".
Drive:	Top battery, 65.1 h.p.
DriveR:	5/5VX4.9
DriveN:	5/5VX18.7
Belt:	5/5VX1500
Center Distance:	56.05"
Tensioning:	Apply force of 7 to 11 pounds, for deflection of 7/8".

Robert Hamm

Page 2

Drive:	Top battery, 91.8 h.p.
DriveR:	6/5VX4.9
DriveN:	6/5VX18.7
Belt:	6/5VX1500
Center Distance:	56.05"
Tensioning:	Apply force of 8 to 12 pounds, for deflection of 7/8".

If you have any questions, please contact me.

Sincerely,

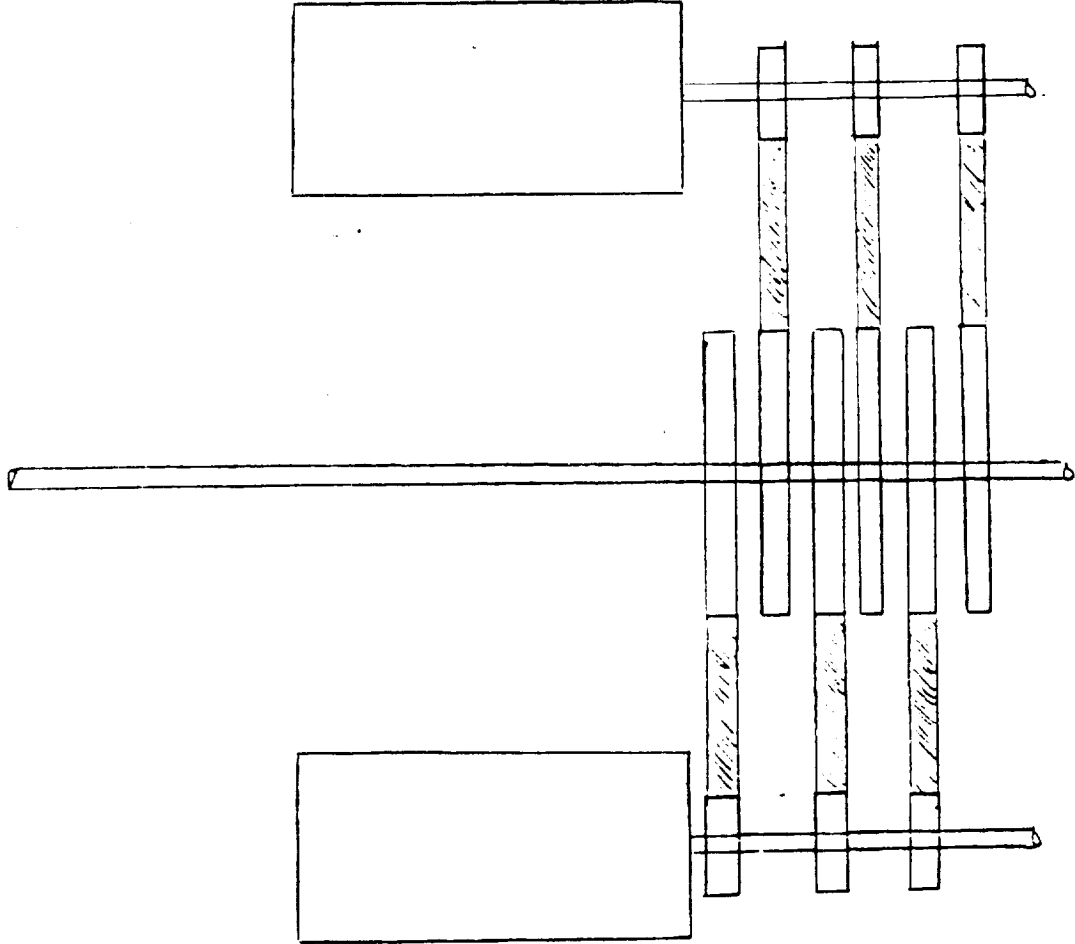


Brent Oman
Application Engineer

BO/cmc

Notes Number Co.
9/7/84

ORIGINAL PAGE IS
OF POOR QUALITY



Top View
(Not to Scale)



The Gates Rubber Company
999 South Broadway
P O. Box 5887
Denver, Colorado 80217
(303) 744-1911

Mr. Robert Hamm
Westinghouse R&D Center
1310 Beulah Road
Pittsburgh, PA 15235

September 24, 1984

Dear Mr. Hamm:

In our telephone conversations of September 17 regarding my previous drive design recommendations for your locomotive drive, you indicated that you preferred to use PowerBand belts.

Using the force-deflection method of tensioning for PowerBand belts is not always convenient since such large forces are required to deflect all of the individual strands in a PowerBand at the same time.

Please use the following information for the elongation method of tensioning in place of my previous tensioning recommendations for single strand belts.

Measure the outside circumference of the belts at zero tension. Tighten the belts until the original outside circumference elongates between the amounts shown below:

<u>Horsepower</u>	<u>Belt</u>	<u>Elongation</u>
65.1	5/5VX1000 PowerBand	3/8" to 9/16"
65.1	5/5VX1500 PowerBand	1/2" to 13/16"
91.8	6/5VX1500 PowerBand	5/8" to 15/16"

If you have any questions, please contact me.

Sincerely,

Brent Oman
Application Engineer

BC/ckw

APPENDIX F

WEIGHT ESTIMATES FOR ORGANIC RANKINE CYCLE SYSTEM COMPONENTS

The weights of the turbine and gearbox for the organic Rankine cycle system in the three applications were based on the designs described in Reference 1. The turbine was scaled using conventional turbomachinery scaling procedures and the planetary gearbox was scaled using the method described in Appendix D.

Table F1 summarizes the results for the turbine and Table F2 summarizes the results for the gearbox.

Table F1

TURBINE DATA FOR ORGANIC RANKINE CYCLE WITH RC-1

<u>Application</u>	<u>Truck</u>	<u>Locomotive</u>	<u>Marine</u>
Total Power - hp	373.3	3600	5600
Rankine Cycle Power - hp	56.2	542.0	904.4
Turbine Rotor Diameter - in	3.5	10.9	13.4
Turbine Rotor Speed - RPM	55,000	17,714	14,349
External Dimensions of Turbine			
Diameter - in	6.68	20.8	23.4
Length - in	10.75	33.5	37.6
Turbine Weight - lb	33.5	1012	1880

Table F2

PLANETARY GEARBOX DATA FOR ORGANIC RANKINE CYCLE WITH RC-1

<u>Application</u>	<u>Truck</u>	<u>Locomotive</u>	<u>Marine</u>
Total Power - hp	373.3	3600	5600
Rankine Cycle Power - hp	56.2	542.0	904.4
Turbine Speed - RPM	55,000	17,714	14,349
Diesel Engine Speed - RPM	1900	1050	1050
Gear Speed - RPM	3000	1050(2)	1800(1)
Speed Ratio	18.3	16.9	8.0
Q-Factor	0.401	10.38	6.74
Weight Ratio	1.00	27.5	15.04
Weight - lbs	36	990	541
Scale Factor	1.00	3.02	2.47
Housing Length - in	7.6	22.9	18.8
Housing Diameter - in	10.0	30.2	24.7

(1) Generator Speed

(2) Engine Speed

APPENDIX G

WEIGHT ESTIMATES FOR STIRLING ENGINE SYSTEM COMPONENTS

The weights of the high and low temperature Stirling engine modules were derived from the MODI reference engine using the scaling procedure described in Appendix C. Table G1 summarizes the results for the three applications. For the truck application, the high temperature module is an 0.89 scale model and the low temperature version is a 1.21 scale model of the reference engine.

For the locomotive application it was found that a single 2.87 scale model high temperature unit would weigh 3.37 times as much as multiple reference engine modules and that a single 3.89 scale model low temperature unit would weigh 3.36 times as much as multiple reference engine modules. It was therefore decided to use multiple reference engine modules for this application rather than single units.

For the marine application, the same advantage of multiple reference engine modules over single units obtained so multiple modules were used for this application also.

In the truck application the two Stirling engine modules drive through a single planetary gearbox. The estimated weight for that gearbox is given in Table G2.

The locomotive application of the Stirling engine does not use a gearbox. The V-belt drive provides the required speed reduction.

The gearboxes for the marine application are gear and pinion type. The weights of these units were estimated.

Table G1
SCALING OF STIRLING ENGINES

Application	Reference	Truck (358.1 hp)	Locomotive (3600 hp)	Marine* (5600 hp)
High Temperature				
Power - hp	35.8	25.3	254.3	404.9
No. of Cylinders	4	4	28	44
Speed - RPM	4000	4000	4000	1200
Height - in	31.9	28.4	31.9	91.6
Width - in	28.0	25.0	28.0	80.4
Length - in	28.0	25.0	196.0	80.4
Weight - lbs	698	494	4900	16522
Low Temperature				
Power - hp	9.28	16.3	163.9	267.7
No. of cylinders	4	4	70	4
Speed - RPM	4000	4000	4000	1200
Height - in	31.9	38.6	31.9	124.1
Width - in	28.0	33.9	28.0	108.9
Length - in	28.0	33.9	490	108.9
Weight - lbs	698	1229	12250	41112
Total Power - Stirling Engine	NA	41.6	418.2	672.6
Total Weight	NA	1723	17150	57634
Specific Weight - lb/hp		41.4	41.4	137.8

*Water Cooled

Table G2

PLANETARY GEARBOXES FOR STIRLING ENGINES

Application	Truck
Total power - hp	358.1
Diesel engine speed - rpm	1900
Stirling engines	
Engine power - hp	41.6
Engine speed - RPM	4000
Gear speed - RPM	3000
Speed ratio	1.33
Q-factor	0.0989
Weight - lbs	8.6
Housing length - in.	4.8
Diameter - in.	6.3

Wale Keairns for J.R. Hamm
J. R. Hamm

Wale Keairns
D. L. Keairns, Manager
Chemical & Process Engineering

Richard A. Newby
R. A. Newby

E. J. Vidt
E. J. Vidt

Thomas E. Lippert
T. E. Lippert

1 Report No NASA CR 174898	2 Government Accession No	3 Recipient's Catalog No	
4 Title and Subtitle Design and Evaluation of Fluidized Bed Heat Recovery for Diesel Engine Systems		5 Report Date July 1985	
		6 Performing Organization Code	
7 Author(s) J. R. Hamm R. A. Newby E. J. Vidt T. E. Lippert		8 Performing Organization Report No.	
		10 Work Unit No.	
9 Performing Organization Name and Address Westinghouse Research & Development Center 1310 Beulah Road Pittsburgh, PA 15235		11 Contract or Grant No. DEN3-345	
		13 Type of Report and Period Covered Contractor Report	
12 Sponsoring Agency Name and Address U. S. Department of Energy Office of Vehicle & Engine R&D Washington, D.C. 20585		14 Sponsoring Agency Code DOE/NASA/0345-1	
		15 Supplementary Notes Prepared under Interagency Agreement DE-AI01-80CS50194, Project Manager M. Murray Bailey, Propulsion Systems Division, NASA Lewis Research Center, Cleveland, OH 44135	
16 Abstract A preliminary conceptual design study was conducted to evaluate the potential of utilizing fluidized bed heat exchangers in place of conventional counter-flow heat exchangers for heat recovery from adiabatic diesel engine exhaust gas streams. Fluidized bed heat recovery systems were evaluated in three different heavy duty transport applications: heavy duty diesel truck, diesel locomotive, and diesel marine pushboat. The three applications are characterized by differences in overall power output and annual utilization. For each application, the exhaust gas source is a turbocharged-adiabatic diesel core. Representative subposed exhaust gas heat utilization power cycles were selected for conceptual design efforts including design layouts and performance estimates for the fluidized bed heat recovery heat exchangers. The selected power cycles were: Organic Rankine with RC-1 working fluid, Turbocompound Power Turbine with Steam Injection, and Stirling Engine. Fuel economy improvement predictions were used in conjunction with capital cost estimates and fuel price data to determine payback times for the various cases. These were based on simple payback assumptions without considerations of maintenance burdens or the cost of money.			
17 Key Words (Suggested by Author(s)) Diesel Engine Economics Heat Recovery Truck Adiabatic Locomotive Fluidized Bed Marine		18 Distribution Statement Unclassified-Unlimited STAR Category 85 DOE Category UC-96	
19 Security Classif. (of this report) Unclassified	20 Security Classif. (of this page) Unclassified	21 No. of pages	22 Price*

